THE ROLE OF PKC EPSILON IN BREAST CANCER CELL SURFACE POLYFIBRONECTIN ASSEMBLY AND PULMONARY METASTASIS

A Dissertation

Presented to the Faculty of the Graduate School

of Cornell University

In Partial Fulfillment of the Requirements for the Degree of

Doctor of Philosophy

by

Lynn Yu Ling Huang

May 2009

ROLE OF PKC EPSILON IN BREAST CANCER CELL SURFACE POLYFIBRONECTIN ASSEMBLY AND PULMONARY METASTASIS

Lynn Yu Ling Huang, Ph. D.

Cornell University 2009

Fibronectin polymerized and assembled into globules on the surface of breast cancer cells has been shown to mediate metastasis to the lungs. Disruption of the binding between these tumor-cell surface-associated fibronectin, or polymeric fibronectin (polyFn), and dipeptidyl peptidase (DPPIV) negatively impacts breast cancer lung colonization. This dissertation was designed to characterize the molecular mechanisms underlying assembly of surface coated polyFn to understand the regulation of breast cancer cell surface polyFn.

In order to investigate the signaling pathways involved in polyFn assembly, we utilized pharmacological inhibitors for various signaling pathways that have been proposed to regulate cellular function. Mutant plasmid expression, siRNA knockdown of proteins and biochemical analyses were carried out to identify the particular kinase involved in regulating polyFn. The ability of rat breast cancer cells to assemble polyFn was impaired by disruption of PKCε function. Knockdown of fibronectin also abolished polyFn formation. Cells with knockdown of either PKCε or fibronectin both had diminished ability to colonize the lungs in rat tail vein injection metastasis model.

To further substantiate the role of PKCε in lung metastasis-mediating polyFn, mass spectrometry analysis was performed on the PKCε complex. Two proteins were identified and tested with corresponding inhibitors to relate cellular function to polyFn assembly. Detailed biochemical analyses, immunofluorescent microscopy, mutant protein expression and pharmacological inhibition demonstrated that the subcellular

localization of PKCε complex with actin cytoskeleton has a great impact on polyFn assembly. A focal adhesion kinase was also identified to be involved. Therefore, PKCε exhibits its effects on polyFn by controlling the activation of downstream signaling proteins.

In summary, the presence of endogenous cellular fibronectin and catalytically competent PKCε is a prerequisite of successful polyFn assembly. Proper subcellular localization of PKCε-actin complex facilitates PKCε downstream signaling, most likely to Pyk2, promoting the formation of polyFn surface formation. These results present a novel potential signaling pathway for therapeutical intervention in breast cancer metastasis.

BIOGRAPHICAL SKETCH

Lynn Yu Ling Huang was born on April 11, 1980, in South Bend, Indiana, USA. She attended a year of elementary school in California and received the remainder of elementary education in the bilingual department of National Experimental High School (NEHS) in Hsinchu, Taiwan, where she was instructed mostly in English. She transferred to the regular high school department of NEHS for preparation of the national college entrance exam and was accepted to the Department of Veterinary Medicine of National Taiwan University, Taipei, Taiwan. She completed veterinary education with one year of internship while working as a part time intern veterinarian at the animal hospital ward and graduated with a Bachelor of Veterinary Medicine (B.V.M.) in 2003. After graduation, she worked as a lab assistant researcher in Academia Sinica, Taipei, Taiwan and National Tsing-Hua University and passed the national examination for licensed veterinarians. In May 2004, she began her doctoral studies in the lab of Dr. Bendicht U. Pauli in the Cancer Biology Laboratories of the Department of Molecular Medicine, College of Veterinary Medicine, Cornell University, Ithaca, NY.

For my lovely family members

Who have stood behind me through the ups and downs of my life

Who

Always had faith in me

ACKNOWLEDGMENTS

First and foremost I would like to thank the chairman of my graduate committee, Dr. Bendicht U. Pauli, whose expertise and support has made an outstanding research environment for my dissertation studies. His scientific counseling has been invaluable during the years of study. Without Dr. Pauli's utmost support, understanding, and encouragement, I would not have been able to complete the work presented here. I am also grateful for the guidance and support from the remaining members of my committee, Drs. James Casey, Roy Levine, and Robert Weiss.

I would like to extend my thanks to previous and current lab members of the "Pauli lab", who has helped created a wonderful environment to learn research techniques and exchange ideas. I thank Dr. Hung-Chi Cheng for assisting me during my earliest years to gain a solid ground in biochemistry and cellular assays, providing the basis for my research in this lab. I also thank Dr. Randolph C. Elble for guiding me through the various approaches in plasmid construction and offering precious advice on graduate life. I thank Dr. Mossaad Abdel-Ghany for his active help and input in various biochemical techniques. I thank Dr. Keyi Liu, who has offered not only scientific interactions but also valuable insights in life. I thank Dr. Roy Levine for the wonderful support as a lab neighbor and for providing advice on experimental design. I thank Dr. James Casey for offering rich encouragements and advice. I also want to thank the lab members of Dr. Jun-lin Guan, Dr. Richard Cerione and Dr. Yung-fu Chang, who have offered accommodating assistance to the lab and at various points of my project. Finally, I would like to thank Dr. Rodman Getchell for his support and guidance on operating the FACS machine, an integral part of my research.

TABLE OF CONTENTS

LIST OF FIGURES

LIST OF TABLES

LIST OF ABBREVIATIONS

ABD	Actin binding domain
DPPIV	Dipeptidylpeptidase IV
ECM	Extracellular matrix
EDA	Extradomain A
EDB	Extradomain B
EGF	Epidermal growth factor
EMT	Epithelial to mesenchymal transition
ERK	Extracellular signal-regulated protein kinase
FACS	Fluorescence Activated Cell Sorting
F-actin	Filamentous actin
FN, Fn	Fibronectin
GFP	Green fluorescent protein
Igtb1	Beta1 integrin
MAP	Mitogen-activated protein
MDA-MB-231	Human breast adenocarcinoma cell line
MEp	Mammary epithelial cell
MFP	Mammary fat pad
MG	Mammary gland
MMTV	Mouse mammary tumor virus
MTF7	Rat breast carcinoma cell line
PKC	Protein Kinase C
PolyFn	Polymeric fibronectin
PYK2	Proline rich kinase 2
RD-PKC	Regulatory domain of PKC

RGD	Arginine-glycine-aspartic acid
RT-PCR	Reverse trascriptase polymerase chain reaction
SDS-PAGE	sodium dodecyl sulfate polyacrylamide gel electrophoresis
TEB	Terminal end bud
TGFβ1	Transforming growth factor β1
VEGF	Vascular endothelial growth factor
V region	Variable region
WT	Wild type

LIST OF SYMBOLS

α	……	Alpha
β	……	Beta
δ	……	Delta
ε	……	Epsilon
η	……	Eta
θ	……	Theta
ζ	……	Zeta

CHAPTER I

FIBRONECTIN IN CANCER PROGRESSION AND METASTASIS

INTRODUCTION

The extracellular matrix (ECM) supports specific interactions with cell surface receptors and is essential for tissue function. Fibronectin (Fn), an abundant ECM glycoprotein, is involved in a variety of cellular functions and disease processes. Fn regulates cellular functions such as cell adhesion, cell migration and cell proliferation. Fn is necessary for proper embryonic development and tissue repair and disregulation of Fn leads to diseases of the skin, liver, lung, cartilage and bones as well as cancer progression. The integral role of Fn in maintenance of normal cell function cannot be undermined. In this review, we will take a look at the structure and domains of Fn, consequences of Fn deletion, Fn matrix assembly and provide a brief overview of Fn function in cancer progression and metastasis.

STRUCTURE OF FIBRONECTIN

Fibronectin (Fn) is a glycoprotein that exists as a dimer comprised of two 220-250 kDa subunits connected at the C-termini by disulfide bonds (1,2) (Fig 1.1). Each subunit consists of repeating modules (Fn repeats) that includes type I, type II and type III repeats. Type I repeats contain two disulfide bonds and contain approximately 40 amino acids; type II repeats are about 60 amino-acid residues in length and contains two intrachain disulfide bonds; and type II repeats are 90 residues in length and have no disulfide bonds. Fn is comprised of 12 type I repeats, 2 type II repeats, 15-17 type III repeats and a variable(V) region not homologous to other areas on Fn (1,2). These domains contain multiple binding sites for heparin and for various cell surface receptors that modulate cellular function.

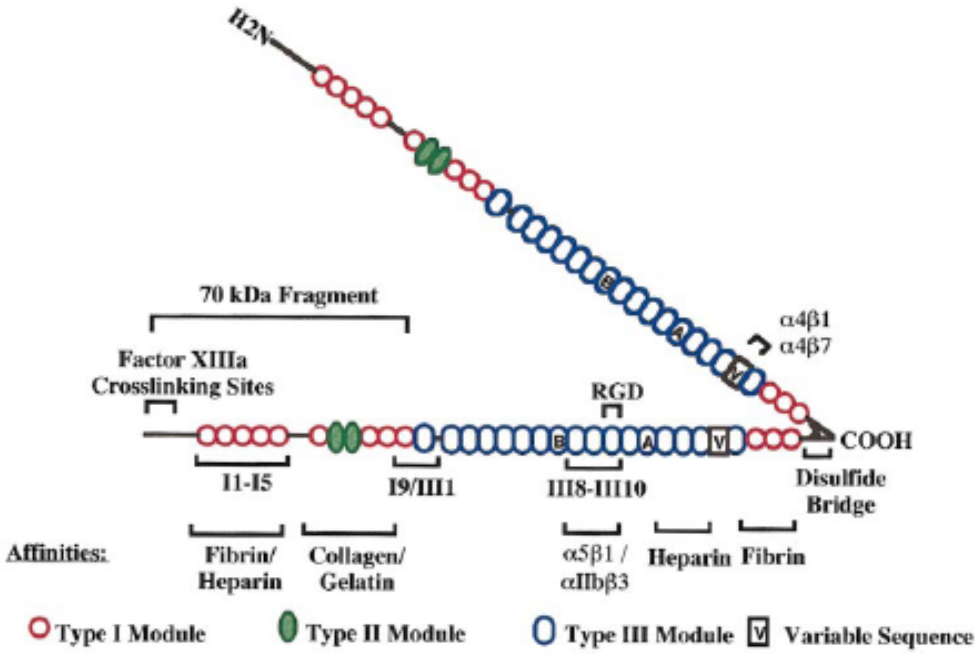

Magnusson, M. K. *et al.* (1998) Arterioscler Thromb Vasc Biol 18(9), 1363-1370

Figure 1.1: Schematic diagram of modular structure of Fn dimer (2).

The 2 type II repeats that undergo alternative splicing are termed EDA (ED, extradomain) and EDB (Fig 1.2). Fn can be subdivided into 2 forms based on solubility: the more soluble plasma Fn and the less soluble cellular FN. Plasma FN (pFn), which is synthesized in hepatocytes, has a simple splicing pattern and contains neither EDA nor EDB while cellular Fn (cFn), which is synthesized in tissues, contains either or both of EDA and EDB and is a more heterogenous group of Fn isoforms as a consequence of cell-type and species-specific alternative splicing (3). In pFn, only one of the subunits contains Variable (V) region whereas most cFn contains V region (1,2).

Individual type III repeats have only 20-40% identity in amino acid sequence but a high degree of structural homology. Type III repeats are organized into 7 anti-parallel β strands with exposed loops within these strands. Fn domains may be structurally modified, which can expose cryptic sites induced by mechanical forces stretching the Fn molecule, proteolysis, or incorporation of one or both of EDA and EDB (4). Exposure of cryptic site allows Fn molecule self association (5) and has a potential role in serving as nucleation sites for Fn polymerization and fibril assembly (6).

FIBRONECTIN SPLICE VARIANTS AND FUNCTIONS

Fibronectin was one of the first genes to be reported to be alternatively spliced and is one of the best studied models of alternative splicing (4). During transcription, the EDA and EDB exons can be included or excluded from Fn mRNA while the V region (also called IIICS, type III connecting segment) can be completely included(V120), partially included, or excluded(V0), depending on species (4) (Fig 1.2). On top of alternatively spliced forms, in zebrafish, 2 Fn genes are present (FN1a

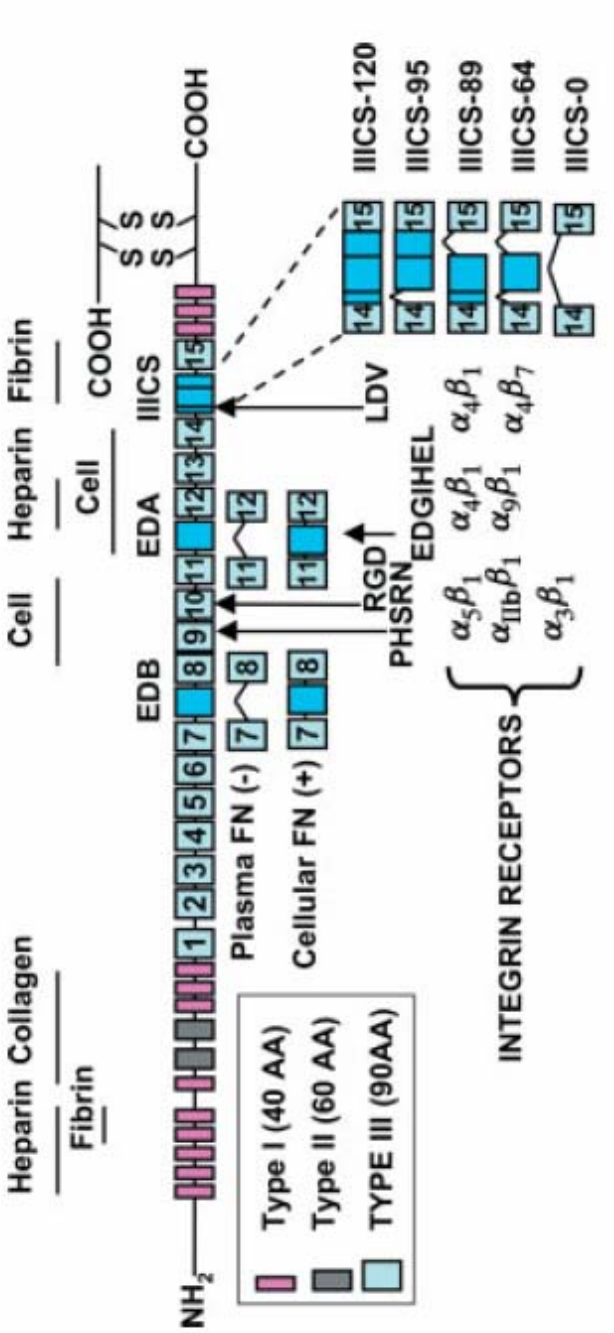

White, E. S. *et al.* (2008) J Pathol 216(1), 1-14

Figure 1.2: Fibronectin alternative splice sites and sites of integrin receptor and cell binding: Splicing of EDA and EDB is similar in all species (total inclusion or exclusion) while splicing of the variable region is species specific (4).

and FN1b) (7). However, the total number of Fn isoforms still correlates with evolutionary scale. The 2 independent genes in zebrafish produce only 1 V-region variant in FN1a and 2 V variants in FN1b and a total of 5 Fn isoforms (8). In other species, frogs and chickens have 2 V variants (generates up to 6 Fn isoforms), rats and mice have 3 (produces 12 Fn isoforms) and humans have 5 V variants that generates up to 20 Fn isoforms (4).

Incorporation of the alternatively spliced region in Fn is increased during embryonic development and decreases dramatically after birth and with aging (4,8,9). A comparison of fetal and nonfetal fibroblasts shows a loss of EDB inclusion in nonfetal cells (10). Analysis of rat embryo mRNA reveals that the entire V region (V120) is included in most FN mRNA while rats in later developmental stages contain V0, V95 and V120, indicating developmentally regulated splicing (11). RNA from mice of different ages after birth up to 24 months revealed the increased inclusion of V0 and decreased inclusion of V120 with aging, while V95 showed no change (12). Under certain situations, the "embryonic" splicing pattern is re-established in adults, such as during tissue repair, tissue fibrosis and angiogenesis. In skin wound healing, EDA and EDB are present in the Fn mRNA in the cells at the base of the wound (13). During pheripheral nerve regeneration, V25 inclusion was increased while V0 levels remain low (14). Cell type specificity of alternative splicing patterns can be seen more clearly in adults. In large vessel wall endothelial cells, inclusion of EDA but not EDB is seen in Fn. The same EDA+EDB- splice form exists within the uterine endometrium. On the other hand, chondrocytes contain EDB+EDA- Fn mRNA (9). The differential distribution of different Fn isoforms certainly suggests different roles for each of the isoforms in cellular function.

(1) EDA DOMAIN

EDA domain has numerous functions which include cell adhesion, wound healing, matrix assembly, dimer formation, protein secretion, cell differentiation, tissue injury and inflammation, cell cycle progression and various disease processes (4). EDA+ Fn is implicated in disease processes such as rheumatoid arthritis (15). A low concentration of pFn and EDA-only polypeptide were synergistic for cell attachment and spreading and lead to cytoskeletal reorganization and focal contact formation compared to either substrate used alone(16). EDA+ Fn was found abundantly expressed only in the ECM of scarred human eyes and not normal conjunctiva (17), indicating a role in wound healing. In airway epithelial cells that secrete Fn from both apical and basal surfaces, EDA+ Fn were only secreted apically, demonstrating a role in directing secretion (18). On the other hand, levels of EDA+ Fn are elevated in plasma and tissues of patients with certain disorders such as pulmonary fibrosis (19), psoriasis, rheumatoid arthritis, diabetes and cancer (4), but the functional role of EDA+ Fn has not be clarified.

(2) EDB DOMAIN

EDB+ Fn has a positive role in matrix assembly, as it is more efficiently incorporated into Fn matrix, along with EDA+ Fn, than EDA-EDB-V-Fn and V+Fn (20). Studies on EDB-/- mice revealed no significant phenotype (21-23), but a mild *in vitro* effect on matrix assembly and proliferation (23). EDB-/- embryonic fibroblasts grew slower and produced shorter and thinner FN fibrils compared to normal cells (23). On the other hand, EDB+ Fn is lost from many cell types upon completion of development and its expression correlates closely to cell proliferation (9). Recently, EDB+ Fn was found to reside in neoplastic tissue blood vessels but absent from mature/adult tissues, highlighting its role in angiogenesis (24). EDB+ Fn may

potentiate and assist in vascular development, suggested by the findings that EDB+ Fn can increase VEGF expression and endothelial proliferation (24), even though in EDB-/- mice a compensatory pathway might exist for angiogenesis. EDB+ Fn is upregulated in the serum of diabetic retinopathy patients (25) and is expressed in hematologic tumors such as Hodgkin and non-Hodgkin lymphoma (26). Future research on these disease models of EDB+ Fn will be able to elucidate the other potential cellular functions of this Fn splice variant.

(3) V REGION

The V region of Fn contains integrin recognition sites that promote cell spreading and migration (9,20). Human Fn contains two cell binding sites within the V region: LDV in V25 (CS1) and REDV in V31 (CS5), both sequence are recognized by α4β1 integrin. LDV is also found in Xenopus, rat and chicken Fn. REDV is not conserved and is RGDV in rat and bovine. The V region mediates tumor invasion, motility and spreading of squamous cell carcinoma (27) and hepatocellular carcinoma (28). Up regulation of V25 has been shown to enhance nerve repair (29). Increased exclusion of the V region has been observed in early disease processes in disease models of lupus nephritis and immune complex nephritis (30). In human primary fibroblasts, the V region induces apoptosis and concomitant transcriptional decreases of c-Myc, p53, p21 and bcl-2 (31). Other roles in Fn secretion and clot formation have also been suggested (32).

PHENOTYPES OF FIBRONECTIN KNOCKOUT MICE

Targeted mutations in the Fn gene in different mouse models have been used to complement experimental data by Fn expression. The first Fn-null mice were

generated by removing the translation initiation codon and part of the 5'exon to disrupt the Fn gene (33). Mice with heterozygous mutation (+/-) are fertile and normal, even with only half the normal level of FN (33). However, homozygous mutations were embryonic lethal. Fn is not required for blastocyst formation and abnormalities in the Fn-null embryos first appear after the onset of gastrulation, which includes shortened anterior-posterior axis, mesoderm deficiencies and distorted ectoderm. These embryos have an abnormal or no heart, no notochord and no somites (33). Heart defects develop depending on genetic background of Fn-null mice: the C57/BL6 background developed a less severe heart and blood vessel phenotype in which the heart tube forms normally while the 129S4 background is affected earlier in development and causes *cardia bifida* (34). More recently, 5 novel modifier genes were identified on chromosome four that were linked to the difference in embryonic heart development by comparing the above two genetic backgrounds in mice with high throughput SNP genotyping (35). The specific functions of these genes are yet to be determined.

Fn-null EDB mutations (EDB-cDNA fusion replacement, no introns) produced similar embryonic lethal and mesoderm defects as the Fn-null mice (36) while EDB-null mutation (deletion of EDB exon) created no obvious phenotype in various healing, organogenesis, tumorigenesis and thrombosis models (21-23). Conditional pFn knockout using ubiquitous Mx-cre recombinase revealed increased neuronal apoptosis and brain infarction following cerebral ischemia treatment but no effect on wound healing or hemostasis (37). Roles for pFn in thrombosis, angiogenesis and bacterial virulence were also suggested in similar pFn knockout models (38-40). Deletion of EDA exon produced mice with reduced atherosclerosis but no differences in tumor growth or thrombus formation was detected (22,23,41). Mice without the EDA exon in the FN protein (EDA-null) and mice having constitutive inclusion of the

EDA exon had reduced life spans, while EDA-null mice had wound healing defects (42). Mice engineered with constitutive inclusion of EDA into the FN molecule had increased thrombosis and thromboembolism, suggesting a pro-thrombotic role for EDA+Fn (43). Roles of EDA+Fn in motor coordination and lung fibrosis were also suggested (19,44).

On the other hand, double knockout of EDA and EDB was embryonic lethal with cardiovascular defects similar but less severe than that of FN-null mice. Deletion of both EDA and EDB exons had no effect on protein synthesis, secretion or cell surface deposition of Fn, indicating embryonic lethality was due specifically to the lack of EIIIA and EIIIB exons from Fn (35). Disruption of the cell binding site RGD by mutation to RGE generated was embryonic lethal at E10 (45), suggesting that the majority of Fn cellular function is mediated through RGD interaction with integrins. Assembly of Fn was normal but embryos had shortened posterior trunk, absent tail bud-derived somites and severe vascular defects similar to the phenotype of α5-integrin deficient mice (45). Although these total knockouts have provide valuable clues for Fn function, with newly available technology and well characterized promoters, tissue specific Fn deletion models will be able to further dissect the specific roles of Fn in various disease models.

CELL-SPECIFIC DELETION OF FIBRONECTIN

Cell-specific deletion of Fn is used to determine roles of Fn in different organs or cell types without the detrimental effects of whole mice Fn knockout. Mice engineered to constitutively express $EDA^{+}Fn$ had a significant decrease of Fn levels in plasma and most tissues while hepatocytes modified to produce EDA+ Fn have normal extracellular matrix Fn levels but secrete less soluble Fn (42). A liver-specific EDA-

exon deletion in these mice restored Fn levels in both plasma and tissues, indicating that a fraction of tissue Fn is plasma derived (46). Future work will be able to reveal the other functional significance of Fn in mouse knockout models.

FIBRONECTIN IN MAMMARY GLAND DEVELOPMENT

The histologic structure of mammary glands varies depending on sex, age and physiologic status. The basic mammary gland structure consists of lobules that consist of several branching intralobular ducts that end in alveoli (acini). During pregnancy and lactation, the mammary gland undergoes striking structural and physiologic change, such as acinar growth, as a result of the synergistic action of various hormones, which includes estrogen, progesterone, prolactin and human placental lactogen (47). Fn levels are regulated by estrogen and progesterone and change considerably during mammary gland development, increasing to 3-fold at puberty and maintains at high level during pregnancy and lactation (48). Fn is expressed around the basal cell surface of acini but downregulated in the late stages of acinar morphogenesis (49). A recent paper of mammary cell 3D culture shows that fibronectin expression regulates mammary epithelial cell growth. Fn in matrigel increases acinar size and Fn supplementation in the medium alters growth arrest state of mammary epithelial cells and increases proliferation and luminal filling. Dysregulated Fn expression affects proper acinar morphogenesis by altering mammary cell proliferative state and prevents lumen formation in mammary gland (49). However, proteolytic fragments of Fn suppress growth and promote apoptosis of tumorigenic mammary epithelial cells through matrix protease dependent pathways (50). ECM proteins like Fn can also influence cell proliferation through regulation of integrin interaction with hormones and growth factors.

ROLE OF FIBRONECTIN IN BREAST CANCER

The interstitial ECM in normal adult mammary tissue mostly lacks fibronectin while increased fibronectin is noted in the stroma of benign mammary hyperplasia and various types of mammary tumors and high levels of fibronectin in tissue sections correlate with decreased patient survival (49). Subtracted cDNA libraries comparing non-breast tissue, normal breast tissue and breast tumors show a threefold expression of Fn in breast tumors (51). Gene expression profile of primary invasive ductal carcinoma of the breast and axillary node with metastasis demonstrated that fibronectin was upregulated in both varieties of isolated tumor compared to disease free mammary epithelium (52). Fibronectin is not only differentially expressed between normal and tumor breast tissue but also differentially upregulated when compared to other cancers such as lung squamous cell cancer, lung adenocarcinoma, and renal cell cancer (53). In fact, fibronectin is most prominently expressed in cell lines selected for enhanced lung colonization and is known as a "pro-metastatic" gene (51). FN1 is also upregulated in a highly lung metastatic breast cancer cell variant isolated from early lung metastasis (54). Bioactive Fn fragments released during remodeling of mammary tissue in post-lactational involution have also been associated with increased breast cancer invasiveness and metastasis to the lung, liver and kidney (55). This result correlates with the high occurrence of metastases in pregnancy-associated breast cancer. These studies strongly indicate a role for fibronectin in breast cancer progression and metastasis.

FIBRONECTIN MATRIX ASSEMBLY

Fibronectin mediates a wide range of cellular functions in normal cells which includes cellular interactions with the extracellular matrix (ECM), cell adhesion, migration, growth and differentiation (1). The single question of utmost importance regarding the function of fibronectin is the mechanism by which cells convert it from a relatively compact soluble protomer to an insoluble form of multimers visible by fluorescence microscopy. This is a highly regulated process that involves interaction between fibronectin and cell surface receptors, matrix components, as well as itself. The ability to interact with the variety of molecules to accomplish the formation of a complex meshwork is conferred in the unique structure and domains within fibronectin (1).

Fibronectin is secreted as a dimer composed of two subunits of 250-kDa fibronectin molecules linked covalently near the C-termini and after secretion, fibronectin is assembled into a fibrillar matrix through interactions with cell surface integrin receptors, other matrix components or via self association (Fig 1.3). The incorporation into the matrix occurs in a two step process. The first step is binding of fibronectin in a deoxycholate (DOC) soluble pool that is reversible. The second step forms a DOC insoluble pool and results in a multimeric insoluble matrix. (1,56). The assembly process is integrin-dependent and fibronectin-integrin interactions trigger sequential events involving extracellular comformational activation of fibronectin and intracellular organization of the actin cytoskeleton. During assembly, the conformational changes of fibronectin expose fibronectin-binding sites and promote intermolecular interactions that result in fibril formation (57).

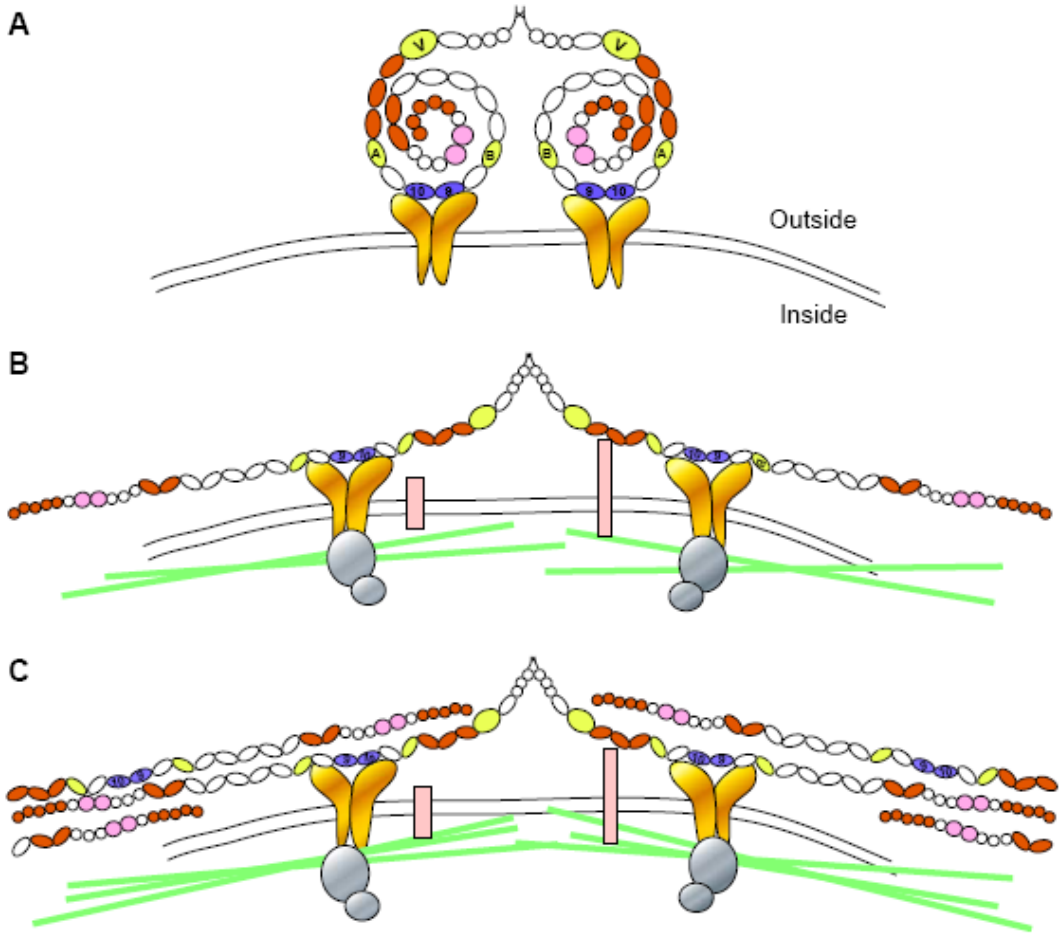

Mao, Y. *et al.* (2005) Matrix Biol 24(6), 389-399

Figure 1.3: Major steps of Fn fibril assembly: (A) Soluble Fn binds to α5β1 integrin via its cell binding domain. (B) Fn binding to integrins and other receptors (pink bars) induces reorganization of the actin cytoskeleton (green lines) and activates intracellular signaling complexes (silver circles). (C) Fn–Fn interactions results in fibrils formation. (57)

(1) INTERACTIONS OF FN AND INTEGRINS

Fibronectin is recognized by at least 10 different integrins. The first of such isolated is the α5β1 integrin, often referred to as the classical fibronectin receptor. It appears to be the main integrin attaching cells to fibronectin and has a partial role in controlling the assembly of fibronectin matrix around cells. (1,58,59). The region spanning the center of the Fn polypeptide chain in the ninth and tenth type III repeats binds to the α5β1 integrin (60). Extensive research had narrowed down the essential sequence for cell adhesion to several minimal integrin-recognition sequences. Two critical amino acid sequences in Fn are required for α5β1 integrin binding: an Arg-Gly-Asp (RGD) sequence and a Pro-His-Ser-Arg-Asn (PHSRN) sequence (Fig 1.2). The well known RGD sequence is located in the tenth type III repeat. The binding to this simple tripeptide sequence depends on many factors including the flanking residues, the three dimensional presentation of the sequence and individual characteristics of the integrin-binding pockets (1). The synergy site PHSRN in the Fn repeat III_9 mediates binding of Fn to α5β1 integrin via interactions with α5. Binding of Fn to α5β1 integrin can also be achieved through interactions with N-terminal fragment that contains I_{1-9} and II_{1-2} and trigger distinct intracellular signals from those elicited through ligation with RGD (1). This PHSRN site has been implicated in regulating matrix metalloproteinase (MMP)-1-dependent invasion of human breast cancer and mammary epithelial cells (61). Other integrins that have been shown to bind fibronectin are α3β1, α4β1, αvβ1, αIIbβ3, αvβ3 αvβ6, α4β7 and α?β8 (62). Many of the other fibronectin binding integrins bind to the RGD sequence, but the α4β1 integrin binds to fibronectin at a different site. The α4β1 binding site in fibronectin resides in the CS1 or V25 site that is located in the alternatively spliced V region of Fn (63-66). Studies have implicated functional differences between α4β1 and α5β1 in fibronectin matrix assembly (67, 68).

(2) INTERACTIONS OF FN AND OTHER MATRIX COMPONENTS

Fibronectin mediates a wide variety of cellular functions through the binding of molecules other than integrins. These include heparin, collagen/gelatin, and fibrin. The interacting domains of Fn to these molecules have been identified by proteolytic fragmentation or recombinant DNA analyses (8,69,70). Fn contains two major heparin-binding domains with the strongest binding site at the C-terminus (Heparin II) and a weaker binding site at the N-terminus (Heparin I). The Heparin II site also binds to glycosaminoglycan, chondroitin sulfate while Heparin I mediates Fn interactions with bacteria. The heparin binding domains of Fn is involved in cell adhesion in some cell types (1, 71). The collagen binding domain includes I_{6-9} and II_{1-2} and binds denatured collagen (gelatin) more effectively than native collagen. This domain has been implicated more in the clearance of collagenous materials than as a mediator of cell adhesion (1). The fibrin binding sites of Fn are Fibrin I and Fibrin II. Interactions at these sites have a role in cell adhesion and cell migration (1).

(3) FN SELF ASSOCIATION

Matrix assembly requires self association of fibronectin and involves domains within fibronectin that are highly specialized for Fn-Fn interactions (3,8,69,72). Two regions of fibronectin has been implicated in Fn binding (self association) and matrix assembly (3). The 70-kDa amino-terminal region was shown to be essential for matrix assembly while the type I repeats I_{1-5} within this region confer fibronectin binding activity. The 70-kDa amino-terminal fragment was shown to have saturable binding to fibroblast monolayers and to be required for *de novo* assembly of newly synthesized recombinant fibronectins into the extracellular matrix. A fragment containing type I repeats I_{1-5} can be covalently cross linked to fibronectin at the cell surface while deletion of the five repeats drastically reduced the binding ability of the fragment to

fibroblasts. An excess of the 70-kDa fragment and antibodies against repeats I_{1-5} had the ability to inhibit matrix assembly. A second site involved in fibronectin binding exists in a fragment spanning the first two type II repeats (II_{1-2}) adjacent to the gelatin binding domain. The 56-kDa fragment spanning this region and antibodies raised against repeats within it also had the ability to inhibit fibronectin binding and matrix formation (3). Other regions involved in matrix assembly include the cell binding domain (3,67,73) and the carboxyl-terminal cysteines that form the interchain disulfide bonds in the Fn dimer (74).

(4) INTERACTION OF FIBRONECTIN WITH DIPEPTIDYLPEPTIDASE IV (DPPIV)

DPPIV (CD26) is a membrane bound ectopeptidase that modulates the activities of several cytokines, chemokines and hormones via its unique proteolytic activity preferentially cleaving N-terminal X-Pro or X-Ala dipeptides (75-77). CD26/DPPIV also exerts biological functions unrelated to its dipeptidase activity. Not only can DPPIV form heterodimers with FAP-alpha, associate with plasminogen 2, ADA, CD45, and CXCR4, it can also bind to the ECM proteins fibronectin and collagen (77).

Binding of fibronectin to hepatocytes in suspension was first observed by Johansson utilizing an 85kDa cell binding peptide that lacks the gelatin- and heparin-binding domains. The 85kDa peptide inhibited initial attachment of hepatocytes to immobilized fibronectin and bound to the cells in suspension at 4 degrees C in a time-dependent, saturable, and partially reversible reaction (62). Piazza et al. later reported that initial binding of fibronectin to the cell surface where it was subsequently cross-linked is accelerated by inhibitors of DPPIV (78). Kinetic studies revealed that increasing amounts of iodinated Fn were irreversibly incorporated into large covalent,

nonreducible complexes that fail to enter the stacking gel during SDS-PAGE. Nitrocellulose binding assays using 125I-labelled DPP IV purified from rat hepatocytes demonstrated a direct interaction of DPP IV with fibronectin. Fibronectin was found to bind DPP IV at a site distinct from its exopeptidase substrate recognition site (78).

Studies were performed in this lab to identify the endothelial cell adhesion molecule responsible for binding multimeric fibronectin presented on the surface of metastatic breast cancer cells (polyFn), which mediates lung colonization, showed the responsible molecule to be the DPPIV expressed on rat lung capillary endothelia (79). Such adhesion could be inhibited in vivo and in vitro by soluble DPPIV and by antibody to Fn but not by soluble Fn (79). Immobilized DPPIV pulls down Fn multimers but not protomers from 35[S]-Met-labeled MTF7 cell extracts. MTF7 cells in suspension accumulate 125[I]-labeled Fn on their surface in a manner similar to that described above and in adherent cells, resulting in deoxycholate-insoluble and nonreducible multimers, seemingly forming a transglutaminase cross-linked matrix. These multimers assembled on tumor cell surface can be visualized as distinct globules under a fluorescent microscope (79). Soluble DPPIV binds to Fn-coated plastic (immobilized Fn) but such binding is not inhibited by soluble Fn, justifying the physiological relevant condition where the cancer cells are able to bind to endothelial DPPIV through its surface associated polyFn in a fibronectin rich environment in the plasma (79).

A detailed study in our lab using proteolytic fragments and maltose-binding protein fusion proteins found that the DPPIV-Fn interaction to be mediated by the consensus motif T (I/L)TGLX (P/R)G (T/V)X on fibronectin. These DPPIV-binding sites are located in type III repeats 13, 14, and 15 (Fn III13, -14, and -15, respectively)

of fibronectin. Peptides spanning the DPPIV-binding domain of FNIII14 blocked DPPIV/polyFn adhesion and suppressed pulmonary metastasis (80).

FN IN EPITHELIAL TO MESENCHYMAL TRANSITION AND INVASION

Tumor cells that migrate must first undergo a process known as epithelial to mesenchymal transition (EMT) to alter their phenotype into a less adhesive, more motile and spindle shaped cell that resembles cells from mesenchymal origin (81,82). EMT is a normal physiologic process that occurs during embryonic development, organogenesis, tissue growth and wound-healing and repair (83) but is also involved in the pathogenesis of many diseases and tumorigenesis. In breast cancer, EMT has been found to occur in 18% of tumors *in vivo* (84). EMT is defined as a variable proportion of tumor cells that express mesenchymal markers like vimentin and tenascin (84). EMT is involved in the appearance of different breast carcinoma types (85). Partial or complete loss of E-cadherin during carcinoma progression, which leads to poor prognosis, has been reported (85). Snail, a gene regulating EMT in Drosophila gastrulation, is expressed in areas of heterogenous tumors that are devoid of E-cadherin and is also found in all ductal invasive carcinomas with lymph node involvement (86). On the other hand, twist, another embryonic regulator, is highly expressed in invasive lobular carcinoma (87). Suppression of twist also inhibits the lung metastatic ability of highly metastatic mammary carcinoma (87). Areas of tumor lesions harboring poorly differentiated tumor cells that exhibited mesenchymal features in mammary sections of Cripto-1 transgenic mice were stained positive for Fn as well as integrins αv,α3, β1 and β3, known Fn receptors (88), strongly correlating EMT to Fn. A blocking antibody of α5β1 integrin signaling resulted in a more epithelial morphology in EGF-treated cells while other integrin antibodies tested have

no effects (89). Inhibition of α5β1 integrin signaling also blocked EGF-mediated increase of EMT markers vimentin and snail and decrease of E-cadherin while application of Fn increased EGF-induced effects on EMT markers. These results indicate that α5β1 integrin signaling and Fn can modulate EGF-induced EMT in cervical cancer cells (89). α5β1 integrin has also been implicated in TGFβ1-induced EMT in mammary epithelial cells (90). Direct evidence of EMT involvement in breast cancer has also recently been shown in three different oncogene-driven mouse mammary tumor models (91). These models found stromal fibroblasts associated with myc-induced tumors were of epithelial origin and these cells lacked cytokeratin and E-cadherin expression while expressing mesenchymal specific markers vimentin and FN (91). However, EMT is not required for breast cancer invasiveness and metastasis because mice and human tumors lacking EMT also had metastatic potential (91). EMT presents one mechanism by which cancer progress to a more aggressive phenotype.

Invasion of cells into a tissue can be a part of tumor progression or a part of normal cell processes. In cancer, invasion of cancerous cells into normal cells leads to metastasis. In inflammatory response or wound healing, migration of cells to the site of infection or wound site is a normal response (92). Fn in the matrix can promote or prevent invasion. In the case where invasive tissue is migrating into an acellular extracellular matrix, such as during embryogenesis or wound repair, Fn promotes invasion. Migration fails when fibronectin is ablated, when cell-Fn interaction is blocked by antifunctional antibodies to Fn or integrin, and when RGD-containing peptide is used, and this typically leads to reduced invasion (92). In developing fetus, when Fn accumulation at the intimal cushion (smooth muscle in the center of arteries that keep arteries open) extracellular matrix is reduced, vascular smooth muscle invasion is blocked and the ductus fails to close properly after birth (93). If invasion occurs towards densely cellular tissue, Fn prevents invasion. Fn contributes to the

stabilization of the organization of tissues, such as in a developing amniote heart, where Fn stabilizes the contact boundary between the myocardium and the epicardial mesenchyme. Loss of crucial mediators of adhesion may result in pathological disorganization of tissues that leads to aggressive malignant invasion (92). An anti-β1 blocking antibody inhibited invasion of both HT-1080 fibrosarcoma cells and MDA-MB-231 breast carcinoma cells through Matrigel basement membrane (94,95). Anti-α5 blocking antibody also inhibited MDA-MB-231 invasion in the presence of chemoattractant but not in the absence of it (95). In this case, the α5 integrin may be functioning as a chemoattractant and not adhesion receptor to promote migration of cells towards Fn (95). Similarly, in cervical cancer, EGF stimulated cancer cell invasiveness was abolished by α5β1 integrin blocking antibody (89). Comparison of normal and fibrotic lung fibroblasts revealed that Fn signaling through α5β1 integrin mediates migration/invasion while Fn signaling through α4β1 integrin suppresses migration/invasion (96). The α4 integrin has also been found to be inversely correlated to invasive potential in B16 melanoma cells (97). The functional roles of Fn in EMT, cell migration and invasion tightly correlate with its role in tumor progression.

FIBRONECTIN IN METASTASIS

The role of Fn in metastasis cannot be simply stated. In some cases, Fn contributes to metastasis and is upregulated in metastatic variants of cancer cells (98-105). In other cases, Fn is found to be negatively correlated to metastasis (51,95,106-110). Various studies on the same type of cancer have pointed towards different functional consequences of Fn expression.

There are generally two broad classes of *in vivo* metastasis models. The "experimental" metastasis models involve injection of tumor cell suspensions into

mice and quantitation of the number or sizes of the metastatic colonies at the metastatic organ. This model studies the later steps of metastasis, skipping the early steps of detachment from the primary tumor mass and invasion into the vessels. The "spontaneous" metastasis models are more complicated and involve the implantation of tumors or cells into mice. This model measures the earlier steps including detachment, intravasation leading to the final steps of adhesion, tumor arrest and migration into the secondary metastatic organ (95).

Fn can have a negative role in metastasis. Fn has been shown to suppress transformed phenotypes in some studies. Overexpression of pFn in human fibrosarcoma cells leads to suppression of tumor features such as a flattened morphology, reduced cell migration and reduced tumor growth (98). Similarly, inverse correlation has also been shown between Fn expression and metastatic potential. Comparison between non-metastatic prostate cancer cell subtype and metastatic subtype (99) and between moderate-metastatic and high-metastatic murine mammary adenocarcinoma subtypes (100) showed decreased Fn expression in non-metastatic or lower metastatic subtypes. Independent experiments that perturb Fn-integrin interactions also showed negatively correlation of Fn and metastasis. Injection of mice with RGD-containing peptides reduced experimental metastasis of murine melanoma cells (101). Intraperitoneal administration of super-Fn (induced multimeric form of fibronectin with enhanced adhesive properties) into mice reduced lung colonization in both experimental and spontaneous metastasis models of KRIB osteosarcoma, C8161 melanoma or HT-29 carcinoma cells (102). Studies using the MM3 murine mammary adenocarcinoma cell line showed inverse correlation between Fn expression and metastatic potential. The highly metastatic MM3 does not express Fn protein or mRNA while the parental M3 moderately expresses Fn and forms Fn ECM (103). Global gene expression comparison between the two cell lines revealed only two

genes significantly down regulated in MM3 , one of which is Fn, reduced by 19 fold (104). LMM3 tumor cells, derived from MM3 spontaneous lung metastasis, like its parent cell line also does not express Fn. Expression of wild type Fn and Fn lacking RGD, which does not form ECM fibrils, in LMM3 cells is shown to be sufficient to reduce the metastatic potential of cancer cells (105). These studies provide a model in which Fn has a negative impact on cancer metastasis.

However, many studies also strongly suggest a role of Fn in metastasis. Global gene profile revealed 3-fold expression of Fn in breast tumors (51), up to 28 fold in colorectal tumors (106), 2.83 fold in head and neck squamous cell carcinoma (107). Fn expression was positively correlated with lymph node involvement and mortality risk of breast cancer (108). In an experimental metastasis model studying B16-F10 murine melanoma cells, the synthetic peptide GRGDS, derived from Fn IIICS cell-binding domain, specifically inhibited the number of lung colonies and results show that the peptide may be interfering with multiple fibronectin-mediated events at different steps of the metastatic process (109). A peptide consisting of Fn central cell-binding domain and heparin-binding domain (CBD-HepII) was able to suppress lung metastasis of B16 melanoma (110) and hepatic metastasis of hepatocarcinoma (111). The importance of Fn-Tumor cell interactions in metastasis can be further supported by the studies that showed the abilities of anti-α5 and anti-β1 monoclonal antibodies to inhibit experimental metastasis in MDA-MB-231 cells. In spontaneous metastasis models, treatment of mice bearing mammary carcinoma transplants with anti-β1 polyclonal antibodies reduced the size of the metastatic colonies but not the number, possibly indicating inhibition of tumor cell interations with the surrounding extracellular matrix (95).

SITE SPECIFIC METASTASIS

In the process of hematogenous metastasis, cancer cells break away from the primary tumor, enter the blood stream, arrest at the vasculature of a secondary organ and either form colonies at the endothelium adhesion site (112) or extravasate to form tumor colonies completing the metastatic cascade (113) (Fig 1.4). Studies have followed labeled tumor cells through the course of hematogenous spread and found that cells initially arrest in the microvasculature of the first organ they encounter. At this site, most tumor cells die (114) and a few survive either to form colonies at that site or colonize another tumor specific metastatic organ (115). Metastasis was once believed to be a mechanistic phenomenon but evidence supports involvement of organ specific molecules in the specific recognition of tumor cells to secondary organs of colonization. This is known as the "seed-and-soil hypothesis (190).The fact that tumors have select specificity for certain organs during metastasis is supported by clinical assessment (116). For instance, prostatic carcinomas and small cell carcinomas of the lungs preferentially colonize bones and the brain, respectively, on the other hand, breast carcinomas most frequently metastasize to the lungs, but also to liver, bones, brain, and adrenals (79). Tracking of GFP tagged tumor cells found that the cells were mainly in pre-capillary arterioles, which had diameters larger than tumor cells, indicating that cells were not merely arrested by capillary trapping. The same study also found extravasation to be a rare event, with no intact cells surviving extravascularly for more than 48 hours, although occasional presence of invadopodia were noted intravascularly (112). Although the extravascular metastasis model is based on the fact that loss of cell contact leads to accelerated cell death in blood circulation, anchorage independent growth in suspension in tumor cells and facilitation of cell proliferation by endothelial attachment have been shown, which

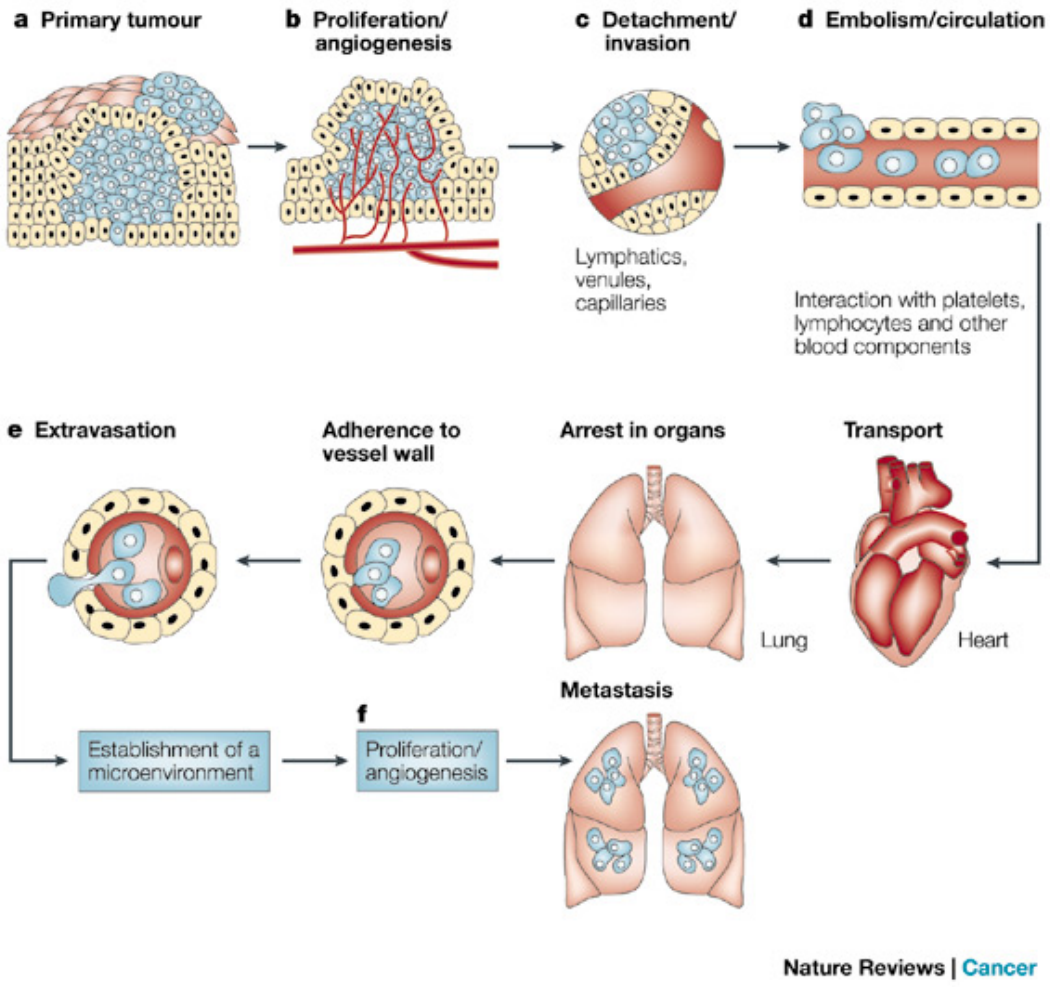

Fidler, I. J. (2003) Nat Rev Cancer 3(6), 453-458

Figure 1.4: The main steps in the formation of a metastasis. (190)

further supports the intravascular metastasis model (112). Opposing to the extravascular metastasis model, which tumor cells extravasate at the endothelial attachment site to form metastatic foci extravascularly, the intravascular metastasis model supports that metastatic colonies originate from intravascular cells, form micrometastases within the vasculature, and finally the colonies will outgrow the vessels and disrupt the vascular walls (112).

Vascular arrest of cancer cells mediated by "organotypic" molecules is responsible for the initial selection of an organ for metastasis (117-119). For example, the lung endothelial cell adhesion molecule-1 (Lu-ECAM-1; bCLCA2, bovine calcium activated chloride channel 2) characterized in this laboratory selectively binds lung-metastatic melanoma cells and its expression on the endothelia of pulmonary venules correlates with the formation of melanoma metastases at these sites (120). Monoclonal antibodies against Lu-ECAM-1 inhibit colonization of the lungs by lung-metastatic murine B16 melanoma cells but have no effect on lung colonization by other types of lung-metastatic cancer cells indicating a tumor cell specific adhesion molecule that mediates lung colonization (79,120). Colonization of the lungs by human breast cancer cells has been shown to be mediated by breast cancer β4 integrin and endothelial hCLCA2, the human counterpart of bCLCA2 (121). The CLCA family members comprise of one group of endothelial tumor homing receptors that facilitate vascular arrest of tumor cells.

Utilizing outside out luminal membrane vesicles, we also show that more vesicles isolated from rat lung microvascular endothelia binds to lung metastatic rat breast carcinoma cells compared to nonmetastatic counterparts (79,122,123). Vesicles isolated from nonmetastatized organ (e.g., hind leg muscle) showed no binding preference for lung-metastatic or nonmetastatic mammary carcinoma cells. Monoclonal antibodies against the lung-derived endothelial vesicles inhibit specific

adhesion of the vesicles to lung-metastatic breast cancer cells. The antibody recognizes a 110-kDa membrane glycoprotein which was found to be dipeptidyl peptidase IV (DPP IV; also known as CD26 or gp110) (123). Studies have previously identified association between cell surface expression of Fn and lung metastasis of rhabdomyosarcoma cells and the DPP IV ligand was identified as tumor cell surface-associated Fn **(**124). Fibronectin assembles on breast cancer cell surfaces into multiple, randomly dispersed globules from cellular and plasma Fn. The level of Fn surface expression correlates to the tumor cells' ability to bind to DPP IV and metastasize to the lungs. Soluble DPPIV blocks DPPIV/Fn mediated adhesion and metastasis while anti-DPPIV and anti-Fn mAb blocks adhesion. Adhesion is unaffected by soluble plasma FN (pFn) and indicates the ability of cancer cells to arrest through this mechanism under high plasma Fn conditions in the blood stream. The ability of many cancer cells to capture Fn molecules on their surface and to augment such deposits by Fn self-association during passage in the blood suggests that DPP IV/Fn binding may be a relatively common mechanism for lung metastasis (79). The CLCA/β4 interaction and the DPPIV/Fn interaction demonstrate the importance of vascular addresses in the adhesion step in metastasis.

POLYMERIC FIBRONECTIN ON SUSPENDED BREAST CANCER CELLS MEDIATES LUNG METASTASIS

The molecular foundation of the original immobilization of Fn on the surface of breast cancer cells is poorly understood. It seems that rat breast cancer cells growing as a solid tumor mass in syngeneic animals support the synthesis of a Fn-containing matrix (116). After tumor cells escape the primary tumor, they become blood-borne and travel passively with the blood stream to other organ sites (113,119).

In the pFn-rich environment of the plasma, tumor cells decorated with a light coat of cellular Fn use this Fn scaffold to attain pFn molecules for the buildup of a prominent Fn coat that is visualized as multiple, densely distributed Fn globules by immunocytochemistry. This suggests that the initial Fn binding to the cell surface occurs around focal adhesion points from which polymerization is then initiated by Fn self-association (125-128). Such adhesion points are anticipated to be sites of integrin clusterings, most likely the classic Fn receptor α5β1 (67,129,130). An alternative mechanism may be that a cellular Fn-α5β1 complex forms intracytoplasmically (e.g. in Golgi vesicles) and serves as a scaffold for build up upon transport to and incorporation into the plasma membrane (79).

The Fn buildup on cancer cell surfaces is comparable with that reported first for normal confluent, adherent cell layers of fibroblasts (56). A 4 hour incubation of lung-metastatic breast cancer cells with 125I-pFn results in cell surface-associated Fn that can be harvested as DOC-soluble and DOC-insoluble fractions. The multimeric Fn on breast cancer cells and normal hepatocytes, both grown in suspension, progressively converted to nonreducible, seemingly covalently bonded Fn complexes (131) not observed on anchorage-dependent normal fibroblasts (56). This conversion is possibly mediated by a cancer cell-associated transglutaminase activity, similar to hepatocytes (131). The similarities between the Fn assembly in suspended, blood-borne breast cancer cells and adherent fibroblasts suggest that commons receptors and signaling molecules might be shared between the two pathways.

SIGNALING EVENTS IN FIBRONECTIN ASSEMBLY

Fibronectin matrix assembly involves regulated intracellular signaling events that include binding to integrins, organization of the actin cytoskeleton and stimulation

of cell contractility and activation of kinase cascades (132) (Fig 1.5). A number of studies have established that binding of Fn by specific integrins is critical in initiating Fn matrix assembly. Fn fragments that contain the RGD integrin binding site or antibodies recognizing the integrin binding site inhibited Fn matrix assembly in cultured cells and developing amphibian embryos (133-138). Also, antibodies to α5β1 integrin decreased the deposition of Fn into extracellular matrix by fibroblasts (72,133,139,140). The role of Fn-binding integrins in Fn matrix assembly has been extensively studied in Chinese hamster ovary (CHO) cells. Overexpression of α5β1 in CHO cells increased Fn deposition in extracellular matrix (141) while CHO B2 cells deficient in α5 did not assemble plasma Fn into the extracellular matrix (67). Transfecting the CHO B2 cells with a full-length α5 chain completely restored fibrillar Fn matrix assembly (67). These studies determined an important role of α5β1 integrin in supporting Fn matrix assembly by CHO cells. On the other hand, cells are also able to support Fn matrix assembly through other integrins. One example of such is fibroblastic cells derived from α5 integrin null mutant embryos being able to assemble a Fn matrix in the absence of α5β1 (142). The primary role of α5β1 integrin in Fn matrix assembly seems to involve the initiation step of Fn matrix assembly, since Fn mutants lacking the α5β1 integrin binding site could not be assembled into Fn matrix if not in the presence of native Fn (74,143).

Integrin links extracellular matrix (ECM) to cytoplasmic molecules mediating initiation of intracellular pathways that control cellular function. One cytoplasmic signaling molecule that is phosphorylated in response to integrin binding to ECM is FAK. FAK controls cell adhesion and spreading, migration, cell survival and proliferation. FAK directly interacts with downstream molecules such as Src, phosphatidylinositol 3-kinase (PI3-kinase) and Grb7 and these molecules have been implicated in regulation of early Fn fibrillogenesis (5,144-146). Cells lacking Src

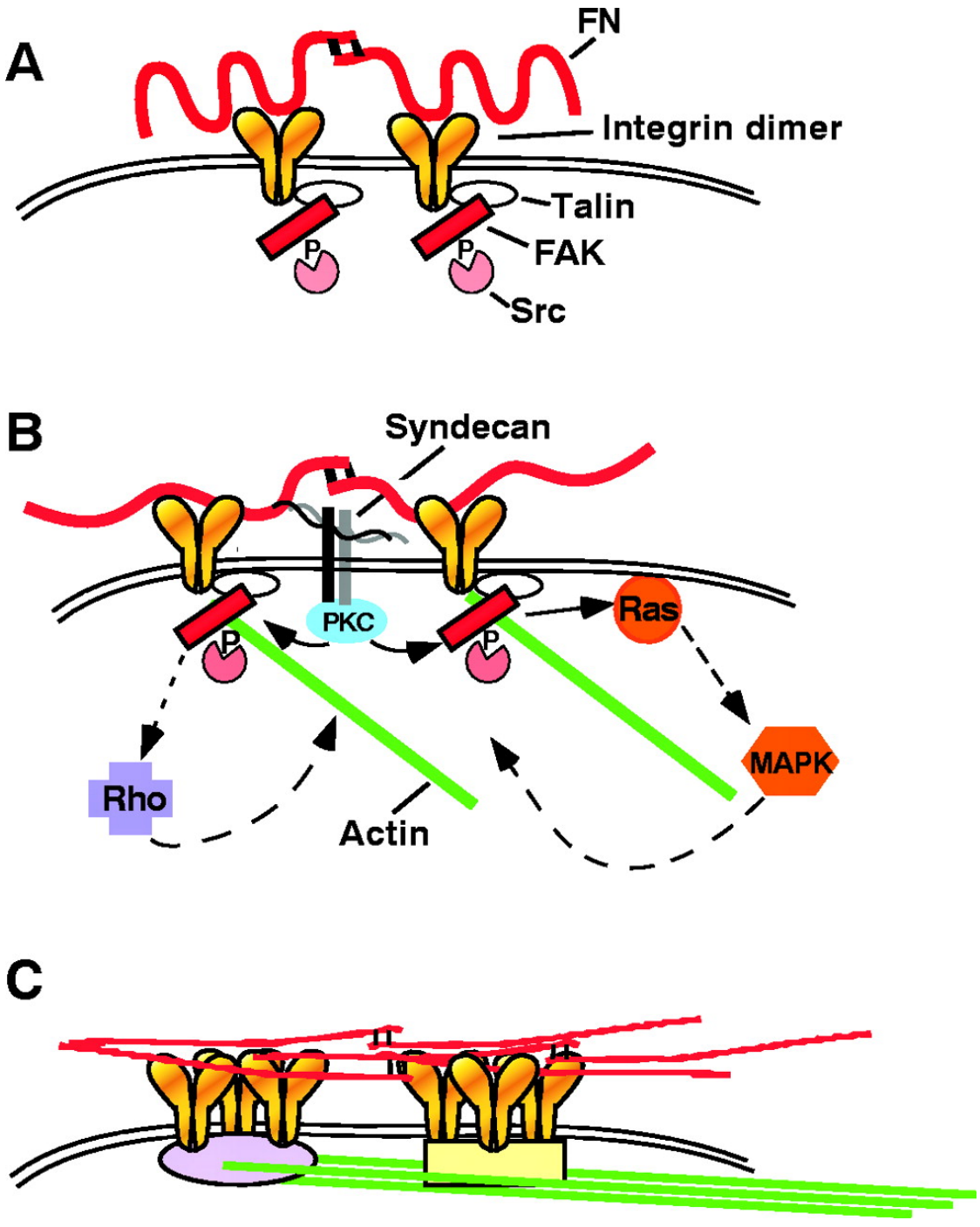

Mao, Y. *et al.* (2005) Matrix Biol 24(6), 389-399

Figure 1.5: Model of Fn matrix assembly. (57)

family kinases, cells treated with Src and PI3-kinase inhibitors, and FAK-null cells and cells with increased Src expression and activity are all associated with a decrease in fibronectin assembly (8,147). These proteins are regulated by phosphorylation on specific tyrosine residues and phosphorylation events may vary depending on the cell type (5).

Integrin ligation can also trigger activation of certain MAP kinases, including extracellular signal-regulated kinase (ERK) 1 members and JNK (JUN kinase) (148-151). Different types of MAP kinases have distinct pathways and functions. ERK activation have been linked to EGF growth factor response pathways, while JNK is not activated by EGF in most cells but is activated by inflammatory cytokines or stress response such as UV irradiation (151,152-154). One study using inhibitors found that herbimycin A and genistein blocked the activation of both types of MAP kinases induced by cell binding to FN coated beads, while Cytochalasin D inhibited the ERK pathway and have no effect on SAPK/JNK1 pathway. The study showed that integrins can mediate activation of two distinct serine/threonine kinase pathways with different kinetics and different responses to disruption of the actin cytoskeleton (154).

A subset of cytoskeletal proteins including tensin, α-actinin, talin and vinculin does not seem to require tyrosine phosphorylation to accumulate locally after integrin ligation (154,155). In contrast, another set of cytoskeletal proteins including paxillin and F-actin, and a group of signaling proteins such as Ras, phospholipase Cγ and ERK require tyrosine phosphorylation for accumulation (155). Cytoskeletal responses to integrin ligation can be studied using beads coated with molecules that interact with integrins. Fibronectin-coated beads induced the local accumulation of a variety of cytoskeletal molecules, including vinculin, talin, α-actinin, and F-actin (154,156-159). This further underlies the importance of cytoskeletal participation in the process of fibronectin matrix assembly.

Oncogenes can also affect fibronectin assembly through regulation of integrin function and localization. Ras proteins, which are small GTPases, link cell surface receptors to intracellular effector pathways regulating cell proliferation, differentiation, and survival (155). Ras proteins exert cell functions through the activation of several downstream effectors, including Raf, Rac, phosphatidylinositol 3-kinase (PI3K), and Ral (160). Through Raf, Ras activates MAPK/ERK kinase (MEK), which then phosphorylates ERKs (161-163). Activation of Raf-1 impedes the ability of α5ß1 integrin to mediate Fn matrix assembly (165). The suppression is similar to what occurs in v-src-transformed cells and correlates with activation of ERK. HT1080 human fibrosarcoma cells possess one activated N-ras allele and can be stimulated to assemble Fn matrix by activation of integrins using Mn2+ or ß1 integrin-activating antibody or by inhibition of Ras signaling through ERK (165). In summary, mutation of at least two oncogenes, ras and src, have negative effects on Fn matrix assembly and, in some cells, exert their effects through a common downstream effector, ERK.

Integrin ligand binding affinity can also be regulated via inside-out signaling, in which intracellular components are able to control extracellular matrix assembly by modulation of ligand preference through interaction with the cytoplasmic tail of integrins. (133,166-170). Constitutively active R-Ras expressed in CHO cells with αIIb3 integrin activated the integrin and caused an increase in Fn matrix assembly (171), whereas activation of Raf-1, probably via the MAPK pathway, suppresses integrin activation and Fn matrix assembly (164). One report shows that overexpression of ILK in epithelial cells dramatically stimulated integrin-mediated Fn matrix assembly (133). ILK, a serine/threonine kinase, binds to the cytoplasmic domains of both β1 and β3 integrins and phosphorylates the β1 cytoplasmic domain in vitro (172). These studies show that cells control integrin activity and Fn matrix

assembly via interactions of cytoplasmic regulatory proteins with integrin cytoplasmic domains (133).

However, integrins do not act alone in transmembrane signaling in Fn matrix assembly (132). Cells with impaired proteoglycan synthesis showed defective Fn matrix assembly, and this has been attributed to reduced activity of syndecans, transmembrane proteoglycans that can bind Fn (173, 174). The major syndecan in fibroblasts, syndecan-2, has been shown to have an indirect regulatory effect on matrix assembly through truncation studies. A truncated version of syndecan-2 lacking a part of its cytoplasmic tail blocks Fn assembly in a dominant negative way. On the other hand, syndecan-2 without its entire cytoplasmic tail had no effect on matrix formation (175). Another syndecan, syndecan-4, has a more direct effect on Fn assembly. Syndecan-4 cooperates with integrins in regulation of Rho-dependent cell adhesion, spreading and actin organization (176). Concomitant ligation of $\alpha_5\beta_1$ integrin and syndecan-4 increases active Rho(177) and phosphorylated FAK and Rho and FAK, when both stimulated, have been shown to favor Fn matrix assembly (178).

Another important signaling molecule that has been implicated in fibronectin assembly is PKC. (179-182). PKC activation has been shown to increase Fn synthesis and fibrillogenesis in a number of cell types, cinluding pulmonary fibroblasts, retinal pigment epithelial cells, vascular smooth muscle cells, osteoblasts, hyperglycemic mesangial cells and Xenopus cells (132, 182, 183-187). Activation of PKC increases I^{125}-labeled Fn binding to the cell surface while inhibition of PKC resulted in a rapid decrease in Fn binding (179). The PKC activator TPA increases extracellular assembly of Fn fibril while the PKC inhibitor forskolin decreased assembly. Moreover, TPA increased α_5 integrin clustering and surface expression while PKC inhibitors inhibited clustering; implicating that PKC regulates the dynamic assembly of Fn through modulation of integrin distribution (180,181). PKC also binds to the cytoplasmic tail

of clustered syndecan-4 (188-189) and may act on Fn assembly through syndecan-4. The strong connection of PKC with integrins and syndecan could potentially be the pathway regulating cell surface polyFn assembly in blood-borne cancer cells.

SUMMARY AND GOALS OF THIS STUDY

In summary, gene expression profiling of breast cancer of different stages and metastatic preference shows that fibronectin is upregulated in breast cancer. Fibronectin interacts with integrins, matrix components and itself during matrix assembly through its integrin interaction sites, collagen, heparin or fibrin binding sites, and self association sites, respectively. Cellular fibronectin has distinct domains from plasma fibronectin and may play a different role in fibronectin assembly. Cells are also able to interact with fibronectin and transduce inside-out or outside-in signals through different integrin receptors. Fibronectin also interacts with DPPIV. In breast cancer cells, multimeric fibronectin (polyFn) assembled on the surface of the cells interact with DPPIV on lung endothelial cells facilitating lung vascular arrest and promotes lung metastasis. The level of polyFn surface expression correlates with cancer cells' ability to metastasize to lungs. The intracellular mediator of the process of polyFn assembly has not been identified, and a further investigation into the regulatory mechanism of fibronectin assembly on the surface of these breast cancer cells might bring forward new insights and novel strategies into the potential targets available for anti-metastatic therapy in breast cancer patients. The goal of this study is to examine the related pathways previously known to be associated in signaling pathways of adherent cell fibronectin matrix assembly in order to discover the molecule(s) regulating polyFn assembly and breast cancer cell lung metastasis.

REFERENCES

1. Pankov, R., and Yamada, K. M. (2002) J Cell Sci 115(Pt 20), 3861-3863

2. Magnusson, M. K., and Mosher, D. F. (1998) Arterioscler Thromb Vasc Biol 18(9), 1363-1370

3. Aguirre, K. M., McCormick, R. J., and Schwarzbauer, J. E. (1994) J Biol Chem 269(45), 27863-27868

4. White, E. S., Baralle, F. E., and Muro, A. F. (2008) J Pathol 216(1), 1-14

5. Geiger, B., Bershadsky, A., Pankov, R., and Yamada, K. M. (2001) Nat Rev Mol Cell Biol 2(11), 793-805

6. Vakonakis, I., Staunton, D., Rooney, L. M., and Campbell, I. D. (2007) Embo J 26(10), 2575-2583

7. Sun, L., Zou, Z., Collodi, P., Xu, F., Xu, X., and Zhao, Q. (2005) Matrix Biol 24(1), 69-77

8. Hynes RO. *Fibronectins* (1st edn). Springer-Verlag: New York, 1990.

9. Ffrench-Constant, C. (1995) Exp Cell Res 221(2), 261-271

10. Borsi, L., Balza, E., Allemanni, G., and Zardi, L. (1992) Exp Cell Res 199(1), 98-105

11. Pagani, F., Zagato, L., Vergani, C., Casari, G., Sidoli, A., and Baralle, F. E. (1991) J Cell Biol 113(5), 1223-1229

12. Chauhan, A. K., Iaconcig, A., Baralle, F. E., and Muro, A. F. (2004) Gene 324, 55-63

13. Ffrench-Constant, C., Van de Water, L., Dvorak, H. F., and Hynes, R. O. (1989) J Cell Biol 109(2), 903-914

14. Mathews, G. A., and Ffrench-Constant, C. (1995) J Neurobiol 26(2), 171-188

15. Przybysz, M., Borysewicz, K., and Katnik-Prastowska, I. (2009) Rheumatol Int

16. Xia, P., and Culp, L. A. (1995) Exp Cell Res 217(2), 517-527

17. Meyer-Ter-Vehn, T., Grehn, F., and Schlunck, G. (2008). Mol Vis 14, 136-41.

18. Wang, A., Cohen, D. S., Palmer, E., and Sheppard, D. (1991) J Biol Chem 266(24), 15598-15601

19. Muro, A. F., Moretti, F. A., Moore, B. B., Yan, M., Atrasz, R. G., Wilke, C. A., Flaherty, K. R., Martinez, F. J., Tsui, J. L., Sheppard, D., Baralle, F. E., Toews, G. B., and White, E. S. (2008) Am J Respir Crit Care Med 177(6), 638-645

20. Guan, J. L., Trevithick, J. E., and Hynes, R. O. (1990) J Cell Biol 110(3), 833-847

21. Fukuda, T., Yoshida, N., Kataoka, Y., Manabe, R., Mizuno-Horikawa, Y., Sato, M., Kuriyama, K., Yasui, N., and Sekiguchi, K. (2002) Cancer Res 62(19), 5603-5610

22. Astrof, S., Crowley, D., George, E. L., Fukuda, T., Sekiguchi, K., Hanahan, D., and Hynes, R. O. (2004) Mol Cell Biol 24(19), 8662-8670

23. Matuskova, J., Chauhan, A. K., Cambien, B., Astrof, S., Dole, V. S., Piffath, C. L., Hynes, R. O., and Wagner, D. D. (2006) Arterioscler Thromb Vasc Biol 26(6), 1391-1396

24. Khan, Z. A., Chan, B. M., Uniyal, S., Barbin, Y. P., Farhangkhoee, H., Chen, S., and Chakrabarti, S. (2005) Angiogenesis 8, 183-96.

25. George, B., Chen, S., Chaudhary, V., Gonder, J., and Chakrabarti, S. (2009) Curr Eye Res 34(2), 134-144

26. Sauer, S., Erba, P. A., Petrini, M., Menrad, A., Giovannoni, L., Grana, C., Hirsch, B., Zardi, L., Paganelli, G., Mariani, G., Neri, D., Durkop, H., and Menssen, H. D. (2009) Blood 113(10), 2265-2274

27. Kapila, Y. L., Niu, J., and Johnson, P. W. (1997) J Biol Chem 272(30), 18932-18938

28. Oyama, F., Hirohashi, S., Sakamoto, M., Titani, K., and Sekiguchi, K. (1993) Cancer Res 53(9), 2005-2011

29. Dufour, S., Duband, J. L., Humphries, M. J., Obara, M., Yamada, K. M., and Thiery, J. P. (1988) Embo J 7(9), 2661-2671

30. Bergijk, E. C., Baelde, H. J., Kootstra, C. J., De Heer, E., Killen, P. D., and Bruijn, J. A. (1996) J Pathol 178(4), 462-468

31. Kapila, Y. L., Wang, S., Dazin, P., Tafolla, E., and Mass, M. J. (2002) J Biol Chem 277(10), 8482-8491

32. Wilson, C. L., and Schwarzbauer, J. E. (1992) J Cell Biol 119(4), 923-933

33. George, E. L., Georges-Labouesse, E. N., Patel-King, R. S., Rayburn, H., and Hynes, R. O. (1993) Development 119(4), 1079-1091

34. George, E. L., Baldwin, H. S., and Hynes, R. O. (1997) Blood 90(8), 3073-3081

35. Astrof, S., Kirby, A., Lindblad-Toh, K., Daly, M., and Hynes, R. O. (2007) Mech Dev 124(7-8), 551-558

36. Georges-Labouesse, E. N., George, E. L., Rayburn, H., and Hynes, R. O. (1996) Dev Dyn 207(2), 145-156

37. Sakai, T., Johnson, K. J., Murozono, M., Sakai, K., Magnuson, M. A., Wieloch, T., Cronberg, T., Isshiki, A., Erickson, H. P., and Fassler, R. (2001) Nat Med 7(3), 324-330

38. Ni, H., Yuen, P. S., Papalia, J. M., Trevithick, J. E., Sakai, T., Fassler, R., Hynes, R. O., and Wagner, D. D. (2003) Proc Natl Acad Sci U S A 100(5), 2415-2419

39. Yi, M., Sakai, T., Fassler, R., and Ruoslahti, E. (2003) Proc Natl Acad Sci U S A 100(20), 11435-11438

40. Nyberg, P., Sakai, T., Cho, K. H., Caparon, M. G., Fassler, R., and Bjorck, L. (2004) Embo J 23(10), 2166-2174

41. Tan, M. H., Sun, Z., Opitz, S. L., Schmidt, T. E., Peters, J. H., and George, E. L. (2004) Blood 104(1), 11-18

42. Muro, A. F., Chauhan, A. K., Gajovic, S., Iaconcig, A., Porro, F., Stanta, G., and Baralle, F. E. (2003) J Cell Biol 162(1), 149-160

43. Chauhan, A. K., Kisucka, J., Cozzi, M. R., Walsh, M. T., Moretti, F. A., Battiston, M., Mazzucato, M., De Marco, L., Baralle, F. E., Wagner, D. D., and Muro, A. F. (2008) Arterioscler Thromb Vasc Biol 28(2), 296-301

44. Chauhan, A. K., Moretti, F. A., Iaconcig, A., Baralle, F. E., and Muro, A. F. (2005) Behav Brain Res 161(1), 31-38

45. Takahashi, S., Leiss, M., Moser, M., Ohashi, T., Kitao, T., Heckmann, D., Pfeifer, A., Kessler, H., Takagi, J., Erickson, H. P., and Fassler, R. (2007) J Cell Biol 178(1), 167-178

46. Moretti, F. A., Chauhan, A. K., Iaconcig, A., Porro, F., Baralle, F. E., and Muro, A. F. (2007) J Biol Chem 282(38), 28057-28062

47. Luiz Carlos Uchoa Junqueira, Jose Carneiro, Robert O. Kelley. Basic Histology. Appleton & Lange; 8th edition (July 1, 1996)

48. Haslam, S. Z., and Woodward, T. L. (2003) Breast Cancer Res 5(4), 208-215

49. Williams, C. M., Engler, A. J., Slone, R. D., Galante, L. L., and Schwarzbauer, J. E. (2008) Cancer Res 68(9), 3185-3192

50. Schedin, P., Strange, R., Mitrenga, T., Wolfe, P., and Kaeck, M. (2000) J Cell Sci 113 (Pt 5), 795-806

51. Jiang, Y., Harlocker, S. L., Molesh, D. A., Dillon, D. C., Stolk, J. A., Houghton, R. L., Repasky, E. A., Badaro, R., Reed, S. G., and Xu, J. (2002) Oncogene 21(14), 2270-2282

52. Zucchi, I., Mento, E., Kuznetsov, V. A., Scotti, M., Valsecchi, V., Simionati, B., Vicinanza, E., Valle, G., Pilotti, S., Reinbold, R., Vezzoni, P., Albertini, A., and Dulbecco, R. (2004) Proc Natl Acad Sci U S A 101(52), 18147-18152

53. Amatschek, S., Koenig, U., Auer, H., Steinlein, P., Pacher, M., Gruenfelder, A., Dekan, G., Vogl, S., Kubista, E., Heider, K. H., Stratowa, C., Schreiber, M., and Sommergruber, W. (2004) Cancer Res 64(3), 844-856

54. Bandyopadhyay, A., Elkahloun, A., Baysa, S. J., Wang, L., and Sun, L. Z. (2005) Cancer Biol Ther 4(2), 168-174

55. McDaniel, S. M., Rumer, K. K., Biroc, S. L., Metz, R. P., Singh, M., Porter, W., and Schedin, P. (2006) Am J Pathol 168(2), 608-620

56. McKeown-Longo, P. J., and Mosher, D. F. (1983) J Cell Biol 97(2), 466-472

57. Mao, Y., and Schwarzbauer, J. E. (2005) Matrix Biol 24(6), 389-399

58. Pytela, R., Pierschbacher, M. D., and Ruoslahti, E. (1985) Proc Natl Acad Sci U S A 82(17), 5766-5770

59. Hay, E.D. (1991) *Cell Biology of the Extracellular Matrix*. 2nd Ed, Springer, 340-351.

60. Akiyama, S. K. (1996) Hum Cell 9(3), 181-186

61. Jia, Y., Zeng, Z. Z., Markwart, S. M., Rockwood, K. F., Ignatoski, K. M., Ethier, S. P., and Livant, D. L. (2004) Cancer Res 64(23), 8674-8681

62. Johansson, S. (1985) J Biol Chem 260(3), 1557-1561

63. Wayner, E. A., Garcia-Pardo, A., Humphries, M. J., McDonald, J. A., and Carter, W. G. (1989) J Cell Biol 109(3), 1321-1330

64. Guan, J. L., and Hynes, R. O. (1990) Cell 60(1), 53-61

65. Mould, A. P., Wheldon, L. A., Komoriya, A., Wayner, E. A., Yamada, K. M., and Humphries, M. J. (1990) J Biol Chem 265(7), 4020-4024

66. Komoriya, A., Green, L. J., Mervic, M., Yamada, S. S., Yamada, K. M., and Humphries, M. J. (1991) J Biol Chem 266(23), 15075-15079

67. Wu, C., Bauer, J. S., Juliano, R. L., and McDonald, J. A. (1993) J Biol Chem 268(29), 21883-21888

68. Wu, C., Fields, A. J., Kapteijn, B. A., and McDonald, J. A. (1995) J Cell Sci 108 (Pt 2), 821-829

69. Mosher, D.F. (1989) Fibronectin. San Diego: Academic Press, Inc.

70. Yamada, K. M. and Clark, R. A. F. (1996). Provisional matrix. In The Molecular and Cellular Biology of Wound Repair (ed. R. A. F. Clark), pp. 51-93. New York: Plenum Press.

71. Mostafavi-Pour, Z., Askari, J. A., Whittard, J. D., and Humphries, M. J. (2001) Matrix Biol 20(1), 63-73

72. Mosher, D. F. (1993) Curr. Opin. Struct. Biol. **3,** 214-222

73. Akiyama, S. K., Yamada, S. S., Chen, W. T., and Yamada, K. M. (1989) J Cell Biol 109(2), 863-875

74. Schwarzbauer, J. E. (1991) J Cell Biol 113(6), 1463-1473

75. Fleischer, B. (1994) Immunol Today 15(4), 180-184

76. Gorrell, M. D., Gysbers, V., and McCaughan, G. W. (2001) Scand J Immunol 54(3), 249-264

77. Havre, P. A., Abe, M., Urasaki, Y., Ohnuma, K., Morimoto, C., and Dang, N. H. (2008) Front Biosci 13, 1634-1645

78. Piazza, G. A., Callanan, H. M., Mowery, J., and Hixson, D. C. (1989) Biochem J 262(1), 327-334

79. Cheng, H. C., Abdel-Ghany, M., Elble, R. C., and Pauli, B. U. (1998) J Biol Chem 273(37), 24207-24215

80. Cheng, H. C., Abdel-Ghany, M., and Pauli, B. U. (2003) J Biol Chem 278(27), 24600-24607

81. Boyer, B., Valles, A. M., and Edme, N. (2000) Biochem Pharmacol 60(8), 1091-1099

82. Savagner, P. (2001) Bioessays 23(10), 912-923

83. Perez-Pomares, J. M., and Munoz-Chapuli, R. (2002) Anat Rec 268(3), 343-351

84. Petersen, O. W., Nielsen, H. L., Gudjonsson, T., Villadsen, R., Rank, F., Niebuhr, E., Bissell, M. J., and Ronnov-Jessen, L. (2003) Am J Pathol 162(2), 391-402

85. Vincent-Salomon, A., and Thiery, J. P. (2003) Breast Cancer Res 5(2), 101-106

86. Blanco, M. J., Moreno-Bueno, G., Sarrio, D., Locascio, A., Cano, A., Palacios, J., and Nieto, M. A. (2002) Oncogene 21(20), 3241-3246

87. Yang, J., Mani, S. A., Donaher, J. L., Ramaswamy, S., Itzykson, R. A., Come, C., Savagner, P., Gitelman, I., Richardson, A., and Weinberg, R. A. (2004) Cell 117(7), 927-939

88. Strizzi, L., Bianco, C., Normanno, N., Seno, M., Wechselberger, C., Wallace-Jones, B., Khan, N. I., Hirota, M., Sun, Y., Sanicola, M., and Salomon, D. S. (2004) J Cell Physiol 201(2), 266-276

89. Lee, M. Y., Chou, C. Y., Tang, M. J., and Shen, M. R. (2008) Clin Cancer Res 14(15), 4743-4750

90. Maschler, S., Wirl, G., Spring, H., Bredow, D. V., Sordat, I., Beug, H., and Reichmann, E. (2005) Oncogene 24(12), 2032-2041

91. Trimboli, A. J., Fukino, K., de Bruin, A., Wei, G., Shen, L., Tanner, S. M., Creasap, N., Rosol, T. J., Robinson, M. L., Eng, C., Ostrowski, M. C., and Leone, G. (2008) Cancer Res 68(3), 937-945

92. Armstrong, P. B., and Armstrong, M. T. (2000) Biochim Biophys Acta 1470(2), O9-20

93. Mason, C. A., Bigras, J. L., O'Blenes, S. B., Zhou, B., McIntyre, B., Nakamura, N., Kaneda, Y., and Rabinovitch, M. (1999) Nat Med 5(2), 176-182

94. Yamada, K. M., Kennedy, D. W., Yamada, S. S., Gralnick, H., Chen, W. T., and Akiyama, S. K. (1990) Cancer Res 50(15), 4485-4496

95. Akiyama, S. K., Olden, K., and Yamada, K. M. (1995) Cancer Metastasis Rev 14(3), 173-189

96. White, E. S., Thannickal, V. J., Carskadon, S. L., Dickie, E. G., Livant, D. L., Markwart, S., Toews, G. B., and Arenberg, D. A. (2003) Am J Respir Crit Care Med 168(4), 436-442

97. Qian, F., Vaux, D. L., and Weissman, I. L. (1994) Cell 77(3), 335-347

98. Akamatsu, H., Ichihara-Tanaka, K., Ozono, K., Kamiike, W., Matsuda, H., and Sekiguchi, K. (1996) Cancer Res 56(19), 4541-4546

99. Schalken, J. A., Ebeling, S. B., Isaacs, J. T., Treiger, B., Bussemakers, M. J., de Jong, M. E., and Van de Ven, W. J. (1988) Cancer Res 48(8), 2042-2046

100. Muro, A., Puricelli, L., Kornblihtt, A. R., and Bal de Kier Joffe, E. (1991) Invasion Metastasis 11(5), 281-287

101. Humphries, M. J., Olden, K., and Yamada, K. M. (1986) Science 233(4762), 467-470

102. Pasqualini, R., Bourdoulous, S., Koivunen, E., Woods, V. L., Jr., and Ruoslahti, E. (1996) Nat Med 2(11), 1197-1203

103. Werbajh, S. E., Urtreger, A. J., Puricelli, L. I., de Lustig, E. S., Bal de Kier Joffe, E., and Kornblihtt, A. R. (1998) FEBS Lett 440(3), 277-281

104. Urtreger, A. J., Werbajh, S. E., Verrecchia, F., Mauviel, A., Puricelli, L. I., Kornblihtt, A. R., and Bal de Kier Joffe, E. D. (2006) Oncol Rep 16(6), 1403-1410

105. Urtreger, A., Porro, F., Puricelli, L., Werbajh, S., Baralle, F. E., Bal de Kier Joffe, E., Kornblihtt, A. R., and Muro, A. F. (1998) Int J Cancer 78(2), 233-241

106. Zhang, L., Zhou, W., Velculescu, V. E., Kern, S. E., Hruban, R. H., Hamilton, S. R., Vogelstein, B., and Kinzler, K. W. (1997) Science 276(5316), 1268-1272

107. Al Moustafa, A. E., Alaoui-Jamali, M. A., Batist, G., Hernandez-Perez, M., Serruya, C., Alpert, L., Black, M. J., Sladek, R., and Foulkes, W. D. (2002) Oncogene 21(17), 2634-2640

108. Ioachim, E., Charchanti, A., Briasoulis, E., Karavasilis, V., Tsanou, H., Arvanitis, D. L., Agnantis, N. J., and Pavlidis, N. (2002) Eur J Cancer 38(18), 2362-2370

109. Humphries, M. J., Yasuda, Y., Olden, K., and Yamada, K. M. (1988) Ciba Found Symp 141, 75-93

110. Gong, W., Liu, Y., Huang, B., Lei, Z., Wu, F. H., Li, D., Feng, Z. H., and Zhang, G. M. (2008) Biochem Biophys Res Commun 367(1), 144-149

111. Liu, Y., Huang, B., Yuan, Y., Gong, W., Xiao, H., Li, D., Yu, Z. R., Wu, F. H., Zhang, G. M., and Feng, Z. H. (2007) Int J Cancer 121(1), 184-192

112. Al-Mehdi, A. B., Tozawa, K., Fisher, A. B., Shientag, L., Lee, A., and Muschel, R. J. (2000) Nat Med 6(1), 100-102

113. Fidler, I. J. (1997) in Cancer: Principles and Practice of Oncology (DeVita, V. T., Hellman, S., and Rosenbvery, S. A., eds), 5th Ed., pp. 135-152, Lipincott-Raven Publishers, Philadelphia

114. Weiss, L., and Dimitrov, D. S. (1986) J Theor Biol 121(3), 307-321

115. Yeatman, T. J., and Nicolson, G. L. (1993) Semin Surg Oncol 9(3), 256-263

116. Sugarbaker, E. V. (1981) Cancer Biol. Rev. **2**, 235-278

117. Albelda, S. M. (1993) Lab Invest 68(1), 4-17

118. Lafrenie, R. M., Buchanan, M. R., and Orr, F. W. (1993) Cell Biophys 23(1-3), 3-89

119. Pauli, B. U., and Lin, H. (1997) in Encyclopedia of Cancer (Bertino, J. R., ed), Vol. 1, pp. 464-476, Academic Press, New York

120. Zhu, D., Cheng, C. F., and Pauli, B. U. (1992) J Clin Invest 89(6), 1718-1724

121. Abdel-Ghany, M., Cheng, H. C., Elble, R. C., and Pauli, B. U. (2001) J Biol Chem 276(27), 25438-25446

122. Johnson, R. C., Augustin-Voss, H. G., Zhu, D. Z., and Pauli, B. U. (1991) Cancer Res 51(1), 394-399

123. Johnson, R. C., Zhu, D., Augustin-Voss, H. G., and Pauli, B. U. (1993) J Cell Biol 121(6), 1423-1432

124. Korach, S., Poupon, M. F., Du Villard, J. A., and Becker, M. (1986) Cancer Res 46(7), 3624-3629

125. Hocking, D. C., Smith, R. K., and McKeown-Longo, P. J. (1996) J Cell Biol 133(2), 431-444

126. Chernousov, M. A., Fogerty, F. J., Koteliansky, V. E., and Mosher, D. F. (1991) J Biol Chem 266(17), 10851-10858

127. Morla, A., and Ruoslahti, E. (1992) J Cell Biol 118(2), 421-429

128. Sakai, K., Fujii, T., and Hayashi, T. (1996) J Biochem 119(1), 58-62

129. Hynes, R. O. (1987) Cell 48(4), 549-554

130. Pierschbacher, M. D., and Ruoslahti, E. (1984) Nature 309(5963), 30-33

131. Fellin, F. M., Barsigian, C., Rich, E., and Martinez, J. (1988) J Biol Chem 263(4), 1791-1797

132. Wierzbicka-Patynowski, I., and Schwarzbauer, J. E. (2003) J Cell Sci 116(Pt 16), 3269-3276

133. Wu, C., Keightley, S. Y., Leung-Hagesteijn, C., Radeva, G., Coppolino, M., Goicoechea, S., McDonald, J. A., and Dedhar, S. (1998) J Biol Chem 273(1), 528-536

134. Wu, C., Keivens, V. M., O'Toole, T. E., McDonald, J. A., and Ginsberg, M. H. (1995) Cell 83(5), 715-724

135. Darribere, T., Koteliansky, V. E., Chernousov, M. A., Akiyama, S. K., Yamada, K. M., Thiery, J. P., and Boucaut, J. C. (1992) Dev Dyn 194(1), 63-70

136. Darribere, T., Guida, K., Larjava, H., Johnson, K. E., Yamada, K. M., Thiery, J. P., and Boucaut, J. C. (1990) J Cell Biol 110(5), 1813-1823

137. McDonald, J. A., Quade, B. J., Broekelmann, T. J., LaChance, R., Forsman, K., Hasegawa, E., and Akiyama, S. (1987) J Biol Chem 262(7), 2957-2967

138. Wu, C., Hughes, P. E., Ginsberg, M. H., and McDonald, J. A. (1996) Cell Adhes Commun 4(3), 149-158

139. Fogerty, F. J., Akiyama, S. K., Yamada, K. M., and Mosher, D. F. (1990) J Cell Biol 111(2), 699-708

140. Roman, J., LaChance, R. M., Broekelmann, T. J., Kennedy, C. J., Wayner, E. A., Carter, W. G., and McDonald, J. A. (1989) J Cell Biol 108(6), 2529-2543

141. Giancotti, F. G., and Ruoslahti, E. (1990) Cell 60(5), 849-859

142. Yang, J. T., Rayburn, H., and Hynes, R. O. (1993) Development 119(4), 1093-1105

143. Sechler, J. L., Takada, Y., and Schwarzbauer, J. E. (1996) J Cell Biol 134(2), 573-583

144. Schlaepfer, D. D., Hauck, C. R., and Sieg, D. J. (1999) Prog Biophys Mol Biol 71(3-4), 435-478

145. Zhao, J. H., and Guan, J. L. (2000) Prog Mol Subcell Biol 25, 37-55

146. Sechler, J. L., and Schwarzbauer, J. E. (1998) J Biol Chem 273(40), 25533-25536

147. Olden, K., and Yamada, K. M. (1977) Cell 11(4), 957-969

148. Chen, Q., Kinch, M. S., Lin, T. H., Burridge, K., and Juliano, R. L. (1994) J Biol Chem 269(43), 26602-26605

149. Morino, N., Mimura, T., Hamasaki, K., Tobe, K., Ueki, K., Kikuchi, K., Takehara, K., Kadowaki, T., Yazaki, Y., and Nojima, Y. (1995) J Biol Chem 270(1), 269-273

150. Schlaepfer, D. D., Hanks, S. K., Hunter, T., and van der Geer, P. (1994) Nature 372(6508), 786-791

151. Derijard, B., Hibi, M., Wu, I. H., Barrett, T., Su, B., Deng, T., Karin, M., and Davis, R. J. (1994) Cell 76(6), 1025-1037

152. Davis, R. J. (1994) Trends Biochem Sci 19(11), 470-473

153. Oehlen, B., and Cross, F. R. (1994) Curr Opin Cell Biol 6(6), 836-841

154. Miyamoto, S., Teramoto, H., Coso, O. A., Gutkind, J. S., Burbelo, P. D., Akiyama, S. K., and Yamada, K. M. (1995) J Cell Biol 131(3), 791-805

155. Yamada, K. M., and Miyamoto, S. (1995) Curr Opin Cell Biol 7(5), 681-689

156. Grinnell, F., and Geiger, B. (1986) Exp Cell Res 162(2), 449-461

157. Mueller, S. C., Kelly, T., Dai, M. Z., Dai, H. N., and Chen, W. T. (1989) J Cell Biol 109(6 Pt 2), 3455-3464

158. Plopper, G., and Ingber, D. E. (1993) Biochem Biophys Res Commun 193(2), 571-578

159. Lewis, J. M., and Schwartz, M. A. (1995) Mol Biol Cell 6(2), 151-160

160. Marshall, C. J. (1996) Curr Opin Cell Biol 8(2), 197-204

161. Alessi, D. R., Saito, Y., Campbell, D. G., Cohen, P., Sithanandam, G., Rapp, U., Ashworth, A., Marshall, C. J., and Cowley, S. (1994) Embo J 13(7), 1610-1619

162. Kyriakis, J. M., App, H., Zhang, X. F., Banerjee, P., Brautigan, D. L., Rapp, U. R., and Avruch, J. (1992) Nature 358(6385), 417-421

163. Shin, I., Kim, S., Song, H., Kim, H. R., and Moon, A. (2005) J Biol Chem 280(15), 14675-14683

164. Hughes, P. E., Renshaw, M. W., Pfaff, M., Forsyth, J., Keivens, V. M., Schwartz, M. A., and Ginsberg, M. H. (1997) Cell 88(4), 521-530

165. Brenner, K. A., Corbett, S. A., and Schwarzbauer, J. E. (2000) Oncogene 19(28), 3156-3163

166. Hynes, R. O. (1992) Cell 69(1), 11-25

167. Schwartz, M. A., Schaller, M. D., and Ginsberg, M. H. (1995) Annu Rev Cell Dev Biol 11, 549-599

168. Ginsberg, M. H., Du, X., and Plow, E. F. (1992) Curr Opin Cell Biol 4(5), 766-771

169. O'Toole, T. E., Katagiri, Y., Faull, R. J., Peter, K., Tamura, R., Quaranta, V., Loftus, J. C., Shattil, S. J., and Ginsberg, M. H. (1994) J Cell Biol 124(6), 1047-1059

170. Dedhar, S., and Hannigan, G. E. (1996) Curr Opin Cell Biol 8(5), 657-669

171. Zhang, Z., Vuori, K., Wang, H., Reed, J. C., and Ruoslahti, E. (1996) Cell 85(1), 61-69

172. Hannigan, G. E., Leung-Hagesteijn, C., Fitz-Gibbon, L., Coppolino, M. G., Radeva, G., Filmus, J., Bell, J. C., and Dedhar, S. (1996) Nature 379(6560), 91-96

173. Chung, C. Y., and Erickson, H. P. (1997) J Cell Sci 110 (Pt 12), 1413-1419

174. Mercurius, K. O., and Morla, A. O. (2001) BMC Cell Biol 2, 18

175. Klass, C. M., Couchman, J. R., and Woods, A. (2000) J Cell Sci 113 (Pt 3), 493-506

176. Saoncella, S., Echtermeyer, F., Denhez, F., Nowlen, J. K., Mosher, D. F., Robinson, S. D., Hynes, R. O., and Goetinck, P. F. (1999) Proc Natl Acad Sci U S A 96(6), 2805-2810

177. Wilcox-Adelman, S. A., Denhez, F., and Goetinck, P. F. (2002) J Biol Chem 277(36), 32970-32977

178. Midwood, K. S., and Schwarzbauer, J. E. (2002) Mol Biol Cell 13(10), 3601-3613

179. Somers, C. E., and Mosher, D. F. (1993) J Biol Chem 268(30), 22277-22280

180. Yang, R. S., Tang, C. H., Ling, Q. D., Liu, S. H., and Fu, W. M. (2002) Mol Pharmacol 61(5), 1163-1173

181. Lin, W., Wang, S. M., Huang, T. F., and Fu, W. M. (2002) Connect Tissue Res 43(1), 22-31

182. Tang, C. H., Yang, R. S., Huang, T. H., Liu, S. H., and Fu, W. M. (2004) Mol Pharmacol 66(3), 440-449

183. Kaiura, T. L., Itoh, H., and Kent, K. C. (1999) J Surg Res 84(2), 212-217

184. Lee, B. H., Park, R. W., Choi, J. Y., Ryoo, H. M., Sohn, K. Y., and Kim, I. S. (1996) Biochem Mol Biol Int 39(5), 895-904

185. Lin, S., Sahai, A., Chugh, S. S., Pan, X., Wallner, E. I., Danesh, F. R., Lomasney, J. W., and Kanwar, Y. S. (2002) J Biol Chem 277(44), 41725-41735

186. Osusky, R., Soriano, D., Ye, J., and Ryan, S. J. (1994) Curr Eye Res 13(8), 569-574

187. Singh, L. P., Andy, J., Anyamale, V., Greene, K., Alexander, M., and Crook, E. D. (2001) Diabetes 50(10), 2355-2362

188. Horowitz, A., and Simons, M. (1998) J Biol Chem 273(40), 25548-25551

189. Oh, E. S., Woods, A., and Couchman, J. R. (1997) J Biol Chem 272(13), 8133-8136

190. Fidler, I. J. (2003) Nat Rev Cancer 3(6), 453-458

CHAPTER II

PKC EPSILON MEDIATES POLYMERIC FIBRONECTIN ASSEMBLY ON THE SURFACE OF BLOOD-BORNE RAT BREAST CANCER CELLS TO PROMOTE PULMONARY METASTASIS*

* Huang L, Cheng HC, Isom R, Chen CS, Levine RA, Pauli BU. Protein kinase C epsilon mediates polymeric fibronectin assembly on the surface of blood-borne rat breast cancer cells to promote pulmonary metastasis. J Biol Chem. 2008 Mar 21;283(12):7616-27. (Huang L: immunofluorescence, FACS, biochemistry; Cheng HC: initial drug screening; Isom R, Chen CS: constructs; Levine R: siRNA constructs advice)

ABSTRACT

Malignant breast cancer cells that have entered the blood circulation from primary mammary fat pad tumors or are grown in end-over-end suspension culture assemble a characteristic, multi-globular polymeric fibronectin (polyFn) coat on their surfaces. Surface polyFn is critical for pulmonary metastasis, presumably by facilitating lung vascular arrest via endothelial dipepidylpeptidase IV (DPP IV; CD26). Here, we show that cell-surface polyFn assembly is initiated by the state of suspension, is dependent upon the synthesis and secretion of cellular Fn, and is augmented in a dose- and time-dependent manner by plasma Fn (pFn). PolyFn assembly is regulated by PKCε, which translocates rapidly and in increasing amounts from the cytosol to the plasma membrane and is phosphorylated. PolyFn assembly is impeded by select inhibitors of this kinase, i.e., bisindolylmaleimide I, Ro-32-0432, Gö6983, and Rottlerin, by the PMA-mediated and time-dependent loss of PKCε protein and decreased plasma membrane-translocation and, more specifically, by stable transfection of lung-metastatic MTF7L breast cancer cells with siRNA-PKCε and dominant-negative PKCε constructs (e.g., RD-PKCε). Inability to assemble a cell surface-associated polyFn coat by knockdown of endogenous Fn or PKCε impedes cancer cells from metastasis to the lungs. The present studies identify a novel regulatory mechanism for polyFn assembly on blood-borne breast cancer cells and depict its effect on pulmonary metastasis.

INTRODUCTION

Fibronectin (Fn) is a “pro-metastatic” gene that is overexpressed in several malignancies (1-7) and, most prominently, in cancer cell lines selected for enhanced

lung colonization (8-11). This pro-metastatic role of Fn is multifaceted, affecting several steps of the metastatic cascade by modulating cell adhesion, motility/invasion, cell cycle progression, and cell survival (reviewed in refs. 12-16). By analyzing cancer cells that had entered the blood circulation from malignant breast cancers implanted into the mammary fat pad of rats or mice, we discovered that blood-borne tumor cells were decorated with a unique, multi-globular coat of polymeric Fn (polyFn) (9,17). PolyFn aggregates appeared to arise from focal accumulations of endogenous, cell surface-immobilized ('linearized') Fn, which served as scaffolds for further Fn-self-assembly from Fn recruited from blood plasma (pFn) (9). Aggregates typically became increasingly deoxycholate-insoluble as they increased in size with time of incubation of suspended cancer cells in serum-containing medium *in vitro*. Biochemically, aggregates impressed as prominent, insoluble (covalently bonded) Fn polymers sitting on top of the stacks of SDS-polyacrylamide gels and, immunocytochemically, as large globules randomly dispersed over the entire cancer cell surface (9). This "cluster arrangement" of polyFn was shown to have the following functional implications: First, the conversion of Fn from the globular state of soluble Fn to the "linearized" state of insoluble, surface-associated Fn aggregates is associated with exposure of a novel, cryptic binding domain for the lung endothelial cell addressin dipeptidylpeptidase IV (DPP IV) (9,17-21). This DPP IV-binding domain is present as consensus motif in each of the 13^{th}, 14^{th}, and 15^{th} type III repeats of Fn (17). Second, the DPP IV binding specificity for linearized (polymeric), but not for globular (soluble) pFn allows tumor cell adhesion to endothelial DPP IV in the presence of high pFn concentrations (9). Third, the large Fn aggregates on cancer cell surfaces allow multiple binding interactions with endothelial DPP IV molecules, thereby generating adhesion strengths between cancer cells and endothelial cells that are able to withstand the rigors of hemodynamic shear stresses (9). The importance of

the Fn/DPP IV-docking mechanism is substantiated by our discovery that synthetic peptides directed against the DPP IV-binding domain in the 13^{th}, 14^{th}, or 15^{th} type III repeats of Fn as well as a polypeptide encompassing the bulk of the extracellular domain of DPP IV dramatically impeded pulmonary metastasis in the MT rat breast cancer model (19,20). These data are consistent with our finding that colonization of the lungs was greatly diminished in Fischer 344/CRJ rats, in which DPP IV is mutated causing a significantly decreased DPP IV protein expression in pulmonary endothelia (21), as well as in DPP IV(-/-) mice (19). DPP IV(-/-) mice injected with lung-metastatic cancer cells lived significantly longer than their wild-type counterparts, an outcome granted by the formation of significantly fewer and smaller lung colonies (Cheng, unpublished data).

Although we have firmly established a critical dependence between the cancer cells' ability to assemble an insoluble, globular polyFn-surface coat and lung colonization in an experimental metastasis model (9,17), we still do not know whether blood-borne cancer cells use their own cellular Fn (cFn) or rely on ubiquitous pFn to assemble their polyFn surface coat, how cancer cells regulate the polyFn build-up, and how Fn cell surface deposits are transformed into covalently bonded, insoluble aggregates (9). To answer some of these questions we examined polyFn genesis in lung-metastatic MTF7L rat breast cancer cells subjected to end-over-end (EoE) suspension culture in serum- or pFn-containing medium, which together induce and augment the build-up of a polyFn surface coat similar to that observed on tumor cells that have entered the blood circulation (9). The data presented here show that assembly of the "pro-metastatic", multi-globular polyFn surface coat on MTF7L breast cancer cells depends upon the synthesis and secretion of endogenous, cellular Fn (Fn1: $EDA^{+}EDB^{+}IIICS_{120}$-Fn) and is regulated by membrane-translocation and Ser/Thr-phosphorylation of protein kinase C epsilon (PKCε). Inhibitors of protein

synthesis, protein secretion, and novel PKC isoforms (nPKCs) as well as transfection of MTF7L cells with the PKCε regulatory domain (RD) or PKCε siRNA species all substantially decrease the cancer cells' ability to assemble a polyFn surface coat. Functionally, inability to assemble polyFn is associated with failure to colonize the lungs. Together, our studies provide novel insights of the regulation of Fn in suspended (blood-borne) breast cancer cells and provide a renewed appreciation for the previously recognized role of Fn in metastasis (1-7).

MATERIAL AND METHODS

Antibodies and Reagents

Rabbit anti-PKCδ, -PKCε, PKCη, PKCθ, PKCζ and anti-hemagglutinin tag (HA-tag) polyclonal antibodies, and mouse anti-Fn (raised against a region in the human Fn-EDA domain; human- mouse- and rat-specific) monoclonal antibody (anti-Fn[EDA]) were from Santa Cruz Biotechnology (Santa Cruz, CA), rabbit anti-Fn polyclonal antibodies that recognized pFn and cFn from both bovine and rat (anti-Fn[pan]: *does not crossreact with fibrinogen, vitronectin, laminin, collagen type IV*) from Sigma (St. Louis, MO), rabbit anti-PKCε polyclonal antibodies from Upstate (Lake Placid, NY), mouse anti-PKCε used for immunoprecipitation from BD Biosciences (San Jose, CA), phycoerythrin (PE)-conjugated donkey anti-rabbit, PE-conjugated goat anti-mouse, horseradish-peroxidase (HRP)-conjugated donkey anti-rabbit, and HRP-conjugated goat anti-mouse antibodies from Jackson ImmunoResearch (West Grove, PA), and rabbit anti-PKCα, -vinculin, and -actin from Dr. Guan (Cornell University). Pertussis toxin ($G\alpha_i$ inhibitor), PD98059 (MEK1/2 inhibitor), SU6656 and PP2 (Src family kinase inhibitors), Wortmannin and LY294002 (PI3K inhibitors), JAKI (Janus-family kinase 1/2 inhibitor), and Y27632

(ROCK1/2 inhibitor), U73122 (inhibitor of phosphatidyl-inositol-specific phospholipase C [PI-PLC]), and the PKC inhibitors calphostin C, Gö6976, HBDDE, bisindolylmaleimide I (BIM I), Gö6983, BIM XI (Ro-32-0432), Rottlerin, Brefeldin A, monensin, and cycloheximide were from EMD Chemicals (San Diego, CA). Fetal bovine serum (FBS) was purchased from Gemini Bio-Products (Woodland, CA). Fn-free FBS (FFS) was generated by successive gelatin- and anti-Fn antibody affinity chromatography (22). All other chemicals and reagents were from Sigma.

Cell Cultures

MTF7L cells were derived from a lung-metastasis generated by tail-vein injection of MTF7 breast cancer cells (obtained from Dr. D.R. Welch, University of Alabama at Birmingham, Birmingham, AL) into Fischer 344 rats. At an i.v. inoculation dose of $2x10^5$ cell per rat, MTF7L cells consistently produce in excess of 400 lung colonies. Cells were grown in culture in Dulbecco's Modified Eagle Medium (DMEM) containing 10% heat-inactivated fetal bovine serum (FBS). For EoE suspension culture, MTF7L cells were grown to 80 to 90% confluence, then removed from the growth surface by trypsinization [0.25% trysin, 0.02% EDTA in phosphate-buffered saline (PBS); 10 min, 37°C], washed twice in DMEM containing 10% FBS, and subjected to EoE suspension culture for 1 hour (or as indicated) in 2ml-centrifuge tubes in DMEM plus 20% FBS at a concentration of $5x10^6$ cells/ml (9,17,20). Tumor cells were used for all experiments within 10 passages from frozen stocks that were tested for metastatic performance immediately prior to freezing.

For metabolic labeling, MTF7L cells in logarithmic growth phase were labeled with [^{35}S]-methionine (0.33 mCi/3-ml) in methionine-free DMEM (both from MP Biomedicals, Solon, OH) containing 20 μM methionine and 10% dialyzed, Fn-free FBS as previously described (9). For [^{32}P]-labeling, cells were serum-starved

overnight, then incubated for 4h in phosphate-free DMEM containing 100 μCi/ml of [^{32}P]orthophosphate (ICN Biochemicals, Irvine, CA), washed in three changes of PBS. Labeled cells were subjected to EoE suspension culture as describe above, and immediately processed for biochemical analyses.

Plasmids Constructs, Transfection, and Selection

The constructs wtPKCε, RD-PKCε, and RD-PKCη cloned into pEGFP-N1 were obtained from Dr. C. Larsson (Lund University, Malmö, Sweden) (23) and wtPKCδ and RD-PKDδ cloned into pcDNA3.1 from Dr. D. Mayer (Deutsches Krebsforschungszentrum, Heidelberg, Germany) (24). For siRNA knockdown of protein expression the following nucleotide (nt.) sequences were cloned into pRNAU6-hygro vector (GenScript, Piscataway, NJ): nt. sequence #1 [5'-acatgagactggtggctat-3' (NM_019143.1, nt. 681-699)] and nt. sequence #2 [5'-aacaaatctcctgcctgggac-3' (NM_019143.1, nt. 4452-4472)] (25) for rat Fn1; nt. sequence #3 [5'-atggtagtgttcaatggc-3' (NM_017171.1, nt. 194-211)] **(26)**; nt. sequence #4 [5'-ccaactctattgctgcttc-3' (NM_017171.1, nt. 1603-1621)] for rat PKCε; and nt. sequence #5 [5'-aactcgcacatagcgactctg-3'] for the non-specific control sequence. The siRNA plasmid pKD™-PKCδ-v6 was purchased from Upstate (Lake Placid, NY). All plasmid constructs were verified by double-stranded sequencing.

MTF7L cells grown to 70% confluence were transiently transfected with above vector constructs or vector alone using LipofectAMINE™ Plus as described by the manufacturer (Invitrogen, Carlsbad, CA). Transfection rates assessed by expression of GFP that is either tagged to the cDNA of interest or co-transfected at a ratio of 1:50 with the cDNA of interest were 20-30%. Cells were used in the various assays 48h after transfection unless otherwise stated. Stable clones were obtained by hygromycin

selection (750µg/ml). In some cases, hygromycin-selected clones were further selected by fluorescence-activated cell sorting (FACS) for optimal expression.

Flow Cytometry

FACS was used to quantify Fn expression on MTF7L breast cancer cell surfaces (9,17). Tumor cells that had been subjected to EoE suspension culture were washed twice in DMEM containing 1% bovine serum albumin (BSA), then incubated with rabbit anti-Fn[pan] antibody diluted 1:100 in PBS containing 1%BSA (PBS-BSA) for 1h at 4°C . After washing in PBS-BSA, tumor cells were stained with phycoerythrin (PE)-conjugated donkey anti-rabbit antiserum in PBS-BSA for 1h at 4°C and fixed in 2% paraformaldehyde in PBS. In select experiments, cells were stained with mouse anti-Fn[EDA] (diluted 1:50) and PE-conjugated goat anti-mouse antiserum. FACS analysis was performed on a Coulter Epics Profile (Coulter Electronics, Hialeah, FL). Nonspecific fluorescence was accounted for by incubating tumor cells with non-immune rabbit serum instead of primary antibody. To quantify the effect of overexpressed or knocked-down proteins on polyFn assembly, we generated bivariate distributions of red fluorescence (y-axis: cells stained with anti-Fn antibodies and PE-conjugated secondary antibodies) and green fluorescence (x-axis: same cells expressing GFP-tagged protein or co-transfected with GFP and cDNA of interest). The levels of polyFn expression in the cell population that emitted high GFP fluorescence were taken as a reflection of the effect of the transfected cDNA on polyFn assembly. To assess the effect of inhibitors of cell signaling, tumor cells were incubated with inhibitor 30-min prior to (adherent) and throughout EoE suspension culture, then subjected to polyFn quantification as described above. Controls were tumor cells incubated in equimolar inhibitor solvent concentration.

Semiquantitative RT-PCR Analyses

Total RNA was prepared from MTF7L grown as adherent monolayers or in EoE suspension cultures by extraction with Trizol as described by the manufacturer (Invitrogen). For every experimental sample, total RNA was quantified both spectrophotometrically and electrophoretically, and amounts were adjusted so that 1µg was reverse-transcribed (SuperScript reverse transcriptase, Invitrogen). cDNA was subjected to PCR (93^{o}C, 30"; 55^{o}C, 30"; 72^{o}C, 30"; 35 cycles) using Taq DNA polymerase (Invitrogen) and primer sets derived from rat Fn1 (NM_019143), PKCδ (NM_133307), PKCε (NM_017171), PKCη (NM_031085), PKCθ (XM_341553), and PKCζ (NM_022507). Controls were run in the absence of reverse transcriptase. GAPDH served as reference standard.

Cell Fractionation

MTF7L cells and transfectants thereof were incubated in EoE suspension culture in DMEM containing 20% FBS for the indicated periods of time. Cells were washed in PBS, collected by centrifugation and resuspended in 0.5 ml ice-cold buffer A [50mM Tris (pH 8.0), 150mM NaCl, 1mM EDTA, 1mM EGTA, 1mM NaF, 0.1mM $NaVO_4$, 20µM leupeptin, 0.1% aprotinin, and 1mM PMSF]. Cells were disrupted by two 15-sec cycles of sonication at 4°C using a microprobe sonicator at maximum power. After removal of unbroken cells and nuclei by centrifugation (500xg for 5 min at 4°C), supernatants were centrifuged at 16,300xg for 15 min at 4°C. The resulting supernatant was designated the cytosolic fraction. The pellet was solubilized in 0.5ml buffer A containing 1% Triton X-100 for 1 hour at 4°C EoE, then centrifuged at 16,300xg for 15 min at 4°C. The detergent-solute was designated the membrane fraction. Twenty micrograms of protein from both the cytosolic and membrane

fractions were separated by SDS–PAGE (10%), transferred to nitrocellulose membrane at 4°C, and probed by Western blotting as described (9).

Cell Lysis, Immunoprecipitation, Western Blotting, and Autoradiography

Cells were extracted with lysis buffer (50mM Tris-HCl, pH 7.4, 150mM NaCl, 1mM EDTA, 1mM EGTA, 1mM benzamidine chloride, 1mM PMSF, 2 µg/ml leupeptin, 0.27 TIU/ml aprotinin, 0.1mM sodium vanadate, and 1% Triton X-100) for 1h at 4°C (9). Total cell lysates or cytosolic and membrane fractions were subjected to: (i) SDS-PAGE (~20-50µg protein) and Western blotting, using anti-Fn[pan], anti-Fn[EDA], or various PKC isoform specific antibodies, HRP-conjugated donkey anti-rabbit or goat anti-mouse secondary antibodies and ECL for detection of bound antibody as described (9); (ii) immunoprecipitation with anti-Fn[pan], anti-PKCε or anti-PKCδ antibodies (27). Immunoprecipitates obtained from lysates of unlabeled, [^{32}P]-orthophosphate-, or [^{35}S]-methionine labeled cells were separated by SDS-PAGE (6-12% polyacrylamide) and analyzed by autoradiography (radio-labeled samples) or blotted to nitrocellulose membranes and probed with either anti-Fn[pan], anti-Fn[EDA], anti-PKC isoform-specific antibodies, or anti-pSer and anti-pThr antibodies (9).

Tumor Cell Proliferation Assay

MTF7L cells and clones thereof were seeded into 96-well microtitration plates (500 cells/well) and incubated in DMEM containing 10% FBS. Cell growth was monitored in daily intervals for up to 4 days. At the end of each incubation period, tumor cells were fixed with 2% paraformaldehyde in PBS and then stained with 0.5% crystal violet in 20% methanol as described (21). Absorbance was read on a

microplate reader (Bio-Teck Instruments) at 562nm and graphed as a function of time of incubation.

Isolation of Blood-Borne Cancer Cells from Tumor-Bearing Rats

MTF7L cancer cells ($1x10^6$ cells/50µl DMEM) were injected into the 4^{th} (left+right) mammary fat pads of six 6-week-old, female Fischer 344 rats. At a tumor diameter of ~2cm, rats were anesthetized by the intraperitoneal injection of sodium pentobarbital (65mg/kg body weight) and blood collected by cardiac puncture. Pooled, EDTA-treated blood was transferred to precooled 50-ml centrifuge trubes containing 15ml of OncoQuick tumor enrichment medium below a porous barrier (Greiner Bio-One, Longwood, FL) and centrifuged at 1600g for 20min at 4°C in a swing-out rotor as described by Rosenberg et al. (28). After a second round of centrifugation of the fluid in the upper compartment, cells were washed with PBS-BSA and stained with anti-Fn antibodies as described above. Tumor cells were readily differentiated from contaminant blood mononuclear cells by size and intensity of anti-Fn staining in comparison with preparations from MTF7L cell-spiked blood.

Lung Colony Assays

To determine the effects of Fn- or PKCε-knockdown on the lung colony efficiency, selected MTF7L clones as well as wt or vector-transfected MTF7 cells ($2x10^5$ cells/0.3ml DMEM/rat) were injected into the lateral tail vein of 5-week-old, female Fischer344 rats (5-9 rats/experiment) as described (9,21). Rats were sacrificed 30 days after tumor cell injection. Means and standard deviations of the lung weights, the number of lung colonies, and the colony diameters were determined for each cell variant (21).

RESULTS

Endogenous Fn Is Required for PolyFn Assembly on Suspended Breast Cancer Cells

Breast cancer cells entering the blood circulation assemble a characteristic surface coat of globular polyFn as evidenced by anti-Fn[pan] staining of cancer cells isolated from the blood of mammary tumor-bearing rats (Fig 2.1A). This phenomenon is mimicked when cancer cells are grown in EoE suspension culture in the presence of serum (9). To examine whether polyFn assembly is mediated by exogenous pFn alone or whether it critically depends on the synthesis of endogenous cFn, we incubated MTF7L breast cancer cells, which express high levels of Fn1 ($EDA^{+}EDB^{+}CSIII_{120}$), in EoE suspension culture in DMEM containing either 20% complete FBS or Fn-free fetal bovine serum (FFS). FFS-treated tumor cells stained with either anti-Fn[pan] (Fig 2.1B) or anti-Fn[EDA] (Fig 2.1B, inset) exhibited similar numbers of polyFn globules on their surfaces as FBS-treated cells (Fig 2.1C). However, the addition of complete FBS to the suspension medium significantly augmented the size of individual polyFn-globules relative to those generated by Fn-free FBS (FFS) (Fig 2.1B&C). The serum-effect on polyFn assembly appeared to be mediated only in part by pFn as shown by FACS analysis of MTF7 cells incubated in EoE suspension culture in the presence of (i) 20% FBS (Fig 1D&E), (ii) 6µg/ml pFn (amount present in 20% FBS [22]), or (iii) 20% FFS (Fig 1E). Both 20% FFS and pFn (6µg/ml) were significantly less effective in promoting polyFn assembly than FBS (Fig 2.1E). The potency of FFS to promote polyFn assembly could be restored to that of FBS by the addition of 6µg/ml pFn (Fig 2.1E, inset). Thus, FFS appeared to promote surface deposition of cellular Fn (Fn1) on suspended MTF7L cells, while pFn in a time- and dose-dependent manner contributed

Figure 2.1: PolyFn globules expressed on the surface of suspended (blood-borne) MTF7L breast cancer cells: (A) MTF7L breast cancer cells were isolated from blood of tumor-bearing rats, using the OncoQuick tumor enrichment medium. The mononuclear cell fraction separated from red blood cells, platelets, and polymorphonuclear leukocyte fractions was washed several times in PBS, then stained with rabbit anti-Fn[pan] antibodies followed by PE-conjugated donkey anti-rabbit IgG antibodies and observed under a fluorescent microscope. There are multiple Fn globules randomly dispersed over the cancer cell surface. (B & C) MTF7L cells subjected to EoE suspension culture in DMEM+20% Fn-free FBS (FFS) (B) or DMEM+20% complete FBS (C). Both are incubated for 1h at 37°C, then stained as described under (A). Notice, the same numerical density of Fn stipples are observed in (B) and (C), but a larger stipple size is present in (C) mimicking those observed in (A). C-Inset: Same treatment, but stained with anti-Fn[EDA]. (D) FACS analysis of MTF7L cells incubated EoE for 1h in DMEM+20% FBS and stained with anti-Fn[pan] antibodies as described under (A). (E) FACS analysis of MTF7L cells incubated EoE for 1h in DMEM+6µg/ml pFn (green), DMEM+20% FFS (red), or DMEM+20% FBS (black). Notice that tumor cells treated with DMEM+20% FBS (containing ~6µg/ml pFn) exhibit a higher mean fluorescence than tumor cells treated with DMEM+20% FFS or DMEM+6µg/ml pFn. E-Inset: Tumor cells incubated with 20% FFS+6µg/ml (red) and 20% FBS (green) show identical polyFn assembly. (F) FACS analysis of MTF7L cells treated for the indicated periods of time with DMEM+20%FBS. There is a time-dependent increase in polyFn assembly. Bars in A-C: 50µm

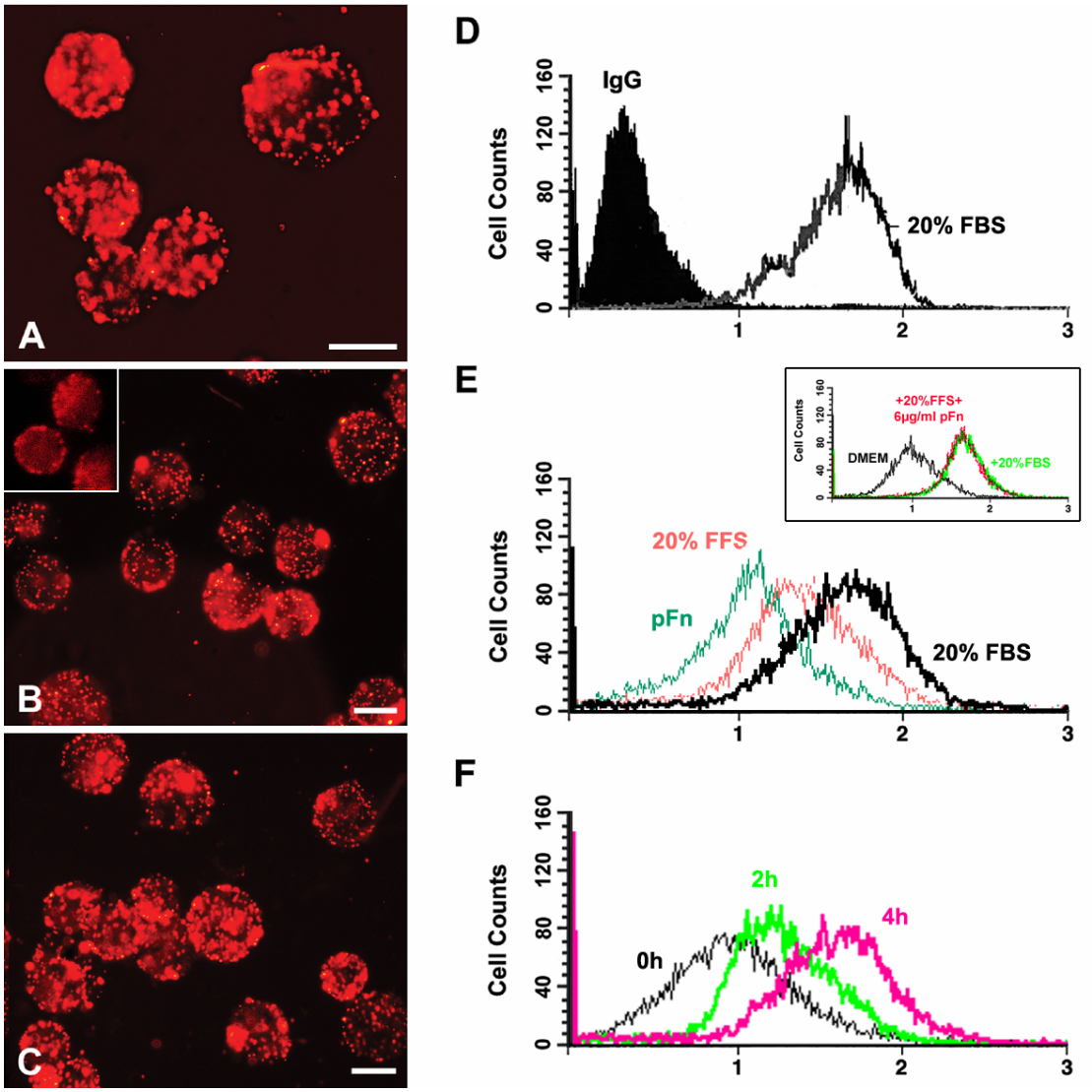
A
B
C
D
IgG
20% FBS
Cell Counts
0
40
80
120
160
1
2
3
E
+20%FFS+
6μg/ml pFn
DMEM
+20%FBS
20% FFS
pFn
20% FBS
F
2h
4h
0h

to augmentation of the Fn polymers by Fn-Fn self assembly (Fig 2.1F).

To further test the hypothesis that surface deposition of a scaffold of endogenous cFn was important for the initiation of polyFn assembly, we examined whether inhibitors of protein synthesis (e.g., cycloheximide) (29) or secretion (e.g., monensin, Brefeldin A) (30,31) would affect polyFn assembly on suspended MTF7L breast cancer cells. Cycloheximide, monensin, and Brefeldin A all dramatically impeded polyFn assembly on MTF7L breast cancer cells in the presence of 20% FBS (Fig 2.2). Since these compounds might have also impaired surface expression of Fn receptors, we used RNA interference to knockdown endogenous cFn in MTF7L (Fn1) cells and to examine whether the specific inhibition of MTF7L-cFn would affect polyFn assembly. Biochemically, stable clones derived from siRNA-Fn transfected cells exhibited a significant decrease in the expression cFn protein as depicted by Western blotting (Fig 2.3A; clones cl1 & cl_2) and by a dramatic decrease in insoluble, metabolically labeled polyFn residing on top of the stack of the polyacrylamide gel (Fig 2.3B, clone cl_1). Functionally, knockdown of endogenous, cellular Fn was associated with impaired surface polyFn assembly on MTF7L cells as shown by FACS (Fig 2.3C) and immunocytochemistry (Fig 2.3D&E), albeit all tumor cells were incubated in the presence of 20%FBS containing ~6µg/ml pFn. An unspecific nucleotide sequences had no affect (Fig 2.3A-E: mcl_{us}). Stable siRNA-Fn clones were also used to test their lung metastatic potential in lung colony assays. In accordance with the level of knockdown of endogenous Fn, lung colonization, assessed by the averages of lung weights, colony numbers, and colony diameters, was significantly decreased relative to wtMTF7L cells or tumor cells that were stably transfected with an unspecific nucleotide sequence (Fig 2.4; siFn-cl_1).

Figure 2.2: Inhibitors of protein synthesis and secretion prevent polyFn assembly: Adherent MTF7L rat breast cancer cells were exposed for 30 min to 10µg/ml of cycloheximide (A), 1µM of monensin (B), or 5µM of Brefeldin A (C), then subjected to EoE suspension cultured in DMEM+20%FBS in the presence of the respective drug or drug solvent (S). After a 1-hr incubation period, cells were stained with anti-Fn[pan] antibodies as described in figure 2.1A (control: MTF7L cell stained with non-immune rabbit IgG [rIgG]). Tumor cells treated with cycloheximide, monensin, and Brefeldin A exhibit a dramatic reduction in the cell surface-associated polyFn, relative to those treated with drug solvent.

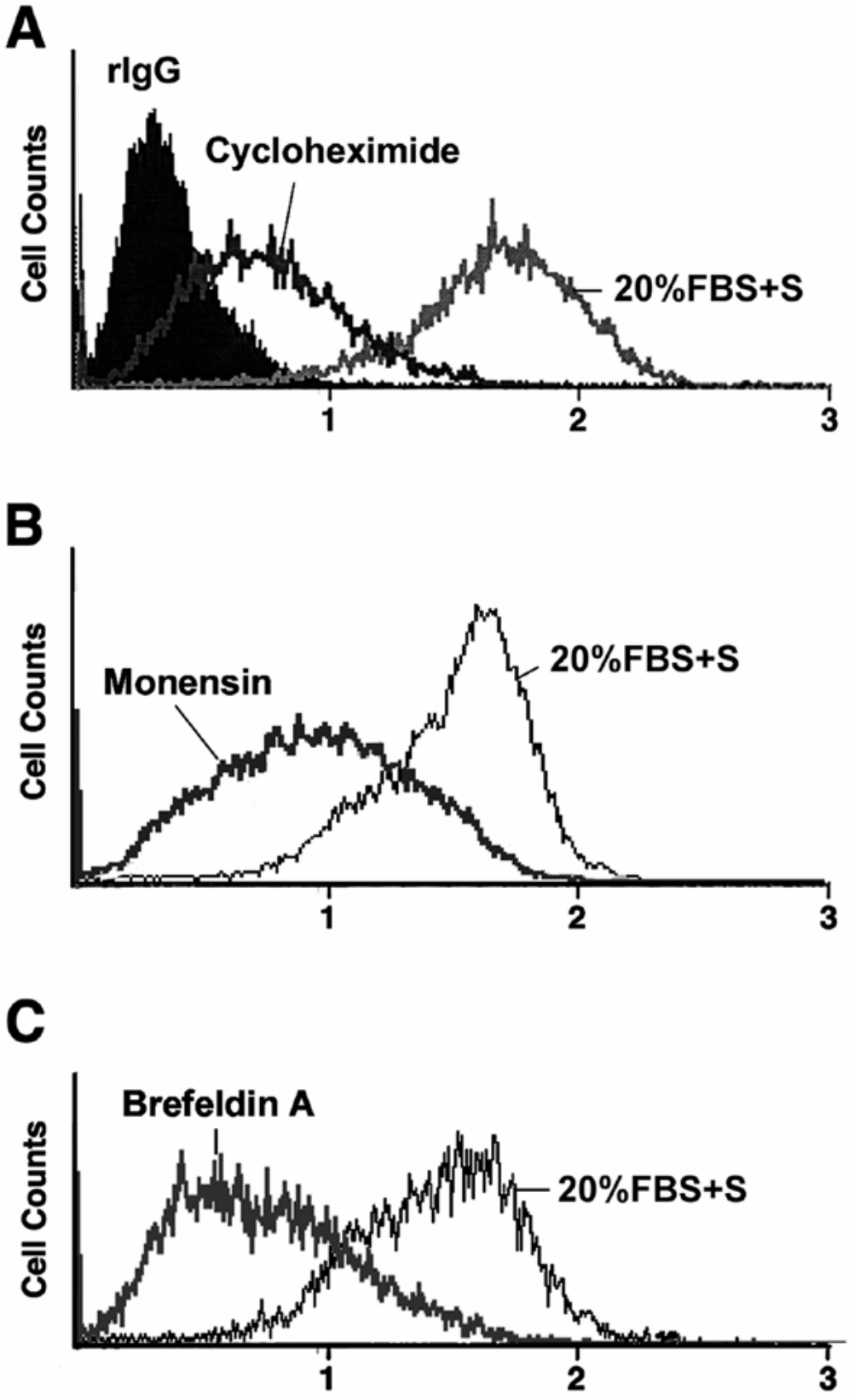
A
rIgG
Cycloheximide
20%FBS+S
Cell Counts
1
2
3
B
Monensin
20%FBS+S
Cell Counts
1
2
3
C
Brefeldin A
20%FBS+S
Cell Counts
1
2
3

Figure 2.3: Effect of siRNA knockdown of cFn on polyFn assembly in the presence of 20% FBS: Hygromycin-resistant clones were selected from MTF7L breast cancer cells transfected with the rat Fn1 nt. sequences #1 (clones cl_1 and cl_2), rat Fn1 nt. sequence #2 (clone cl_3), or unspecific nt. sequence #5 (multi-clone mcl_{us}) all cloned into pRNAU6-Hygro for siRNA targeting as described in Material and Methods. (A) Anti-Fn[pan] Western blot from lysates of siFn clones cl_1 and cl_3, and the contol clone mcl_{us}. (B) MTF7L cells metabolically labeled with [^{35}S]-methionine as described in Material and Methods and ref. 9 were subjected to EoE culture in DMEM+20% FBS for 4h, then extracted in lysis buffer containing 1% NP-40 (9). Lysates were immunoprecipitated with anti-Fn[pan] and immunoprecipitated proteins separated by SDS-PAGE (6%) under non-reducing conditions. Notice the significant reduction in the amount of anti-Fn[pan] immunoprecitable material (polyFn) residing on top of the stacking gel. (C) FACS analysis of MTF7L siFn clones cl_1, cl_2, and cl_3 (green) and the control clone mcl_{us} (black: control), cultured and stained with anti-Fn[pan] as described in figure 1A. Mc=mean fluorescence of multi-clone mcl_{us} (back); M_{siFn}= mean fluorescence of siFn clones cl_1, cl_2, and cl_3 (green). (D &E) Micrographs from MTF7L siRNA-Fn clone cl_1 (D) and control-clone mcl_{us} (E), both processed and stained with anti-Fn[pan] as described in figure 2.1A. Notice a significantly decreased polyFn assembly in MTF7L siFn clone cl_1 (C), relative to MTF7L control clone mcl_{us} (D), even though both clones (D&E) were incubated with DMEM+20% FBS for the same period of time (1h at 37°C) in EoE suspension culture. Bars in D&E: 50μm.

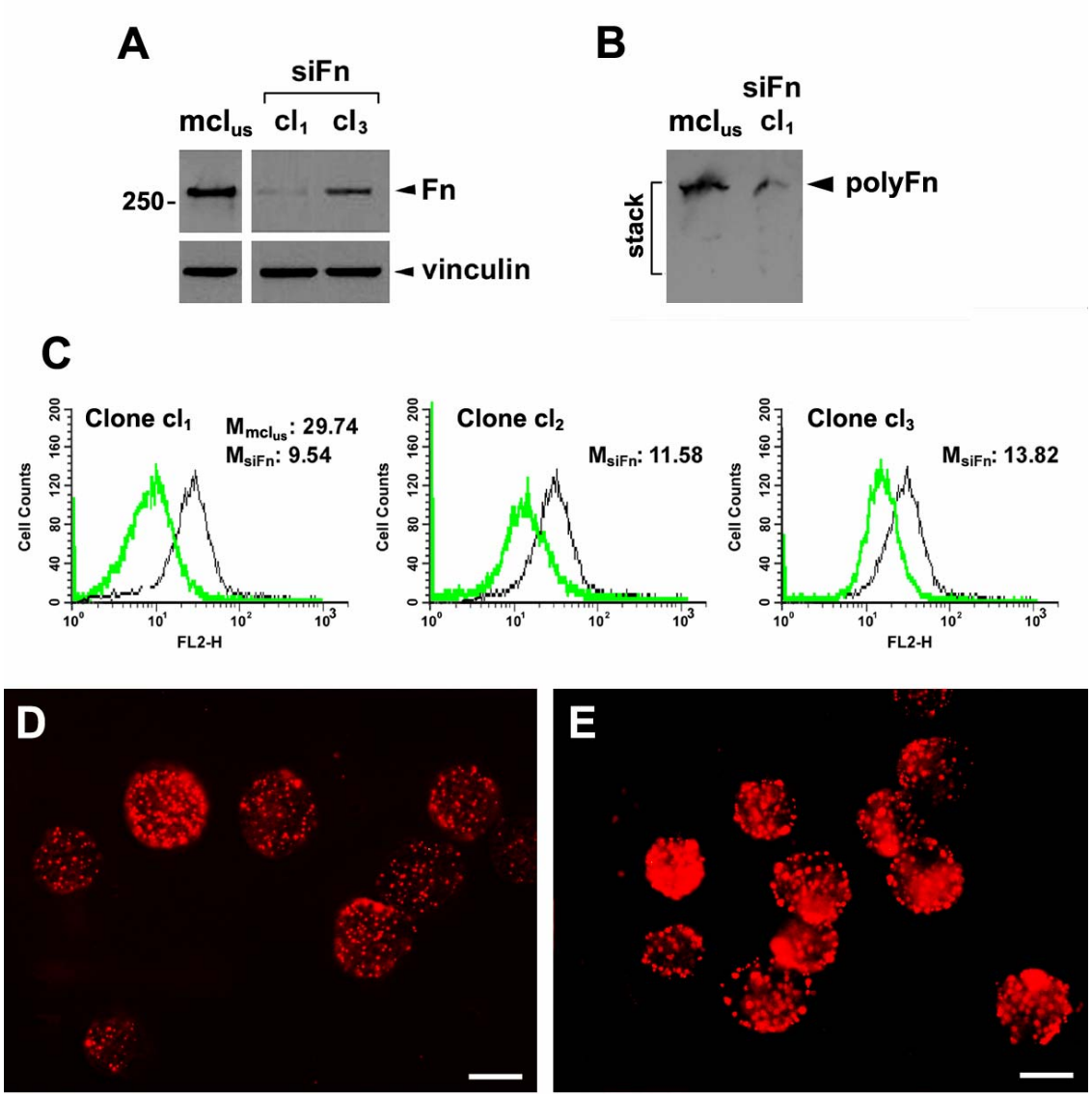
A
siFn
mcl$_{us}$
cl$_1$
cl$_3$
250-
Fn
vinculin
B
siFn
mcl$_{us}$
cl$_1$
stack
polyFn
C
Clone cl$_1$
M$_{mcl_{us}}$: 29.74
M$_{siFn}$: 9.54
Clone cl$_2$
M$_{siFn}$: 11.58
Clone cl$_3$
M$_{siFn}$: 13.82
Cell Counts
FL2-H
D
E

Figure 2.4: Fn and PKCε siRNA-knockdown inhibit pulmonary metastasis: Cells ($2x10^5$ cells/0.3ml DMEM/rat) derived from MTF7L clone mcl_{us} (control clone), clone siFn-cl_1 (*see Fig 2.3*) and MTF7L clone siPKε-cl_1 (*see Fig 2.8*) were injected into the lateral tail vein of female Fischer344 rats as described in Material and Methods. Numbers of lung colonies were significantly decreased in rats injected with MTF7L-siFn-cl_1 (*) and, most prominently, with MTF7L-siPKCε-cl_1 (*) relative to rats injected MTF7L-mcl_{us} cells. Colony diameters were reduced by approximately 5-fold in MTF7L-siFn-cl_1 (*) and 2-fold in MTF7L-siPKCε-cl_1 relative to MTF7-mcl_{us}, in which the coalescence of individual colonies to large aggregates might have led to an inflated estimate of the colony diameter. [Results presented in this figure may reflect to some extent a reduced *in vitro* growth rate of 29% for MTF7L-siFn-cl_1 and 12% for MTF7L-siPKCε-cl_1 cells relative to MTF7-mcl_{us} observed after a 4-day culture period *in vitro*]. *, Student's t-test: $p<0.01$.

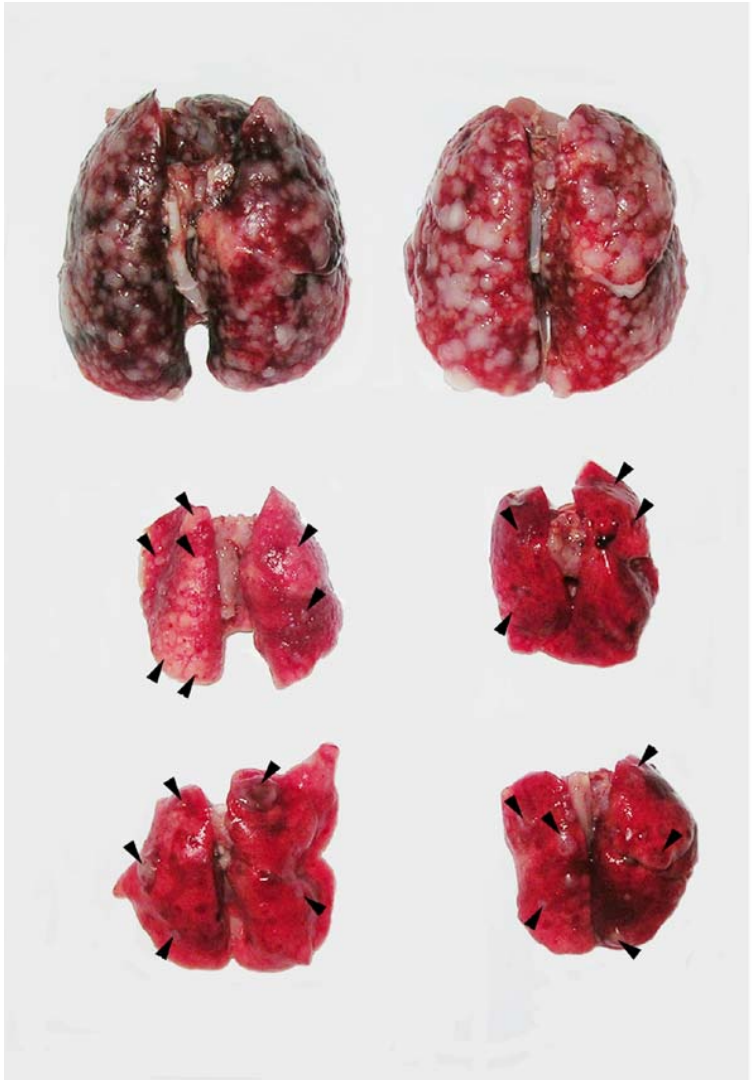

MTF7L-mcl$_{us}$

Lung Weight: 6.04±0.85 gm
Colony Number: >500
Colony Diameter: 1.77±1.32 mm

MTF7L-siFn-cl$_1$

Lung Weight: 1.54±0.14 gm*
Colony Number: 289±36*
Colony Diameter: 0.34±0.30 mm*

MTF7L-siPKCε-cl$_1$

Lung Weight: 1.75±0.32 gm*
Colony Number: 74±23*
Colony Diameter: 0.85±0.72 mm

PolyFn Assembly Occurs in a PKC-Dependent Manner

To identify the signaling cascade that regulates polyFn assembly, we screened a diverse group of inhibitors of cell signaling for their ability to impede polyFn assembly as determined by routine FACS analyses of anti-Fn[pan] stained MTF7L breast cancer cells subjected for 1 hour to EoE suspension culture in FBS (20%)-containing medium in the presence or absence of inhibitor. These inhibitors included pertussis toxin, PD98059, SU6656, PP2, Wortmannin, LY294002, JAKI, and Y27632. None of these inhibitors had any effect on the assembly of the polyFn surface coat of MTF7L breast cancer cells (data not shown). Consistent with the negative result obtained with the ROCK1/2 inhibitor Y27632 is the finding that the Rho activity, associated with Fn-matrix assembly and stress fiber formation in adherent cells (32,33), steadily decreased during the polyFn assembly phase on suspended breast cancer cells. Moreover, transfection with constitutively active Rho (RhoA*Q63L*) suppressed polyFn assembly, while transfection with dominant negative Rho (RhoA*T19N*) appeared to promote polyFn assembly (Cheng and Pauli, manuscript in preparation). In contrast, polyFn assembly was dramatically reduced by U73122, an inhibitor of phospholipase C (PLC) (34) and the PKC inhibitor calphostin C, which competes with the diacylglyceral and phorbol ester binding site of conventional PKCs (cPKCs) and nPKCs (35) (Fig 2.5A). Together, these findings suggest involvement of a cPKC or nPKC isoform, but not an atypical PKC (aPKC) isoform, presumably acting downstream of PLC in polyFn assembly on MTF7L cancer cell surfaces (36).

PKCε Is the Mediator of polyFn Assembly and Metastasis

Our attempts to identify the PKC isoform responsible for polyFn assembly were preceded by determining the c- and nPKC expression levels in MTF7L breast cancer cells. As reported for adherent, metastatic MT tumor variants by Kiley *et al*.

Figure 2.5: Inhibitors of PLC and PKC diminish polyFn assembly: (A) MTF7L breast cancer cells were incubated in the presence of U73122 (PLC inhibitor) and calphostin C (inhibitor of cPKCs and nPKCs) at the indicated concentrations or inhibitor solute (DMSO, control) for 30min, then subjected to EoE suspension culture for 1h in DMEM+20%FBS+inhibitor (or inhibitor solute [S]). Cells were then stained for Fn surface expression as described in figure 2.1A and analyzed by FACS (negative control: cells stained with non-immune rabbit IgG). Strong, dose-dependant inhibition of polyFn assembly was observed with both U73122 and calphostin C. (B) Expression of c- and nPKC isoforms in MTF7L cells: MTF7L breast cancer cells were subjected to EoE suspension culture for 1h in DMEM+20%FBS. One half of the cells were extracted with Trizol and RNA purified as described by the manufacturer (Invitrogen), the other half was extracted with lysis buffer. One microgram of purified RNA was subjected to RT-PCR (35 cycles) using PKC isoform-specific primers (upper panel). GAPDH served as reference message. Controls were samples run in the absence of reverse transcriptase (RTase). Cell lysates were subjected to SDS-PAGE and Western blotting with isoform-specific anti-PKC antibodies (lower panel). Strong message levels were recorded for PKCα, δ, and ε, moderate for PKCη, and weak for PKCθ. Protein expression was strong for PKCα, δ, and ε, weak for PKCη, and non-detectable for PKCθ.

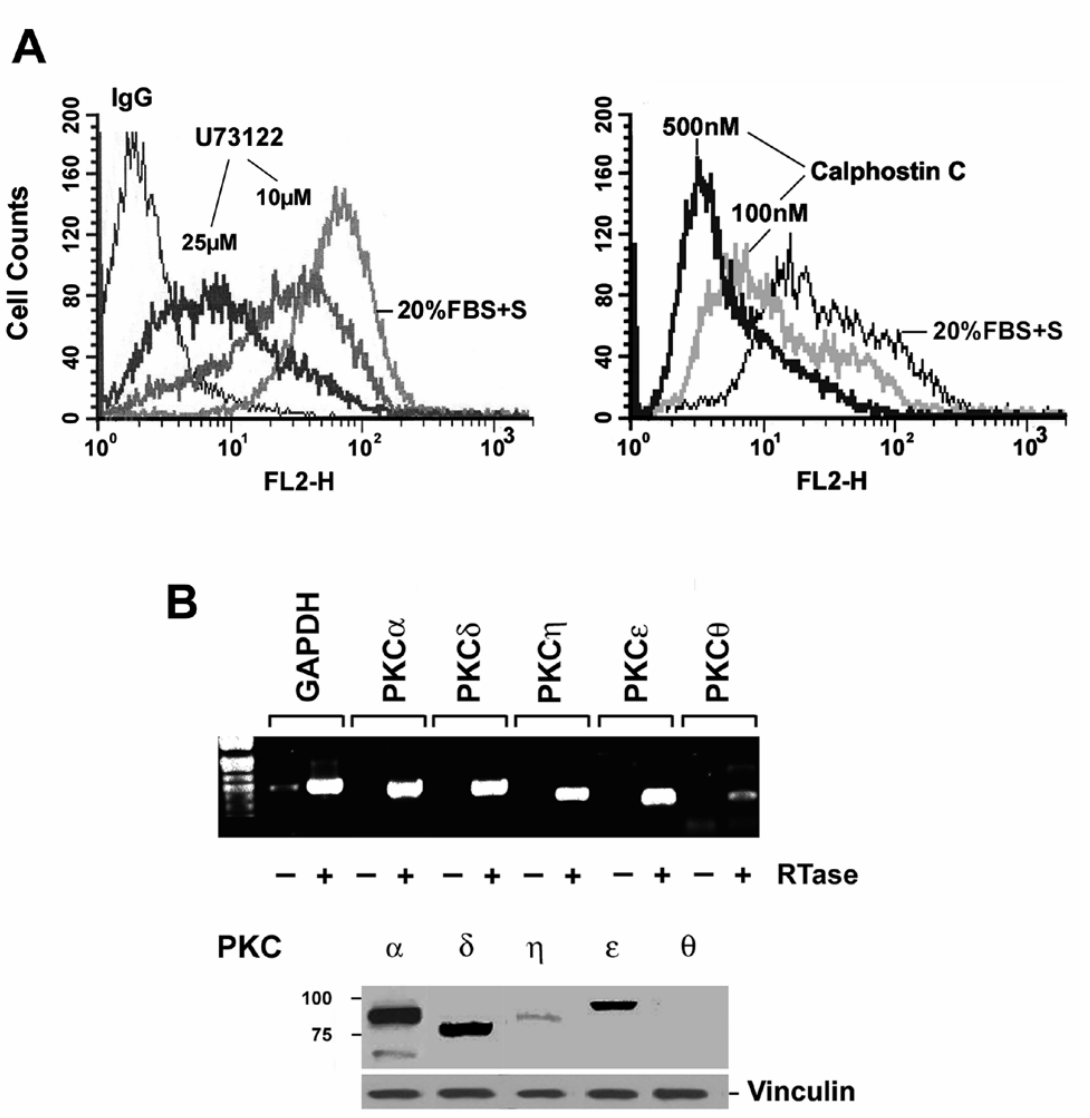
A
IgG
U73122
10μM
25μM
20%FBS+S
Cell Counts
FL2-H
500nM
Calphostin C
100nM
20%FBS+S
FL2-H
B
GAPDH
PKCα
PKCδ
PKCη
PKCε
PKCθ
RTase
PKC
α
δ
η
ε
θ
100
75
Vinculin

(37), suspended MTF7L cells strongly express PKCα, PKCδ, and PKCε, both at the mRNA and protein levels (Fig 2.5B). PKCη mRNA is expressed moderately and protein weakly, and PKCθ mRNA weakly and protein non-detectably (Fig 2.5B). Next, we used select PKC inhibitors to narrow the spectrum of PKC isoforms involved in polyFn assembly. Failure of high doses of the cPKC inhibitors Gö6976 and HBDDE (38) to prevent polyFn assembly ruled out participation of PKCα in polyFn assembly (Fig 2.6A). In contrast, inhibitors that in addition to cPKCs also inhibited nPKCs, including BIM I, Gö6983, BIM XI (Ro-32-0432), and Rottlerin (39-43), decreased polyFn assembly in dose-dependant manners (Fig 2.6B). Albeit these inhibitor data do not provide conclusive evidence of the nPKC isoform involved in polyFn assembly, PKCδ (preferentially, but not specifically, inhibited by Rottlerin, ref. 43) and PKCε (preferentially inhibited by BIM XI) are our most likely candidates for involvement in polyFn assembly based on high protein expression levels and inhibitor activity.

To examine the roles of PKCδ, PKCε and PKCη (nPKC isoforms previously associated with breast cancer metastasis, see refs. 44-46) in polyFn assembly, we transfected MTF7L cells with the regulatory domains (RD) of these isoforms or knocked down their expression by PKC isoform-specific siRNA oligonucleotides. The RD domains of PKCδ (co-transfected with GFP at a ratio of 1:50), PKCη-GFP and PKCε-GFP were transiently expressed in MTF7L breast cancer cells. Forty-eight hours after transfection, cancer cells were subjected to EoE suspension culture in serum-containing medium for 1 hour, then stained with anti-Fn antibodies, and Fn visualized by PE-conjugated secondary antibodies. Cells were analyzed by bivariate, dual-color (red-green) FACS. Among the three nPKC isoforms, only RD-PKCε inhibited polyFn assembly as depicted by a significant down-shift in the number of

Figure 2.6: Effect of various PKC inhibitors on polyFn assembly: (A) Inhibitors of cPKCs such as Gö6976 and HBDDE have no effect on polyFn assembly. (B) However, other PKC inhibitors such as BIM I, BIM XI, Gö6983, and Rottlerin inhibit polyFn assembly in a dose-dependant manner. Experiments were conducted as described in figure 2.5A. Significant differences in polyFn assembly by BIM XI at 100nM and 500nM and Rottlerin at 3μM and, more notably, at 100μM provide strong clues of a possible involvement of PKCε or PKCδ, given the fact that these isoforms are also strongly expressed in suspended MTF7L cells. S, drug solvent.

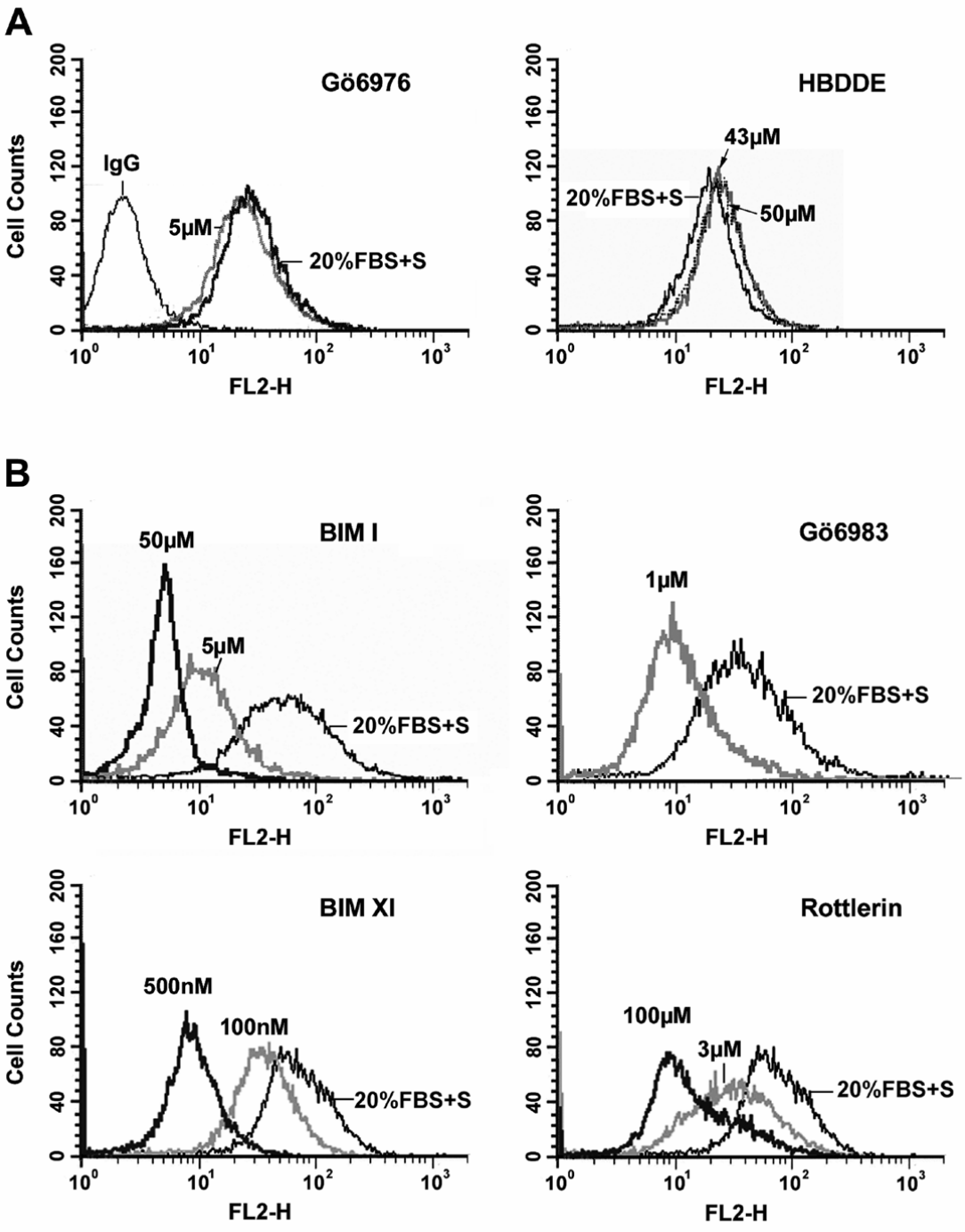
A
Gö6976
IgG
5μM
20%FBS+S
HBDDE
43μM
20%FBS+S
50μM
B
BIM I
50μM
5μM
20%FBS+S
Gö6983
1μM
20%FBS+S
BIM XI
500nM
100nM
20%FBS+S
Rottlerin
100μM
3μM
20%FBS+S
Cell Counts
FL2-H

GFP-positive cells that strongly stained with anti-Fn antibody, i.e., only 21% of tumor cells that expressed high levels of GFP also expressed high levels of polyFn, relative to 56% in vector transfected cells (Fig 2.7A). The RD sequences of PKCη had no effect on polyFn assembly, while the RD sequence of PKCδ caused an increase in the number of strongly GFP-positive cells that expressed high levels of polyFn (Fig 2.7A), suggesting that PKCδ might exert a negative regulatory role in polyFn assembly.

A similar effect on polyFn assembly to that of RD-PKCδ and RD-PKCε was observed when MTF7L cells were co-transfected transiently with GFP and siRNA-PKCδ or siRNA-PKCε and subjected to bivariate FACS analyses 48h or 72h after transfection. Again, knockdown of PKCε suppressed polyFn assembly, while knockdown of PKCδ resulted in increased polyFn assembly on MTF7L cell surfaces (Fig 2.7B). These results were confirmed by the analysis of stable MTF7L clones with "siRNA-knockdown" of PKCε. PKCε-knockdown resulted in a significant decrease in polyFn assembly relative to a control clone transfected with an unspecific siRNA nucleotide sequence (Fig 2.8A). As expected, the FACS-measured decrease in polyFn paralleled decreased PKCε protein expression (Fig 2.8B) as well as decreased amounts of polyFn residing on top of the stack of polyacrylamide gels (Fig 2.8C, top), generated from anti-Fn[pan]-immunoprecipitates of metabolically labeled siRNA-PKCε and control clones. The biochemically identified decrease in polyFn was reflected in decreased surface-association of polyFn on MTF7L cells stained with anti-Fn[pan] (Fig 2.8C, bottom). Functionally, impaired polyFn assembly in siRNA-PKCε clones is associated with a dramatic decrease in lung colonization (Fig 2.4).

Figure 2.7: (A) Effect of RD-PKCδ, RD-PCη, and RD-PKCε on polyFn assembly: MTF7L breast cancer cells grown to a density of 70-80% were transiently transfected with the regulatory domains (RD) of PKCδ, PKCη, and PKCε as described in Material and Methods. Forty-eight hours after transfection, cells were subjected to EoE suspension culture in DMEM+20%FBS for 1h at 37°C, then stained with anti-Fn[pan] antibodies as described in Figure 2.1A and immediately analyzed by bivariate, dual-color [red fluorescence (FnF) vs. green fluorescence (GF)] FACS. Gates were selected based on the staining of wtMTF7L cells with non-immune rabbit IgG and Fn staining of vector-transfected MTF7L cells. Cells in the upper right quadrant of the scatter gram (=strong expressers of RD-PKC and Fn) were expressed as percent of the sum of cells in the right upper and lower quadrants (=strong RD-PKC expressers: gray area), thereby providing a quantitative measure of the inhibitory activity of each RD-PKC isoform on polyFn assembly. Data show inhibitory activity of RD-PKCε, stimulatory activity of RD-PKCδ, and no effect of RD-PKCη. (B) Effect of PKCδ and PKCε siRNA-knockdown on polyFn assembly: MTF7L breast cancer cells grown to a density of 70-80% were transiently co-transfected with either pRNAU6-Hygro-siRNA-PKCε (sequence #3), pKD™-PKCδ-v6, or pRNAU6-Hygro-siRNA-us (unspecific nt. sequence #5) and GFP at a cDNA ratio of 50:1 as described in Material and Methods. Forty-eight hours after transfection, tumor cells were analyzed by FACS. Using a similar gate setting as in (A) [MTF7L cells stained with non-immune rabbit IgG and MTF7L cells transfected with siRNA-us and stained with anti-Fn[pan] antibodies], only 33% of the siPKCε-transfectants exceeded the ~50% threshold in polyFn assembly of siRNA-US transfectants, while in siPKCδ-transfectants this value was 73%. Fn-F, Fn fluorescence; GFP-F, GFP fluorescence.

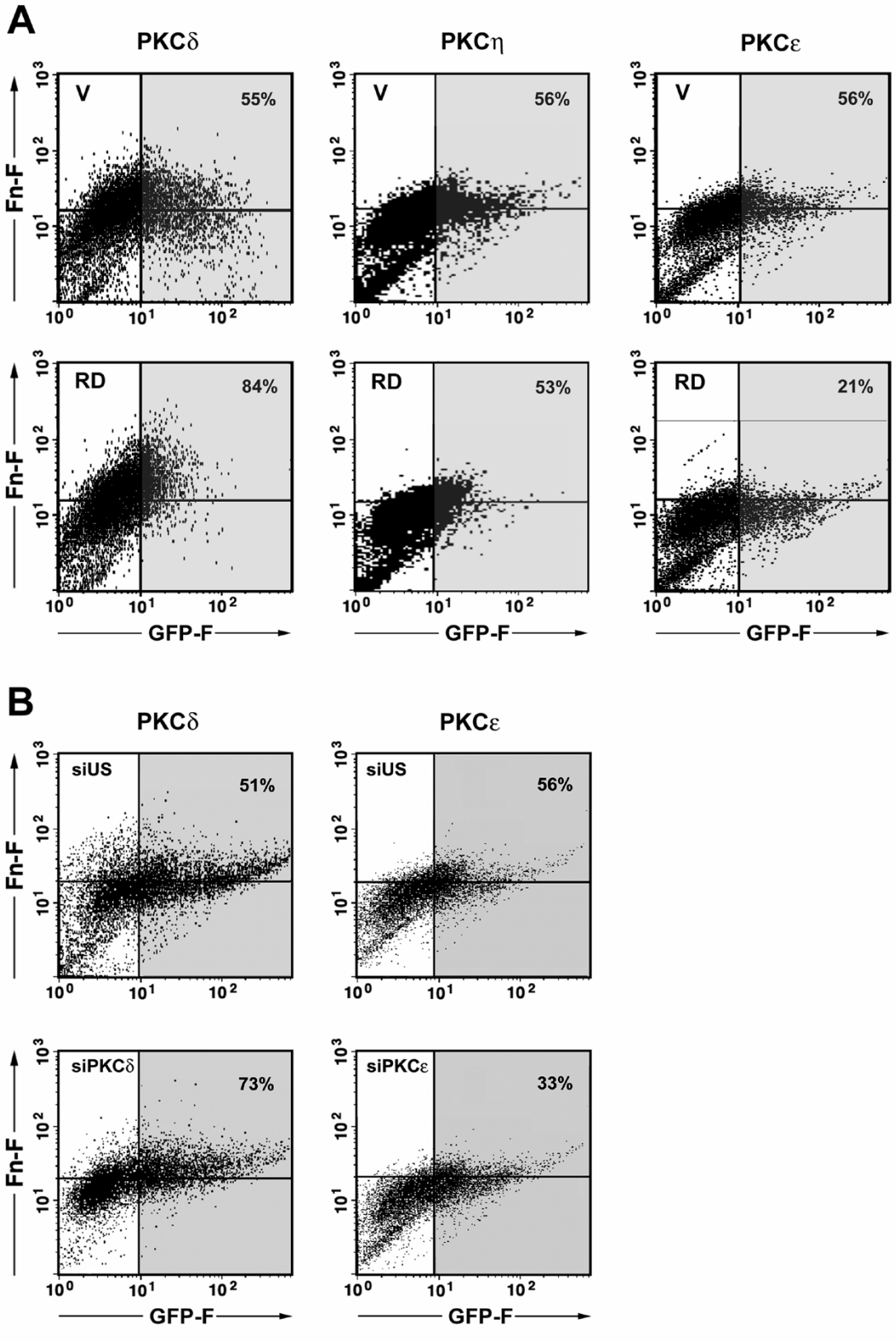
A
PKCδ
PKCη
PKCε
V
55%
56%
56%
RD
84%
53%
21%
Fn-F
GFP-F
B
PKCδ
PKCε
siUS
51%
56%
siPKCδ
73%
siPKCε
33%

Figure 2.8: Analysis of stable clones selected from siRNA-PKCε transfected MTF7L cells: siRNA-PKCε clones (cl_1 and -cl_2) were hygomycin-selected from MTF7L cells transfected with the nt. sequence #3, siRNA-PKCε-cl_3 from MTF7L cells transfected with the nt. sequence #4, andcontrol clone mcl_{us} from MTF7L cells transfected with the unspecific nt. sequence #5 [see Material and Methods]: (A) Clones PKCε-cl_1 and -cl_2 and control clone mcl_{us} subjected to EoE suspension culture in DMEM+20% FBS for 1h were stained with anti-Fn[pan] and analyzed by FACS as described in Material and Methods, then analyzed by FACS. PolyFn assembly by MTF7L clones PKCε-cl_1 and PKCε-cl_2 was significantly decreased relative to the mcl_{us} control clone. (B) Western blot analysis for PKCε– and vinculin-expression in lysates from siPKCε-cl_1, -cl_2 and -cl_3 and the mcl_{us} clone: PKCε protein is decreased in siPKCε clones relative to the unspecific siRNA-mcl_{us} control clone. (C) Lysates from MTF7L clones mcl_{us} and siPKCε-cl_1 labeled with [^{35}S]-methionine and processed as described in Fig 2.3B were subjected to anti-Fn[pan]-immunoprecipitation followed by SDS-PAGE and autoradiography. There is a significant decreased in polyFn residing on top of the stacking gel in siPKCε-cl_1 relative to the mcl_{us} control, mimicking the degree of tumor cell surface-associated polyFn of these clones stained with anti-Fn[pan] (C, bottom).

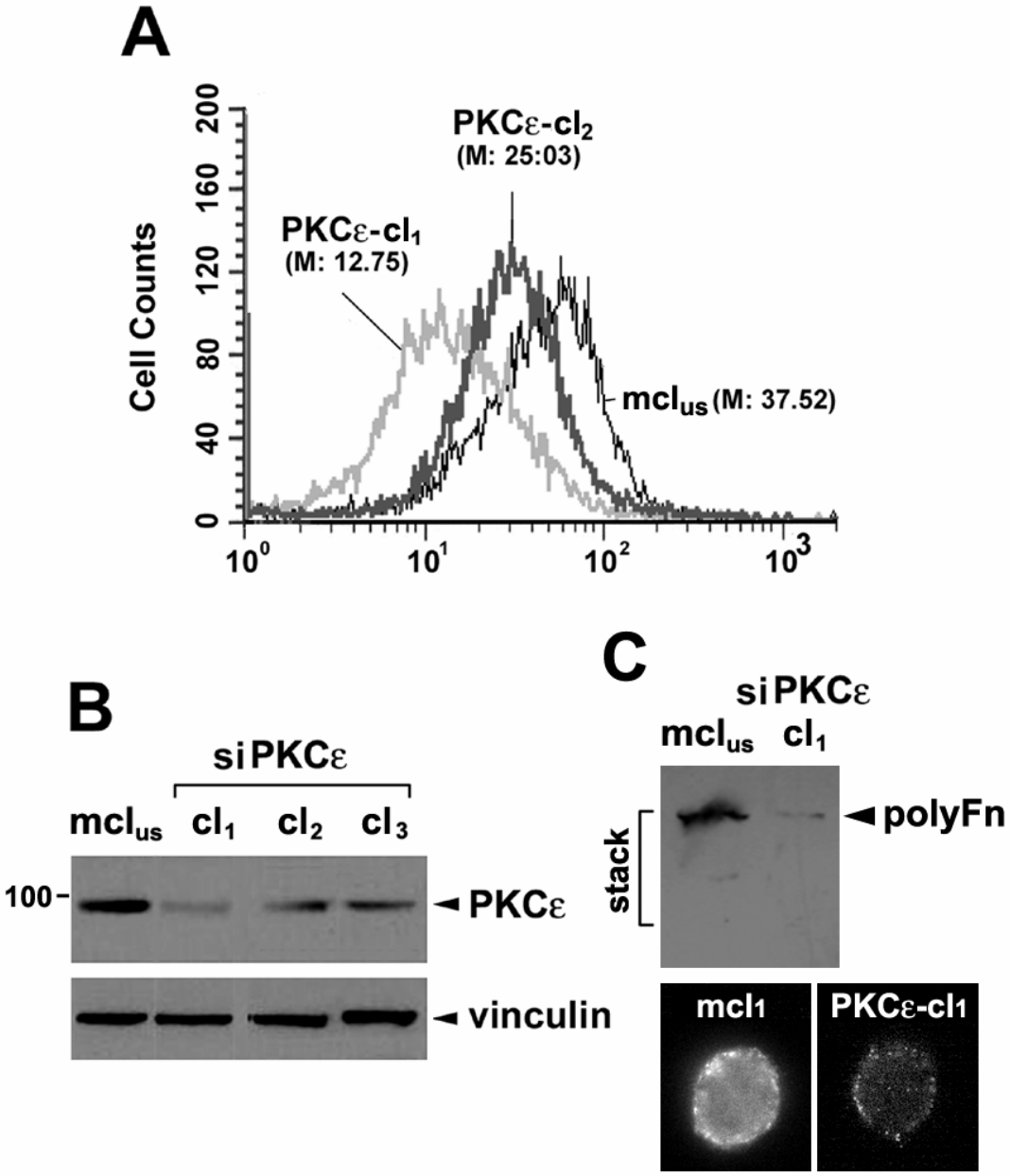
A
PKCε-cl2
(M: 25:03)
PKCε-cl1
(M: 12.75)
mclus (M: 37.52)
Cell Counts
0
40
80
120
160
200
10^0
10^1
10^2
10^3
B
siPKCε
mclus
cl1
cl2
cl3
100
PKCε
vinculin
C
siPKCε
mclus
cl1
stack
polyFn
mcl1
PKCε-cl1

Plasma Membrane Translocation and Activation of PKCε Promote and PMA Suppresses polyFn Assembly

The process of polyFn assembly was associated with a time-dependent translocation of PKCε to the plasma membrane. In adherent MTF7L cells, PKCε was present predominantly in the cytosolic fraction (Fig 2.9A: Time 0), but translocated in increasing amounts to the plasma membrane when MTF7L cells were subjected to EoE suspension culture in the presence of pFn-containing serum (Fig 2.9A: Time 15-60 min). Peak values for membrane-associated PKCε were observed at 30 min of incubation in EoE suspension culture and remained high for the remainder of the 1h incubation period. Translocation of PKCε to the plasma membrane was associated with a noticeable gain of its molecular weight, presumably caused by the observed serine- and threonine phosphorylation of PKCε. PKCε phosphorylation, again, was most prominent at 30 min of EoE suspension culture, then rapidly declined to barely detectable levels at 60 min (Fig 2.9B). This decline was accompanied with a backward shift to the lower molecular weight form of PKCε (Fig 2.9A). The PKC inhibitor BIM XI totally blocked PKCε phosphorylation (Fig 2.9B). This result was confirmed when ^{32}P-labeled MTF7L were examined for PKCε-phosphorylation (Fig 2.9C). Control experiments conducted with PKCδ yielded no phoshorylation of this PKC isoform (Fig 2.9D). Interestingly, PMA (1μM) caused a time-dependent loss of PKCε protein from both the cytosolic and membrane fractions of MTF7L cells (Fig 2.10A). The PMA-mediated loss of PKCε protein, and to a slightly lesser extent of PKCδ protein, was most striking after an 18h incubation period of tumor cells with PMA. No effect was observed for the PMA-insensitive aPKC isoform PKCζ (Fig 2.10B). Concomitantly, loss of PKCε protein and decreased plasma membrane translocation in PMA-treated cells resulted in a dose-dependent, diminished polyFn assembly (Fig 2.10C).

Figure 2.9: Membrane translocation and phosphorylation of PKCε: (A) PKCε translocates in increasing amounts from the cytosol to the plasma membrane during 0, 15, 30, and 60 min of EoE suspension culture of MTF7L in DMEM+20% FBS. Notice a slightly higher molecular weight of PKCε harvested from the membrane fraction (M) relative to that from the cytosolic fractions (C). (B) Time course of PKCε phosphorylation: MTF7L were incubated in EoE suspension culture for the indicated periods of time in DMEM+20% FBS in the presence or absence of BIM XI (500nM). At the end of the indicated time periods, cells were lysed, and lysates subjected to anti-PKCε immunoprecipitation. Precipitates were probed by Western blotting with anti-PKCε, anti-pSer, and anti-pThr antibodies. Maximal phosphorylation of PKCε was observed at 30 min of EoE suspension culture. Thereafter, the PKCε phosphorylation decreased to barely detectable levels at 60 min. PKCε of MTF7 cells treated with BIM XI stained weakly or non-detectably with anti-pSer and anti-pThr. (C & D) [^{32}P]-incorporation into PKCε (C) and PKCδ (D): MTF7 cells labeled for 4h in phosphate-free DMEM containing 100μCi/ml of [^{32}P]orthophosphate as described in Material and Methods were subjected for 30min to EoE suspension cultures in DMEM+20μg/ml pFn (lane 2), DMEM+20%FBS (lane 3), and DMEM+20%FBS+500nM BIM XI (lane 4) [control: [^{32}P]orthophosphate-labeled, adherent cells incubated for 30min in DMEM+20%FBS (lane 1)]. Anti-PKCε (C) and anti-PKCδ (D) immunoprecipitates were analyzed by autoradiography. RG, radiograph; WB, Western blot; IP, immunoprecipitation.

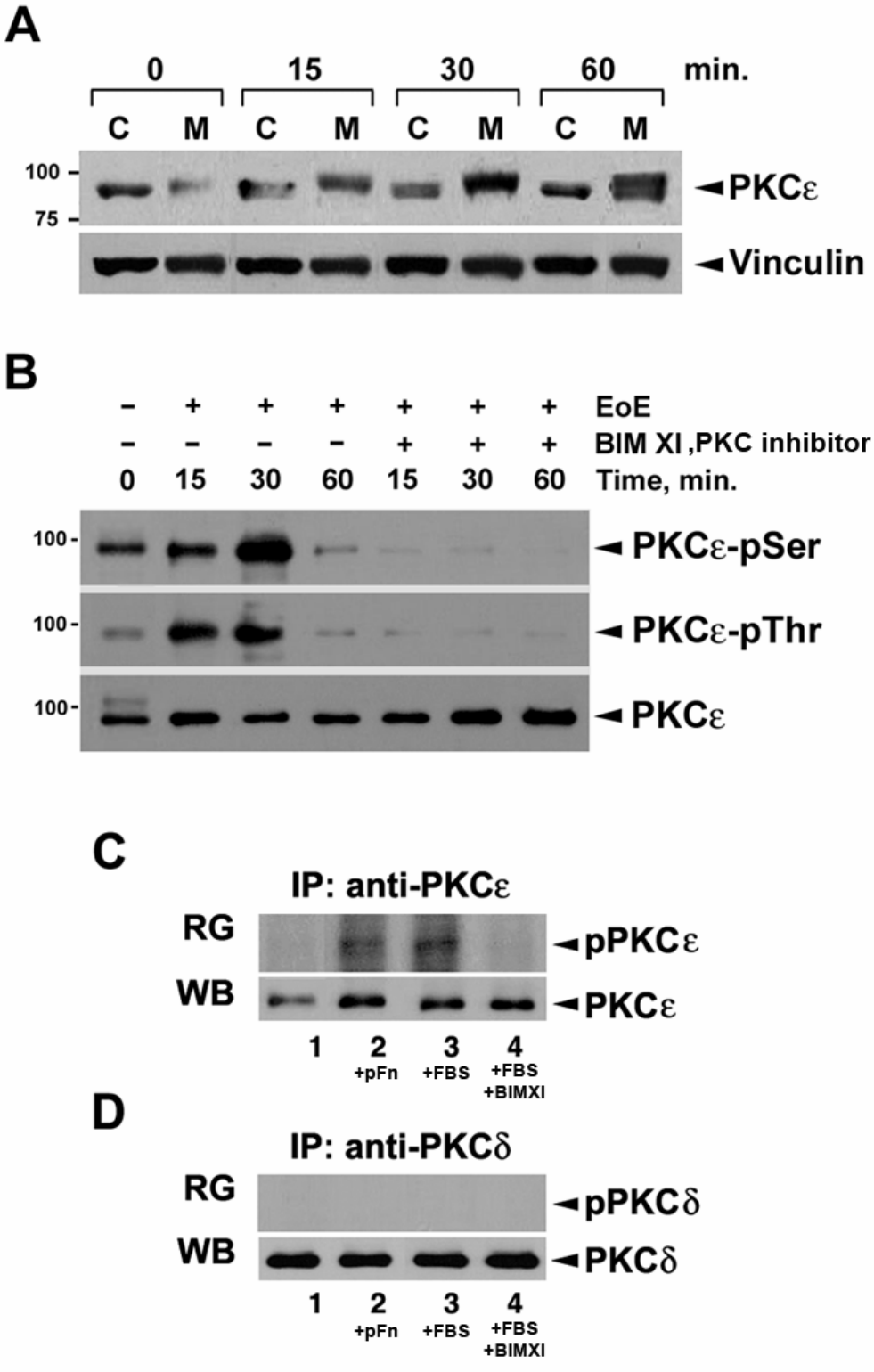
A
0
15
30
60
min.
C
M
C
M
C
M
C
M
100
75
PKCε
Vinculin
B
–
+
+
+
+
+
+
EoE
–
–
–
–
+
+
+
BIM XI ,PKC inhibitor
0
15
30
60
15
30
60
Time, min.
100
PKCε-pSer
100
PKCε-pThr
100
PKCε
C
IP: anti-PKCε
RG
WB
pPKCε
PKCε
1
2
+pFn
3
+FBS
4
+FBS
+BIMXI
D
IP: anti-PKCδ
RG
WB
pPKCδ
PKCδ
1
2
+pFn
3
+FBS
4
+FBS
+BIMXI

Figure 2.10: Effect of PMA on PKCε and polyFn assembly: (A) PMA treatment (1μM) of MTF7L cells caused a time-dependent loss of PKCε from both cytosolic and membrane fractions relative to untreated cells, in which PKCε decreased in the cytosolic fraction, but increased in the membrane fraction with time of incubation. (B) MTF7L cells pretreated with 1μM PMA for 18h, then subjected to EoE suspension culture in DMEM+20%FBS+1μM PMA exhibited decreased amounts of PKCδ protein and, particularly, PKCε protein relative to cells treated without PMA, while protein expression of the atypical PKC isoform PKCζ was unaffected by PMA (control). (C) PMA caused a dose-dependent decrease in polyFn assembly on MTF7L cells subjected to EoE suspension culture in DMEM+20%FBS for 1h. (S=PMA solvent).

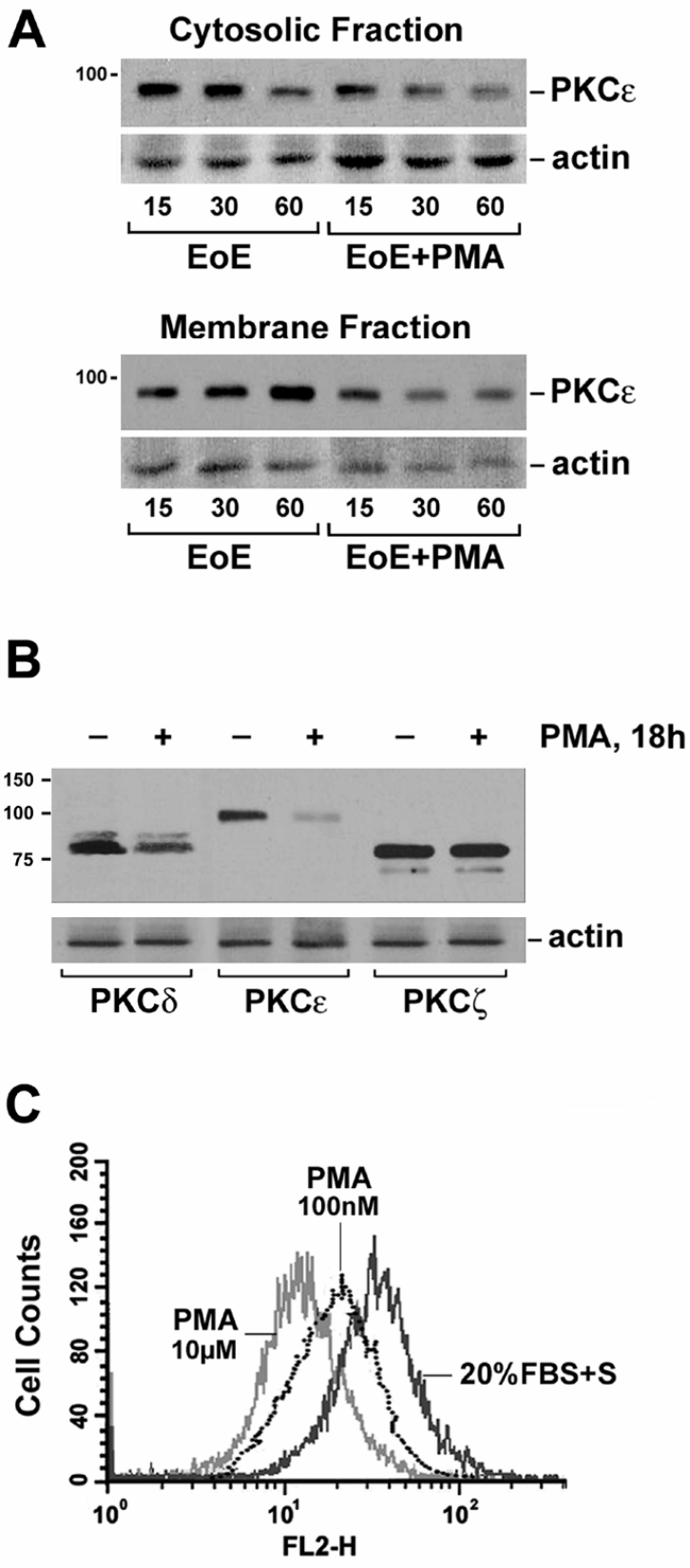
A
Cytosolic Fraction
100
PKCε
actin
15 30 60 15 30 60
EoE
EoE+PMA
Membrane Fraction
100
PKCε
actin
15 30 60 15 30 60
EoE
EoE+PMA
B
– + – + – + PMA, 18h
150
100
75
actin
PKCδ
PKCε
PKCζ
C
Cell Counts
0 40 80 120 160 200
PMA
100nM
PMA
10μM
20%FBS+S
10^0 10^1 10^2
FL2-H

DISCUSSION

The role of Fn in cancer progression is controversial. Early studies suggest that Fn may act as a *tumor suppressor gene*, promoting differentiation and suppressing proliferation, migration, invasion, and metastasis (reviewed in refs. 13-16). In accordance, expression of pFn in Fn-negative LMM3 murine mammary cancer cells reduced the rate of migration as well as spontaneous and experimental metastasis (47), and forced expression of the α5β1 integrin, which was thought to capture secreted cFn at the cell surface, convert it into fibrils and then deposit it in the extracellular matrix, reduced motility and tumorigenicity of transfected tumor cells (48). These findings are contrasted by cDNA or oligonucleotide microarray analyses that attempted to identify genes whose expression was associated with malignant behavior of breast cancers. In several of these studies, Fn (Fn1: $EDA^{+}EDB^{+}IIICS_{120}$) was found to be consistently overexpressed in invasive/metastatic breast tumors *in toto* as well as in tumor cells isolated by laser capture microdissection from a primary invasive ductal carcinoma and an axillary node harboring metastatic breast cancer (5-7). Interestingly, ErbB2 overexpression, observed in 25-30% of invasive ductal breast carcinomas and correlated with a poor clinical prognosis, was associated with Fn1 overexpression in 11 out of 36 cases (49). Overexpression of Fn was also noticed in cancer cell lines that exhibited an invasive/metastatic phenotype, including MDA-MB-231, MeWo-70W, PC3-ML, 4T1, LLC1, B16-F10, K7M2, MTF7, and RPC-2 (17), and was most dramatic in cancer cell lines that were subjected to a selection process for enhanced lung metastatic performance (9,11,17) or in highly metastatic clones derived from a rabdomyosarcoma (8) or B16 melanoma (10), but not in non-metastatic clones (8). Moreover, expression of the metastasis suppressor gene nm23 in MDA-MB-435 breast cancer cells resulted in a down regulation of genes associated with adhesion and

motility, including Fn1 (50). On the other hand, neither the *poor prognosis signature* obtained by large-scale transcript profiling of human breast cancers (51,52) nor the gene expression profile that was associated with lung-metastasis of selected MDA-MB-231 clones (i.e., *lung-metastatic signature*) contained Fn (53). A possible explanation for this result may be related to the multi-functional role of Fn in tumor progression, requiring high levels of Fn expression throughout tumor progression. For example, in early stages of progression Fn promotes survival, cell cycle progression, and angiogenesis and in later stages motility/invasiveness and dissemination and implantation in secondary organs (reviewed in refs. 12-16). Support for this notion can be found in the observation that tumor cell lines that do not express Fn such as MCF-7 cells exhibit poor tumorigenicity, growth, and angiogenesis (54), while overexpresssion of c-Jun in MCF7 cells stimulated Fn synthesis and, concomitantly, increased tumorigenicity and invasiveness (55,56).

In recent years our laboratory has been interested in the role of Fn in breast cancer lung metastasis. This interest was triggered by the fact that a survey of all our highly lung-metastatic breast cancer cell lines, including MTF7, MTF7L, MDA-MD-231 and 4T1 cells, revealed high levels of Fn expression (17) and by the observation that tumor cells isolated from the blood of tumor-bearing animals exhibited a characteristic cell surface coat of multi-globular polyFn. This phenotype could be reproduced *in vitro*, when cancer cells were subjected to EoE suspension culture in the presence of serum (9,17). As indicated in the introduction, this unique surface expression of Fn was responsible for the docking of MTF7 to the lung endothelial addressin DPP IV (9,17-21) and for facilitating lung colonization (9,17,20,21). Interference with the polyFn/DPP IV adhesion by monoclonal antibodies (9), peptides directed against the DPP IV-binding domains in the 13^{th}, 14^{th} and 15^{th} type III repeats of Fn (17), and a polypeptide representing the extracellular domain of DPP IV (20)

abrogated metastatic colonization of the lungs. Here, we have presented some of the molecular underpinnings that regulate polyFn assembly in a rat model of hematogenous dissemination of breast cancer cells. We show that polyFn assembly critically depends upon the expression of endogenous cFn (Fn1) and is regulated by PKCε. This is evidenced by a significantly decreased polyFn assembly in cells transfected with either siRNA-PKCε or dominant-negative RD-PKCε, and in cells treated with select PKC inhibitors. During a 1-hour polyFn assembly phase, PKCε translocates in increasing amounts from the cytosol to the plasma membrane. This translocation is accompanied by PKCε Ser/Thr-phosphorylation and is crucial for successful polyFn assembly, since overexpression of dominant-negative RD-PKCε, which blocks DAG-mediated plasma membrane-docking and activation of endogenous PKCε (57,58), prevents polyFn assembly. In contrast, both RD-PKCδ and siRNA knockdown of PKCδ promoted polyFn assembly, mimicking the previously recognized opposing effects of PKCε and PKCδ in ischemic injury of the heart (59) and suggesting a dominant-negative regulatory effect of PKCδ over PKCε in MTF7L cells. A PKCε regulatory effect was also observed for PMA, which in a dose- and time-dependent manner inhibited PKCε protein synthesis and, in accordance, impaired polyFn assembly on MTF7L cells in a manner similar to that reported for other cell-types (60,61). Together, PMA/DAG competition for plasma membrane-docking, overall loss of PKCε protein, and competition between related PKC isoforms appear to be primarily responsible for the observed decrease in polyFn assembly on cancer cell surfaces.

The role of PKCε in polyFn assembly appears to be dualistic in that it may facilitate surface expression of endogenous, cellular Fn by promoting Fn exocytosis (62-66) and protein synthesis (67). In accordance, inhibitors of protein synthesis (e.g., cycloheximide) and exocytosis (e.g., monensin and Brefeldin B) strongly impeded

polyFn assembly (Fig 2), albeit cells were kept in suspension culture in the presence of high concentrations of pFn. However, at this writing we have not identified any of the PKCε partner proteins that are required in regulating these processes. Nonetheless, inhibition of PKCε has been shown to trap integrin β1, a possible receptor for cellular Fn, in a CD81-positive intracellular compartment and electron microscopy demonstrated the co-localization of PKCε and integrin β1 on vesicular membranes (68). Translocation of the integrin β1 from cytosolic vesicles to the plasma membrane appears to involve the PKCε-mediated phosphorylation of the cytoplasmic tail of β1-integrin at threonine 788/789 (69) or cytoskeletal intermediaries such as vimentin (70) and actin (62). Accordingly, interaction of PKCε with actin has been linked to the formation of invadopodia-like structures, increased pericellular metalloproteinase activity and, ultimately, invasiveness and metastasis in PKCε-transformed NIH3T3 fibroblasts (71). Whether the concomitant downregulation of RhoC in MDA-MB-231 cells, in which PKCε expression was knocked down by RNA interference resulting in a cell phenotype that was significantly less proliferative, invasive, and metastatic (45), is intertwined in PKCε-actin remodeling is unclear and needs further investigation. Supporting evidence for such role may be deduced from the thrombin-induced PKCε-Rho-actin complex formation in actin reorganization in myofibroblasts (72). However, in our system of suspended (blood-borne) breast cancer cells, the Rho activity is significantly suppressed and expression of constitutively active Rho suppresses polyFn assembly (Cheng and Pauli, manuscript in preparation).

In conclusion, our studies suggest that surface expression of polyFn occurs in PKCε-dependant manner presumably involving the transport of Fn-receptor complexes from cytosolic vesicles to the plasma membrane and that such complexes serve as scaffolds for the subsequent augmentation of polyFn aggregates on tumor cells during their journey in Fn-rich blood plasma. This notion is supported by a

dramatic inhibition of polyFn assembly by inhibitors of exocytosis and by siRNA-knockdown of PKCε, that occurs even when cancer cells are exposed to high exogenous Fn concentrations and express several integrin and syndecan Fn-receptors on their surfaces (Cheng, unpublished data). Thus, we have disclosed here a novel regulatory principle for the recognized "pro-metastatic" role of Fn that may spur the design of new anti-metastatic therapies.

REFERENCES

1. Zhang L, Zhou W, Velculescu VE, Kern SE, Hruban RH, Hamilton SR, Vogelstein B, and Kinzler KW. (1997) Science 276, 1268-1272

2. Bittner M, Meltzer P, Chen Y, Jiang Y, Seftor E, Hendrix M, Radmacher M, Simon R, Yakhini Z, Ben-Dor A, Sampas N, Dougherty E, Wang E, Marincola F, Gooden C, Lueders J, Glatfelter A, Pollock P, Carpten J, Gillanders E, Leja D, Dietrich K, Beaudry C, Berens M, Alberts D, and Sondak V. (2000) Nature 406, 536-540

3. Al Moustafa AE, Alaoui-Jamali MA, Batist G, Hernandez-Perez M, Serruya C, Alpert L, Black MJ, Sladek R, and Foulkes WD. (2002) Oncogene 21, 2634-2640

4. Jiang Y, Harlocker SL, Molesh DA, Dillon DC, Stolk JA, Houghton RL, Repasky EA, Badaro R, and Xu J. (2002) Ongoene 21, 2270-2282

5. Amatschek S, Koenig U, Auer H, Steinlein P, Pacher M, Gruenfelder A, Dekan G, Vogl S, Kubista E, Heider KH, Stratowa C, Schreiber M, and Sommergruber W. (2004) Cancer Res. 64, 844-856

6. Hao X, Sun B, Hu L, Lähdesmäki H, Dumire V, Feng Y, Zhang SW, Wang H, Wu C, Wang H, Fuller GN, Symmans WF, Shumulevich I, and Zhang W. (2004) Cancer 100, 1110-1122

7. Zucchi I, Mento E, Kuznetsov VA, Scotti M, Valsecchi V, Simionati B, Vicinanza E, Valle G, Pilotti S, Reinbold R, Vezzoni P, Albertini A, and Dulbecco R. (2004) Proc. Natl. Acad. Sci. U S A 101, 18147-18152

8. Korach S, Poupon MF, Du Villard JA, and Becker M. (1986) Cancer Res. 46, 3624-3629

9. Cheng HC, Abdel-Ghany M, Elble RC, and Pauli BU. (1998) J. Biol. Chem. 273, 24207-24215

10. Clark EA, Golub TR, Lander ES, and Hynes RO. (2000) Nature 406, 532-535

11. Bandyopadhyay A, Elkahloun A, Baysa SJ, Wang L, and Sun LZ. (2005) Cancer Biol. Ther. 4, 168-172, 2005

12. Hynes RO, and Yamada KM. (1982) J. Cell Biol. 95, 369-377

13. Humphries MJ, Obara M, Olden K, and Yamada KM. (1989) Cancer Invest. 7, 373-393

14. Rouslahti E. (1999) Adv. Cancer Res. 67, 1-20

15. Danen EHJ, and Yamada KM. (2001) J. Cell Physiol. 189, 1-13

16. Labat-Robert J. (2002) Cancer Biol. 12, 187-195

17. Cheng HC, Abdel-Ghany M, and Pauli BU. (2003) J. Biol. Chem. 278, 24600-24607

18. Johnson RC, Augustin-Voss HG, Zhu D, and Pauli BU. (1991) Cancer Res. 51, 394-399

19. Johnson RC, Zhu D, Augustin-Voss HG, and Pauli BU. (1993) J. Cell Biol. 121, 1423-1432

20. Abdel-Ghany M, Cheng HC, Levine RA, and Pauli BU. (1998) Invasion & Metastasis 18: 35-43

21. Cheng HC, Abdel-Ghany M, Zhang S, and Pauli BU. (1999) Clin. Exp. Metastasis 17, 609-615

22. Hayman EG and Ruoslahti E. (1979) J. Cell Biol. 83, 255-259

23. Zeidman R, Löfgren B, Pahlman S, and Larsson C. (1999) J. Cell Biol. 145, 713-726

24. De Servi B, Hermani A, Medunjanin S, and Mayer D. (2005) Oncogene 24, 4946-4955

25. Sakai T, Larsen M, and Yamada KM. (2003) Nature 423, 876-881

26. Cheng JJ, Wung BS,Chao YJ, and Wang DL. (2001) J. Biol. Chem. 276, 31368-31375

27. Abdel-Ghany M, Cheng HC, Elble RC, and Pauli BU. (2001) J. Biol. Chem. 276, 25438-25446

28. Rosenberg R, Gertler R, Friedrichs J, Fuehrer K, Dahm M, Phelps R, Thorban S, Nekarda H, and Siewert JR. (2002) Cytometry 49, 150-158

29. Barr RK, and Bogoyevitch MA. (2001) Int. J. Biochem. Cell Biol. 33, 1047-1063

30. Dinter A, and Berger EG. (1998) Histochem. Cell Biol. 109, 571-590

31. Nebenfuhr A, Ritzenthaler C, and Robinson DG. (2002) Plant Physiol. 130, 1102-1108

32. Narumiya S, Ishizaki T, and Watanabe N. (1997) FEBS Lett. 410, 68-72

33. Hall A. (2005) Biochem. Soc. Trans. 33(Pt 5), 891-895

34. Gloyna W, Schmitz F, and Seebeck J. (2005) Regul. Pept. 125, 179-184

35. Valledor AF, Xaus J, Comalada M, Soler C, and Celada A. (2000) J. Immunol. 164, 29-37

36. Munakata M, Stamm C, Friehs I, Zurakowski D, Cowan DB, Cao-Danh H, McGowan FX Jr, and del Nido PJ. (2000) Ann. Thorac. Surg. 73, 1236-1245

37. Kiley SC, Clark KJ, Duddy SK, Welch DR, and Jaken S. (1999) Oncogene 18, 6748-6757

38. Schreckenberg R, Taimor G, Piper HM, and Schluter KD. (2004) Cardiovasc. Res. 63, 553-560

39. Wilkinson SE, Parker PJ, and Nixon JS. (1993) Biochem. J. 294, 335-337

40. Gschwendt M, Müller HJ, Kielbassa K, Zang R, Kittstein W, Rincke G, and Marks F. (1994) BBRC 199, 93-98.

41. Di-Capua N, Sperling O, and Zoref-Shani E. (2003) J. Neurochem. 84, 409-12

42. Imamdi R, de Graauw M, and van de Water B. (2004) J. Pharmacol. Exp. Ther. 311, 892-903

43. Tapia JA, Jensen RT, and Garcia-Marin LJ. (2006) Biochim. Biophys. Acta 1763, 25-38

44. Kiley SC, Clark KJ, Goodenough M. Welch DR, and Jaken S. (1999) Cancer Res. 59, 3230-3228

45. Pan Q, Bao LW, Kleer CG, Sabel MS, Griffith KA, Teknos TN, and Merajver SD. (2005) Cancer Res. 65, 8366-8371

46. Masso-Welch PA, Winston JS, Edge S, Darcy KM, Ascxh H, Vaughan MM, and Ip MM. (2001) Breast Cancer Res. Treat. 68, 211-223

47. Urtreger A, Porro F, Puricelli L, Werbajh S, Baralle FE, De Joffe EB, Kornblihtt AR, and Muro AF. (1998) Int. J. Cancer 78, 233-241

48. Giancotti FG, and Ruoslahti E. (1999) Science 285, 1028-1032

49. Mackay A, Jones C, Dexter T, La Silva R, Bulmer K, Jones A, Simpson P, Harris RA, Jat PS, Neville AM, Reis LFL, Lakhani S, and O'Hare MJ. (2003) Oncogene 22, 2680-2688

50. Zhao H, Jhanwar-Uniyalk M, Datta PK, Yemul S, Ho L, Khitrov G, Kupershmidt I, Pasinetti GM, Ray T, Athwal RS, and Achary MP. (2004) Int. J. Cancer 109, 65-70

51. van 't Veer LJ, Dai H, van de Vijver MJ, He YD, Hart AA, Mao M, Peterse HL, van der Kooy K, Marton MJ, Witteveen AT, Schreiber GJ, Kerkhoven RM, Roberts C, Linsley PS, Bernards R, and Friend SH. (2002) Nature 425, 530-536

52. Ramaswamy S, Ross KN, Lander ES, and Golub TR. (2003) Nat. Genet. 33, 49-54

53. Minn AJ, Gupta GP, Siegel PM, Bos PD, Shu W, Giri DD, Viale A, Olshen AB, Gerald WL, and Massague J. (2005) Nature 436, 518-524

54. Levenson AS, Thurn KE, Simons LA, Valiceasa D, Jarrett J, Ospio C, Jordan VC, Volpert OV, Satcher, Jr. RL and Gartenhaus RB. (2005) Cancer Res. 65, 10651-10656

55. Smith LM, Wise SC, Hendricks DT, Sabichi AL, Bos T, Reddy P, Brown PH, and Birrer MJ. (1999) Oncogene 18, 6063-7070

56. Reinehart-Kim J, Johnston M, Birrer M, and Bos T. (2000) Int. J. Cancer 88, 180-190

57. Lopez-Andreo MJ, Gomez-Fernandez JC, and Coirbalan-Garcia S. (2003) Mol. Biol. Cell 14, 4885-4895

58. Stahelin RV, Digman MA, Medkova M, Ananthanarayanan B, Melowic HR, Rafter JD, and Cho W. (2005) J. Biol. Chem. 280, 19784-19793

59. Chen L, Hahn H, Wu G, Chen CH, Liron T, Schechtman D, Cavallero G, Bancil L, Olli R, Dorn II GW, and Mochly-Rosen D. (2001) Proc. Natl. Acad. Sci. USA 98, 111114-111119

60. Ways DK, Messler BR, Garris TO, Qin W, Cook PP, and Parker PJ. (1992). Cancer Res. 52, 5604-5609

61. Fujihara M, Connolly N, Ito N and Suzuki T. (1994) J. Immunol. 15, 1898-906

62. Chun J, Auer KA, Jacobson BS. (1997) J. Cell Physiol. 173, 361-370

63. Hoy M, Berggren PO, and Gromada J. (2003) J. Biol. Chem. 278, 35168-35171

64. Mendez CF, Leibiger IB, Leibiger B, Hoy M, Gromada J, Berggren PO, and Bertorello AM. (2003) J. Biol. Chem. 278, 44753-4477

65. Jerdeva GV, Yarber FA, Trousdale MD, Rhodes CJ, Okamoto CT, Dartt DA, and Hamm-Alvarez SF. (2005) Am. J. Physiol. Cell Physiol. 289, C1052-C1068

66. Park YS, Hur EM, Choi BH, Kwak E, Jun DJ, Park SJ, and Kim KT. (2006) J. Neurosci. 26, 8999-9005

67. Lee HB, Yu MR, Song JS, and Ha H. (2004) Kidney Int. 65, 1170-1179

68. Ivaska J, Whelan RD, Watson R, and Parker PJ. (2002) EMBO J. 21, 3608-3619

69. Stawowy P, Margeta C, Blaschke F, Lindschau C, Spencer-Hansch C, Leitges M, Biagini G, Fleck E, and Graf K. (2005) Cardiovasc. Res. 67, 50-59

70. Ivaska J, Vuoriluoto K, Huovinen T, Izawa I, Inagaki M, and Parker PJ. (2005) EMBO J. 24, 3834-3845

71. Tachado SD, Mayhew MW, Wescott GG, Foreman TL, Goodwin CD, McJilton MA, and Terrian DM. (2002) J. Cell Biochem. 85, 785-7697

72. Bogatkevich GS, Tourkina E, Abrams CS, Harley RA, Silver RM, and Ludwicka-Bradley A. (2003) Am. J. Physiol. Lung Cell Mol. Physiol. 285, L334-L343

CHAPTER III

POLYMERIC FIBRONECTIN ASSEMBLY ON THE SURFACE OF BREAST CANCER CELLS IS DEPENDENT ON SUBCELLULAR LOCALIZATION OF PKC EPSILON-ACTIN COMPLEX AND PYK2 ACTIVITY*

* Huang L, Pauli BU. Polymeric fibronectin assembly on the surface of breast cancer cells is dependent on subcellular localization of PKCε-actin complex and PYK2 activity. To be submitted to Experimental Cell Research.

ABSTRACT

Lung colonization by breast cancer cells is mediated, at least in part, by interaction of lung endothelial dipeptidyl-peptidase IV (DPPIV; CD26) with breast cancer cell surface polymeric fibronectin (polyFn). PolyFn on the surface of MTF7L rat breast cancer cells has been shown previously to be regulated by protein kinase C epsilon (PKCε). Here, we introduce β-actin and proline-rich tyrosine kinase-2 (Pyk-2) as partners of PKCε in orchestrating the successful polyFn assembly on MTF7L cells. Mimicking conditions of cancer cells disseminating in the blood, MTF7L cells subjected to end-over-end suspension culture exhibit an increasing accumulation of PKCε and F-actin in the subplasmalemmal space beneath emerging polyFn surface aggregates. Translocation of these proteins and polyFn assembly is abrogated by Cytochalasin D, an actin barbed-end capping drug, and to a lesser extent latrunculin B, an actin monomer sequestering drug. PKCε-actin interaction is dependent on PKCε catalytic activity, as shown by treatment of suspended cancer cells with the PKCε inhibitor bisindolylmaleimide XI (BIMXI; Ro-32-0432), but does not involve the unique PKCε actin binding domain. Catalytic activity of Pyk2 is required for successful assembly of polyFn, as shown by the absence of polyFn assembly upon transfection of cancer cells with kinase dead Pyk2. The present study provides new insights into the regulation of the PKCε-mediated polyFn assembly and pulmonary metastasis of breast cancer cells that may harbor new therapeutic potentials.

INTRODUCTION

Cancer cells isolated from blood of rats or mice from malignant breast tumors implanted into the mammary fat pad are adorned with a multi-globular coat of polymeric fibronectin (polyFn) (1). These polyFn aggregates increase in size with time of incubation in suspension and assemble into increasingly deoxycholate-insoluble polymers that can be seen in the top of the stacks of SDS-polyacrylamide gels (1) and on the surface of cancer cells with immunofluorescent staining. Conversion of Fn from the globular (soluble) to the linearized state (insoluble, surface-associated) exposes a cryptic domain in Fn responsible for binding to DPPIV on lung endothelial cells. The DPPIV domain of Fn has been identified as a consensus motif in each of the 13^{th}, 14^{th} and 15^{th} type III repeats of Fn. DPPIV binding is specific for the linearized form of Fn and not for the globular form, facilitating cancer cell adhesion in the presence of high Fn concentrations in the plasma under physiological conditions (1). The cluster arrangement of polyFn aggregates presents multiple binding sites for interaction with DPPIV that strengthens cancer cell and endothelial cell adhesion and enables cancer cell vascular arrest under hemodynamic shear stress (1). These findings are consistent with our studies with rodent models showing reduced lung colonization in Fischer 344/CRJ rats with mutated DPPIV and diminished pulmonary endothelia expression (2) and in DPPIV-/- mice (3).

We have recently elucidated one of the PKCs responsible in mediating polyFn assembly on breast cancer cells. In the rat model of hematogenous dissemination of breast cancer cells, polyFn assembly and lung metastasis critically depends on expression of endogenous cellular Fn (cFn) and is regulated by PKCε (4). Pharmacological inhibition, expression of dominant negative forms of PKCε and knockdown of PKCε lead to decreases in the levels of polyFn on cancer cell surface

and lung colonization (4). Several possible pathways may account for the ability of PKCε to mediate polyFn formation. PKCε may regulate polyFn assembly on the cell surface by phosphorylation of cytoskeletal regulators, through signaling to other signaling pathways and/or control extracellular matrix receptors (5-11). To promote substrate recognition, PKC may directly interact with its substrates (substrates that interact with C-kinase, STICK) or bind to proteins that facilitate substrate phosphorylation (receptors for activated C-kinase, RACK). STICKs localize to a range of specific cellular compartments which includes plasma membrane, cortical cytoskeleton, focal contacts, nucleus and vesicles (5) and allow PKC to perform specialized function. Several PKC substrates, such as myristoylated alanine-rich protein kinase C substrate (MARCKS), have a role of anchoring the actin cytoskeleton to the plasma membrane (6). On the other hand, PKCε may also directly phosphorylate kinases that are able to activate polyFn receptors. PKCε has been shown to play a role in the activation of Pyk2 (7), which is able to bind the phosphorylated integrin beta3 cytoplasmic tail (8) and promote integrin ligand binding ability. Lastly, PKCε may control integrin function. PKCε is involved in inside-out signaling for beta integrin mediated cell adhesion (9-11) and RACK1 has been shown to be one of the mediators of binding between integrin beta chains and PKCε. Whether direct or indirect, integrin activation may indeed be an important pathway in PKCε-mediate polyFn assembly remains to be seen.

In order to further elucidate the role of PKCε in polyFn assembly, we have utilized matrix-assisted laser desorption/ionization time of flight mass spectrometry (MALDI TOF/ m/s) fingerprinting to identify proteins that reside in the PKCε complex under cancer cell-activating conditions. Two cytoskeletal proteins, β-actin, cytoplasmic-2 and myosin IIa (Myh9) have been identified in PKCε immunoprecipitates. Focusing on the contribution of β-actin-2, we report that polyFn

assembly is dependent on PKCε/actin interaction and cytoskeletal integrity. With time of incubation of cancer cell in suspension, PKCε and F-actin translocated in increasing amounts in the subplasmalemmal space at the base of globular polyFn aggregates. This translocation is associated with activation and phosphorylation of Pyk2. Disruption of the PKCε/actin association by actin polymerization blocking agents such as Cytochalasin D and kinase-dead Pyk2 prevent polyFn assembly. Together, our study presents a role of PKCε in the regulation of polyFn assembly through interaction with the actin cytoskeleton and activation of Pyk2.

MATERIAL AND METHODS

Antibodies and Reagents

Rabbit and mouse anti-PKCε polyclonal antibody and mouse anti-β actin antibody for western blotting were from Santa Cruz Biotechnology (Santa Cruz, CA), rabbit anti-Fn polyclonal antibodies that recognized pFn and cFn from both bovine and rat (anti-Fn[pan]: *does not crossreact with fibrinogen, vitronectin, laminin, collagen type IV*) were from Sigma (St. Louis, MO), mouse anti-PKCε used for immunoprecipitation was from BD Biosciences (San Jose, CA), phycoerythrin (PE)-conjugated donkey anti-rabbit, horseradish-peroxidase (HRP)-conjugated donkey anti-rabbit, and HRP-conjugated goat anti-mouse antibodies were from Jackson ImmunoResearch (West Grove, PA), rabbit anti-Pyk2 antibody werefrom Upstate (Lake Placid, NY), and phospho-specific anti-Pyk2(Tyr402) were from Cell Signaling (Danvers, MA). PKC inhibitor BIM XI (Ro-32-0432) was from EMD Chemicals (San Diego, CA). Actin inhibitor Cytochalasin D and Latrunculin B was from Sigma (St. Louis, MO). Fetal bovine serum (FBS) was purchased from Gemini Bio-Products (Woodland, CA). All other chemicals and reagents were from Sigma.

Cell Cultures

MTF7L cells were derived from a lung-metastasis generated by tail-vein injection of MTF7 breast cancer cells (obtained from Dr. D.R. Welch, University of Alabama at Birmingham, Birmingham, AL) into Fischer 344 rats. At an i.v. inoculation dose of $2x10^5$cells/0.3ml PBS per rat, MTF7L cells consistently produce in excess of 400 lung colonies. Cells were grown in culture in Dulbecco's Modified Eagle Medium (DMEM) containing 10% heat-inactivated fetal bovine serum (FBS). For end-over-end (EoE) suspension culture, MTF7L cells were grown to 80 to 90% confluence, then removed from the growth surface by trypsinization [0.25% trypsin, 0.02% EDTA in phosphate-buffered saline (PBS); 10 min, 37°C], washed twice in DMEM containing 10% FBS, and subjected to EoE suspension culture for 1 hour (or as indicated) in 2ml-centrifuge tubes in DMEM plus 20% FBS at a concentration of $5x10^6$ cells/ml (1,13). Tumor cells were used for all experiments within 10 passages from frozen stocks that were tested for metastatic performance immediately prior to freezing.

Plasmids Constructs, Transfection, and Selection

The construct Wild type PKCε (PKCε–WT) cloned into pEGFP-N1 was obtained from Dr. C. Larsson (Lund University, Malmö, Sweden) (12). PKCε with actin binding domain 223-228 deleted (PKCε–ΔABDε) was constructed from PKCε–WT using Quickchange XL Site-directed mutagenesis kit from Stratagene (La Jolla, CA). Wild type FAK, kinase dead FAK (K454R), wild type Pyk2 and kinase dead Pyk2 (K457R) cloned into pKH3 vector were obtained from Dr. Jun-Lin Guan (Cornell University, Ithaca, NY). All plasmid constructs were verified by double-stranded sequencing.

MTF7L cells grown to 70% confluence were transiently transfected with above vector constructs or vector alone using ExGen 500 (Fermentas, Glen Burnie, MD) as described by the manufacturer. Transfection rates were assessed by expression of GFP that is either tagged to the cDNA of interest or co-transfected at a ratio of 1:50 with the cDNA of interest, which were 30-40 %. Cells were used in the various assays 24h after transfection unless otherwise stated.

Flow Cytometry

FACS was used to quantify Fn expression on MTF7L breast cancer cell surfaces (1, 13). Tumor cells that had been subjected to EoE suspension culture were washed twice in DMEM containing 1% bovine serum albumin (BSA), then incubated with rabbit anti-Fn[pan] antibody diluted 1:100 in PBS containing 1%BSA (PBS-BSA) for 1h at 4°C. After washing in PBS-BSA, tumor cells were stained with phycoerythrin (PE)-conjugated donkey anti-rabbit antiserum in PBS-BSA for 1h at 4°C and fixed in 2% paraformaldehyde in PBS. FACS analysis was performed on a Coulter Epics Profile (Coulter Electronics, Hialeah, FL). Nonspecific fluorescence was accounted for by incubating tumor cells with non-immune rabbit serum instead of primary antibody. To quantify the effect of overexpressed proteins on polyFn assembly, we generate bivariate distributions of red fluorescence (y-axis: cells stained with anti-Fn antibodies and PE-conjugated secondary antibodies) and green fluorescence (x-axis: same cells expressing GFP-tagged protein or co-transfected with GFP and cDNA of interest). The levels of polyFn expression in the cell population that emitted high GFP fluorescence were taken as a reflection of the effect of the transfected cDNA on polyFn assembly. X-axis gates were selected based on the staining of MTF7L cells with non-immune rabbit IgG. Y-axis gates were selected based on 50% Fn staining intensity of the vector transfected GFP-positive cells. Cells

in the upper right quadrant of the scatter gram (strong expressers of PKCε and Fn) were expressed as percent of the sum of cells in the right upper and lower quadrants (strong PKCε expressers), providing a quantitative measure of the inhibitory activity of transfected plasmids or pharmacological inhibitors. To assess the effect of inhibitors of cell signaling, tumor cells were incubated with inhibitor 30-min prior to and throughout EoE suspension culture in DME/FBS, then subjected to polyFn quantification as described above. Controls were tumor cells incubated in equimolar inhibitor solvent concentration.

Cell Lysis, Immunoprecipitation, and Western Blotting

Cells were extracted with lysis buffer (50mM Tris-HCl, pH 7.4, 150mM NaCl, 1mM EDTA, 1mM EGTA, 1mM benzamidine chloride, 1mM PMSF, 2 μg/ml leupeptin, 0.27 TIU/ml aprotinin, 0.1mM sodium vanadate, and 1% Triton X-100) for 1h at 4°C (9). Total cell lysates were subjected to: (i) SDS-PAGE (~20-50μg protein) and Western blotting, using anti-Fn[pan], anti-PKCε, anti-PYK2, phospho-specific anti-PYK2 antibodies, anti-β-actin, HRP-conjugated donkey anti-rabbit or goat anti-mouse secondary antibodies and ECL for detection of bound antibody as described (1); (ii) immunoprecipitation with anti-PKCε antibodies (14). Immunoprecipitates obtained from cell lysates were separated by SDS-PAGE (8-10% polyacrylamide) and blotted to nitrocellulose membranes and probed with either anti-PKCε, anti-βactin or anti-pSer and anti-pThr antibodies (1).

Mass Spectrometry

PKCε monoclonal antibody was conjugated to protein-G (PG) agarose beads by incubating antibody with beads for 2 hours at room temperature. PG beads were washed with PBS, washed with borate buffer (0.2M Sodium Borate pH9.0), then

incubated with borate/DMP buffer (0.2M Sodium Borate pH9.0, 20mM dimethyl pimelimidate) for 1 hour at room temperature. After incubation, the beads were incubated with 0.2M ethanolamine twice then incubated in 0.2M ethanolamine for 2 hours room temperature. Beads were transferred to a column and washed with 1% OG lysis buffer (1% Octylglucoside, 50mM Tris-HCl pH 7.4, 150mM NaCl, 1mM $CaCl_2$, 2mM $MgCl_2$, 1mM PMSF, 1mM benzamidine, 0.01 % aprotinin, 0.1% BSA). PKCε was immunoprecipitated on the column from lysates of MTF7L cells activated for 30 minutes in 20%FBS/DME in suspension and immunoprecipitates resolved by SDS–PAGE on 8% or 10% gels. Proteins were visualized with Colloidal Coomassie blue for MALDI TOF m/s, and protein bands were excised and sent for mass spectrometry analysis on MALDI-TOF/TOF 4700 Analyzer (Applied Biosystems) by The Proteomics and Mass Spectrometry Core Facility, Cornell University.

Filamentous actin assay

An actin binding spin-down assay kit, for non-muscle actin (Cytoskeleton Inc, Denver, CO) was used to examine the interaction between PKCε and actin. Briefly, filamentous actin was allowed to form in compatible buffer from globular actin and purified PKCε was added to the solution to react for 30 min. The reaction mixture was ultracentrifuged and separated into supernatant (S) and pellet (P) fractions. S and P fractions were resolved by SDS-PAGE, stained with Coomassie blue and Western probed with anti- PKCε.

Confocal microscopy

Confocal microscopy was used to monitor cytoskeletal actin structure in MTF7L breast cancer cells. Tumor cells that had been subjected to EoE suspension culture were washed twice in DMEM containing 1% bovine serum albumin (BSA),

permeabilized with permeabilization buffer (0.5% TX-100, 20mM HEPES, 3mM $MgCl_2$, 50mM NaCl, 300mM sucrose, 0.02% NaN_3) at room temperature for 10 min, then incubated with phalloidin—fluorescein (to stain for filamentous actin) or mouse anti-PKCε diluted 1:50 or 1:300, respectively, in PBS containing 1%BSA (PBS-BSA) for 1h at 4°C . After washing in PBS-BSA, tumor cells stained with phalloidin were fixed in 2% paraformaldehyde in PBS and those stained with PKCε were washed twice with 0.1% Tween20 in PBS, stained with PE conjugated anti-mouse antiserum for 1h at 4°C, washed twice, then fixed. In select experiments, cells were stained with rabbit anti-Fn as described. Coverslips were mounted onto glass slides using Prolong Antifade (Molecular Probes, Eugene, OR) and viewed by laser scanning confocal microscopy (LSCM). An Olympus Fluoview 500 confocal laser scanning imaging system equipped with argon, krypton, and He-Ne lasers on an Olympus IX70 inverted microscope with a PLAPO 60× objective was used (Olympus America, Inc., Melville, NY). Confocal images were processed using Adobe Photoshop 6.0 (Adobe Systems, Inc., Mountain View, CA).

RESULTS

Mass spectrometry of PKCε complex in MTF7L reveals two cytoskeletal interacting proteins

To identify potential interacting proteins within the PKCε signaling complex, we used a PKCε immunoaffinity column. Proteins that co-immunoprecipitated with PKCε were visualized with Coomassie staining (Fig 3.1A). The bands were excised from the SDS-PAGE gels and subjected to MALDI TOF m/s analysis. Analysis revealed two cytoskeletal proteins that were associated with PKCε, myosin IIa and β-actin-2. In this paper, we shall examine the contribution of β-actin-2 to PKCε-

Figure 3.1: PKCε associates with β-actin: (A) Coomassie blue staining and western blot of PKCε complex: MTF7L cells were suspended in 20% FBS/DMEM for 30 minutes then lysed and immunoaffinity purified on an anti-PKCε antibody conjugated protein G column. Bound proteins were resolved by SDS-PAGE, the gel was stained with Colloidal Coomassie blue, and protein bands were excised for MALDI TOF m/s analysis. Corresponding fractions were ran in duplicate for Western blotting. **(B) β-actin co-immunoprecipitates with PKCε.** Immunoaffinity-purified PKCε fractions #E3 and #E4 from lysed MTF7L cells treated as described above were Western probed with anti-β-actin antibodies. PKCε and β-actin co-immunoprecipitate, while corresponding control mIgG fraction is negative for both PKCε and β-actin. **(C,D) PKCε binds F-actin.** Immunoaffinity purified PKCε was subjected to an F-actin binding assay using Biochem Actin binding spin-down assay kit as described in Material and Methods. Coomassie blue staining (CB) reveals F-actin co-sedimentation of positive control α-actinin, no co-sedimentation for negative control bovine serum albumin (BSA) (C) and PKCε co-sedimentation with F-actin in both eluted fractions E3 and E4 of purified PKCε (D), as confirmed by Western blotting (WB). S, supernatant. P, pellet.

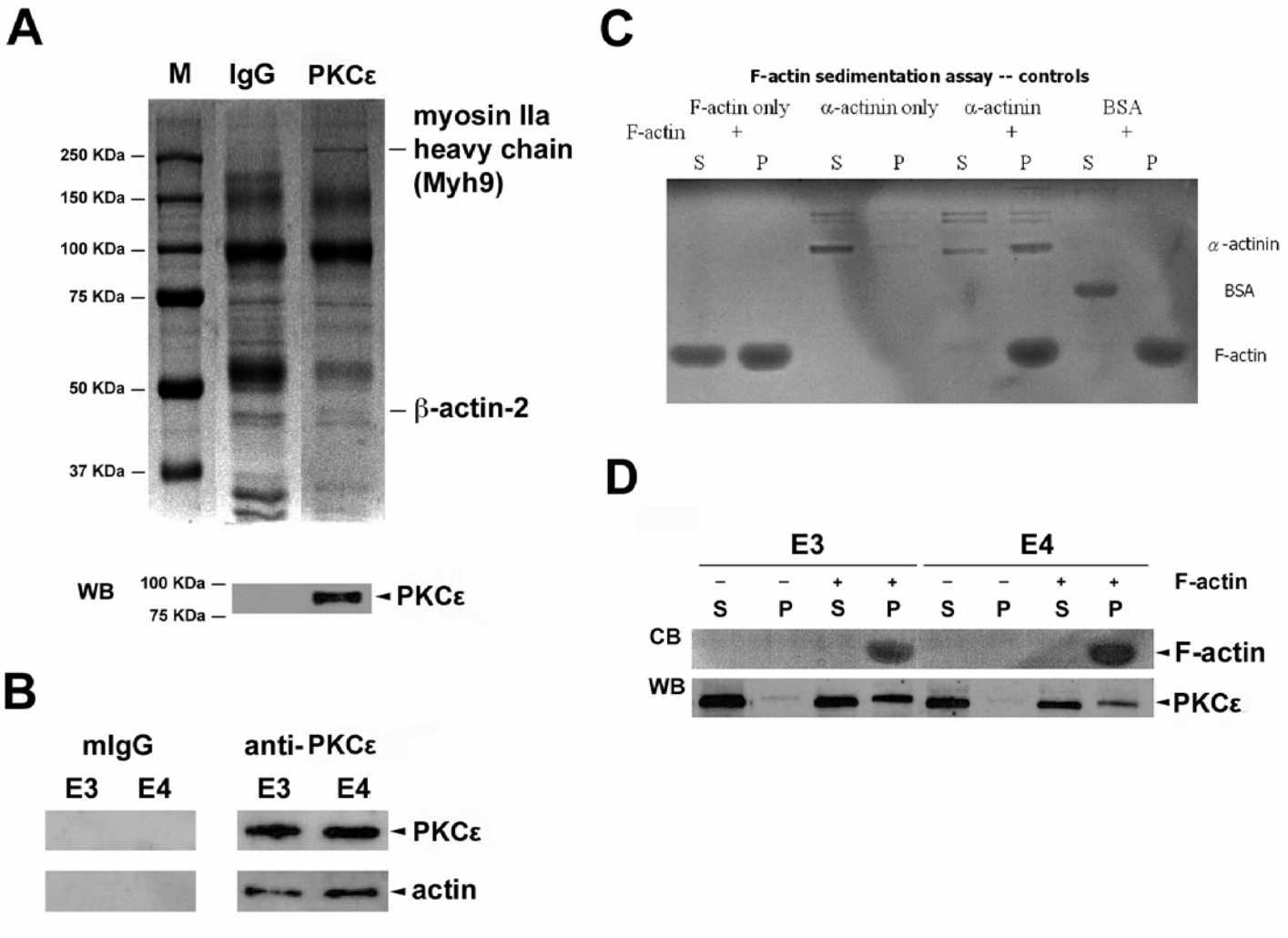
A
M
IgG
PKCε
250 KDa
150 KDa
100 KDa
75 KDa
50 KDa
37 KDa
myosin IIa heavy chain (Myh9)
β-actin-2
WB
100 KDa
75 KDa
PKCε
B
mIgG
anti-PKCε
E3
E4
E3
E4
PKCε
actin
C
F-actin sedimentation assay -- controls
F-actin only
α-actinin only
α-actinin
BSA
F-actin
+
+
+
S
P
S
P
S
P
S
P
α-actinin
BSA
F-actin
D
E3
E4
F-actin
S
P
S
P
S
P
S
P
CB
WB
F-actin
PKCε

mediated polyFn assembly. To confirm the results of MALDI TOF m/s analysis, we used anti-β actin antibody to specifically detect β actin in immunoprecipitates of PKCε. β actin co-immunoprecipitates (co-IP) with PKCε, but not with control mouse(m)IgG nonspecific immunoprecipitates (Fig 3.1B).

To determine whether PKCε binds to functional actin filaments, an in vitro filamentous actin (F-actin) binding assay was performed. Results reveal that PKCε does indeed bind to F-actin, suggesting a cytoskeletal involvement in PKCε-mediated polyFn assembly (Fig 3.1C).

PKCε and F-actin co-immunoprecipitate and colocalize at the subplasmalemmal space beneath polyFn aggregates

PKC subcellular localization determines the specificity of kinase action on cellular function. Interactions with actin-binding proteins, RACKs or direct interaction with actin can position activated PKC at specific membrane domains in proximity of suitable substrate proteins, and further promote substrate phosphorylation. To determine whether PKCε and actin colocalizes at a certain cellular compartment, we utilized fluorescent confocal microscopy to examine the redistribution of activated PKCε in MTF7L cells following suspension culture in FBS. MTF7L cells were treated in EoE suspension in 20% FBS and endogenous PKCε was stained with red fluorescence while filamentous actin (F-actin) was stained with green fluorescence with phalloidin-fluorescein. Staining of PKCε and F-actin and their co-localization is monitored as a function of time in EoE suspension culture (Fig 3.2). At 5 min of EoE suspension culture, much of the PKCε and F-actin are dispersed in a punctate manner throughout the cytoplasm with some F-actin lining the subplasmalemmal space. There is no co-localization of the two molecules. At 10 min of incubation, PKCε and F-actin

Figure 3.2: PKCε colocalization with F-actin in activated MTF7L cells is time and cytoskeletal integrity-dependent: MTF7L cells subjected to EoE suspension for 5, 10 or 30 minutes were stained with anti-PKCε or phalloidin-FITC (for F-actin) and analyzed by confocal microscopy. Confocal images of cells were merged and colocalized images isolated. MTF7L cells show increasing, time-dependent colocalization of PKCε-F-actin in the subplasmalemmal region.

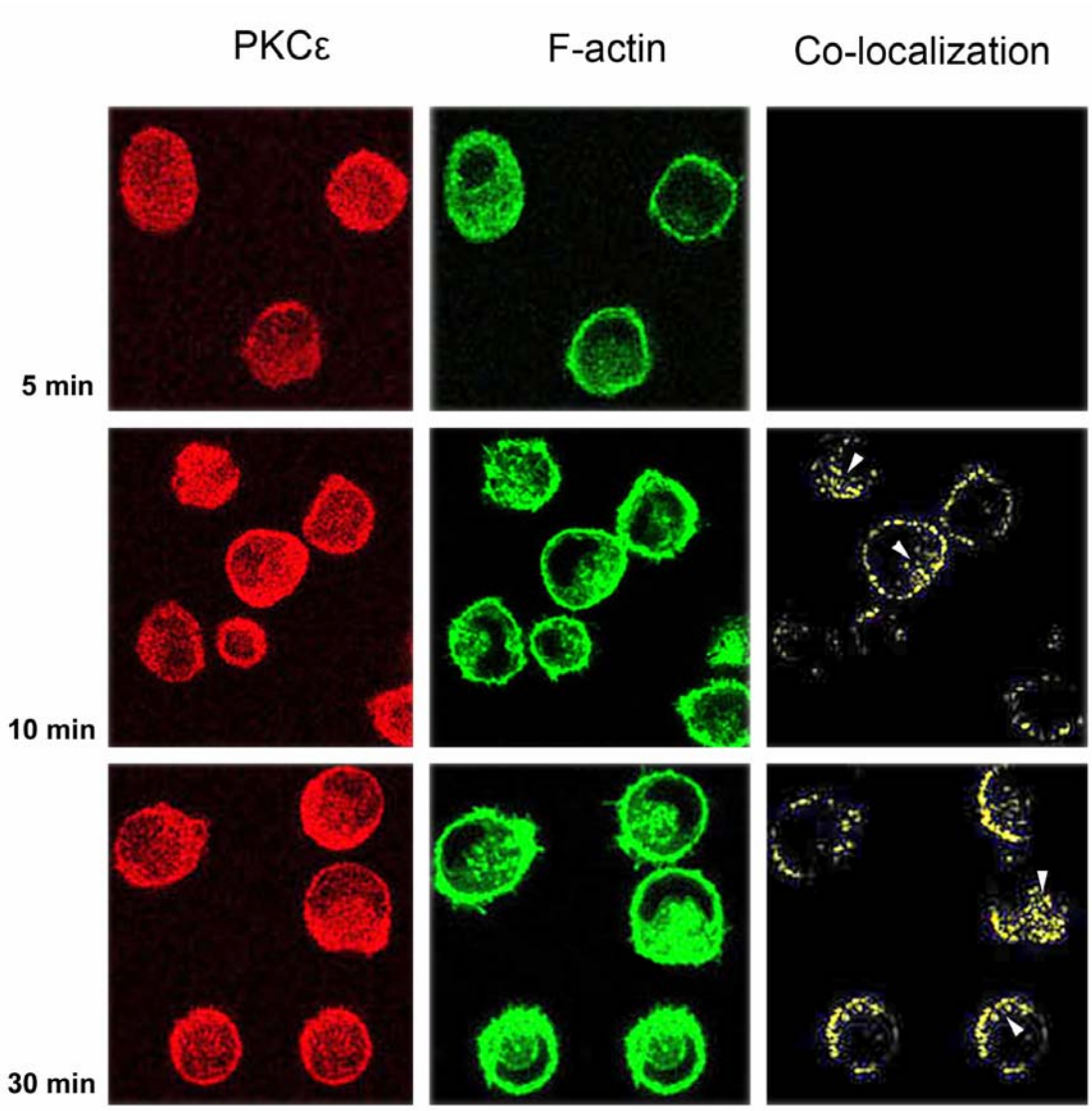
PKCε
F-actin
Co-localization
5 min
10 min
30 min

have both co-segregated to the subplasmalemmal space, where they co-localize in a punctate manner reminiscent of the distribution of polyFn globules on the cancer cell surface. At 30 min of incubation, co-localization of PKCε and F-actin in the subplasmalemmal space is further pronounced.

Confocal microscopy data were complemented by biochemical analyses. MTF7L cells subjected to EoE suspension culture for various periods of time were lysed, and lysates subjected to immunoprecipitation with anti-PKCε antibody. Western blotting of anti-PKCε immunoprecipitates shows that the association of PKCε and actin peaks at 15 minutes, then decreases drastically afterwards (Fig 3.3A). As we have shown previously (4), PKCε phosphorylation peaks at 15 minutes in suspension, correlating to the time point at which PKCε and actin binding occurs at maximum as detected by Western blotting. To determine whether PKCε activity is required for this PKCε-actin association, the inhibitor BIMXI was used at PKCε-inhibitory concentration. BIMXI caused a significant decrease in the association of PKCε and actin after drug inhibition (Fig 3.3B), indicating that PKCε activity is critical in mediating binding of PKCε to the actin cytoskeleton and activation of PKCε most possibly occurs before PKCε-actin association.

F-Actin cytoskeletal integrity is necessary for polyFn assembly and proper PKCε localization

The presence of an intact cytoskeleton has been shown to be critical for Fn matrix assembly in adherent cells (15). The ability of cytoskeleton to control fibronectin assembly may be mediated through regulation of the integrin functional state by interaction with cytoplasmic tails of β integrin (15) or to support proper PKC signaling complex localization (16). To examine whether cytoskeletal integrity is

Figure 3.3: PKCε and actin association: (A) PKCε-actin association is time-dependent. MTF7L cells are treated with FBS for the time points 0, 15, and 30 minutes and PKCε was immunoprecipitated and detected by Western blotting. Blots were subjected to staining with anti-β-actin antibody or anti-PKCε antibody. (B) PKCε -actin association is inhibited by BIMXI**.** MTF7L cells were trypsinized and treated BIMXI (500nM, PKCε inhibitor) for 15 minutes and suspended in 20% FBS/DMEM for 0, 15 and 30 minutes, and processed as above.

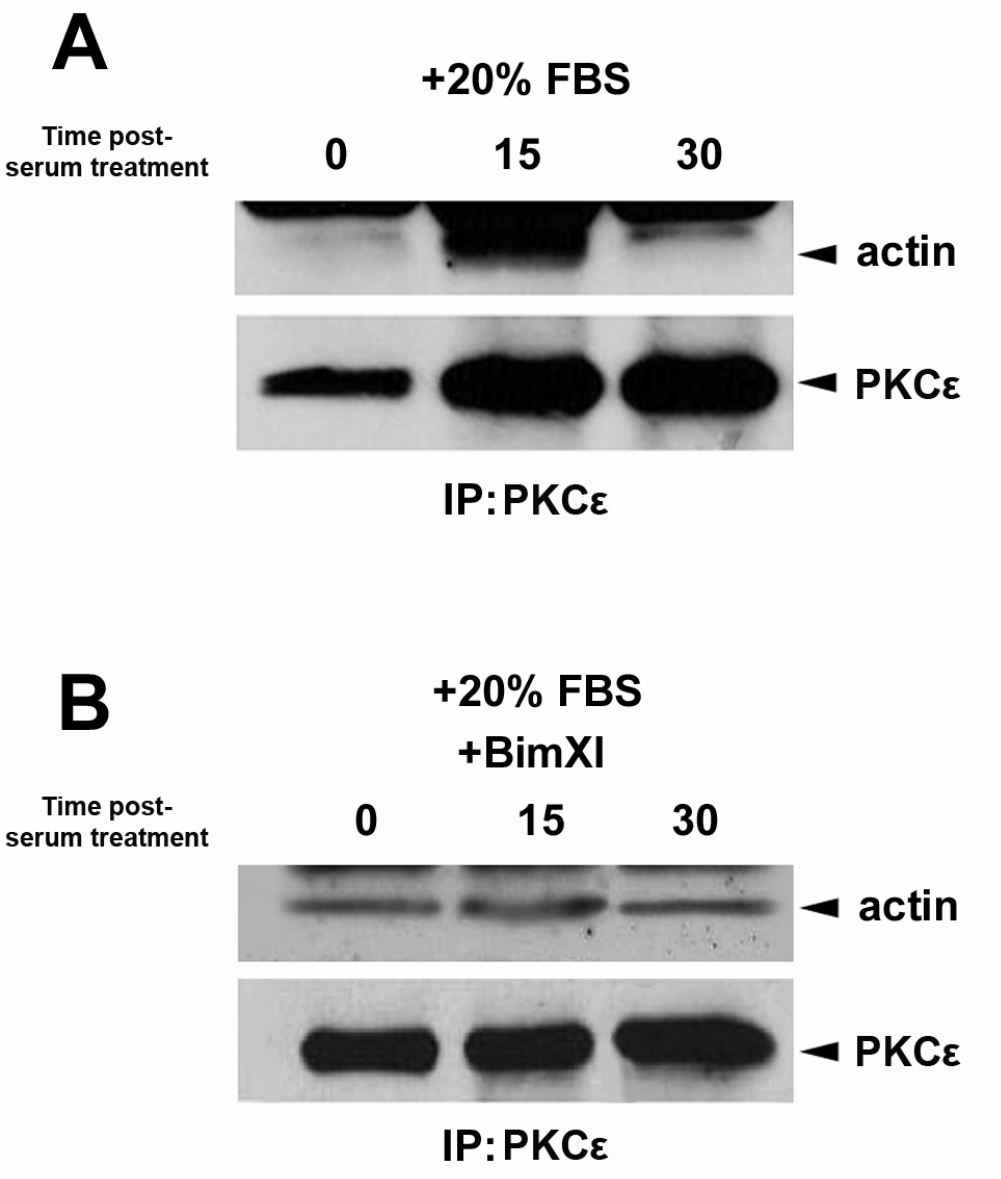
A
+20% FBS
Time post-serum treatment
0
15
30
actin
PKCε
IP: PKCε
B
+20% FBS
+BimXI
Time post-serum treatment
0
15
30
actin
PKCε
IP: PKCε

Figure 3.4: PolyFn assembly is dependent on cytoskeletal integrity: Actin depolymerizing drugs, Cytochalasin D (A) and Latrunculin B (B), block polyFn assembly. MTF7L rat breast cancer cells were exposed for 30min to 1uM, 10uM and 20uM of Cytochalasin D or 200nM and 1uM of Lantrunculin B, and then subjected to EoE suspension culture for 1 hour in the presence of the drug. Cells were stained for poly-Fn and analyzed by FACS, showing a dose-dependent inhibition of polyFn assembly that is confirmed densitometrically and by immunocytochemistry. (C) Cells treated with solvent (DMSO) or Cytochalasin D (CytD), were EoE cultured for 30 minutes in 20% FBS, and then immunostained and processed as described in Figure 3.2. Data show co-localization of PKCε and F-actin in the subplasmalemmal space of DMSO-treated cancer cells and cytoplasmic clusters of PKCε/F-actin complexes in Cytochalasin D-treated cells.

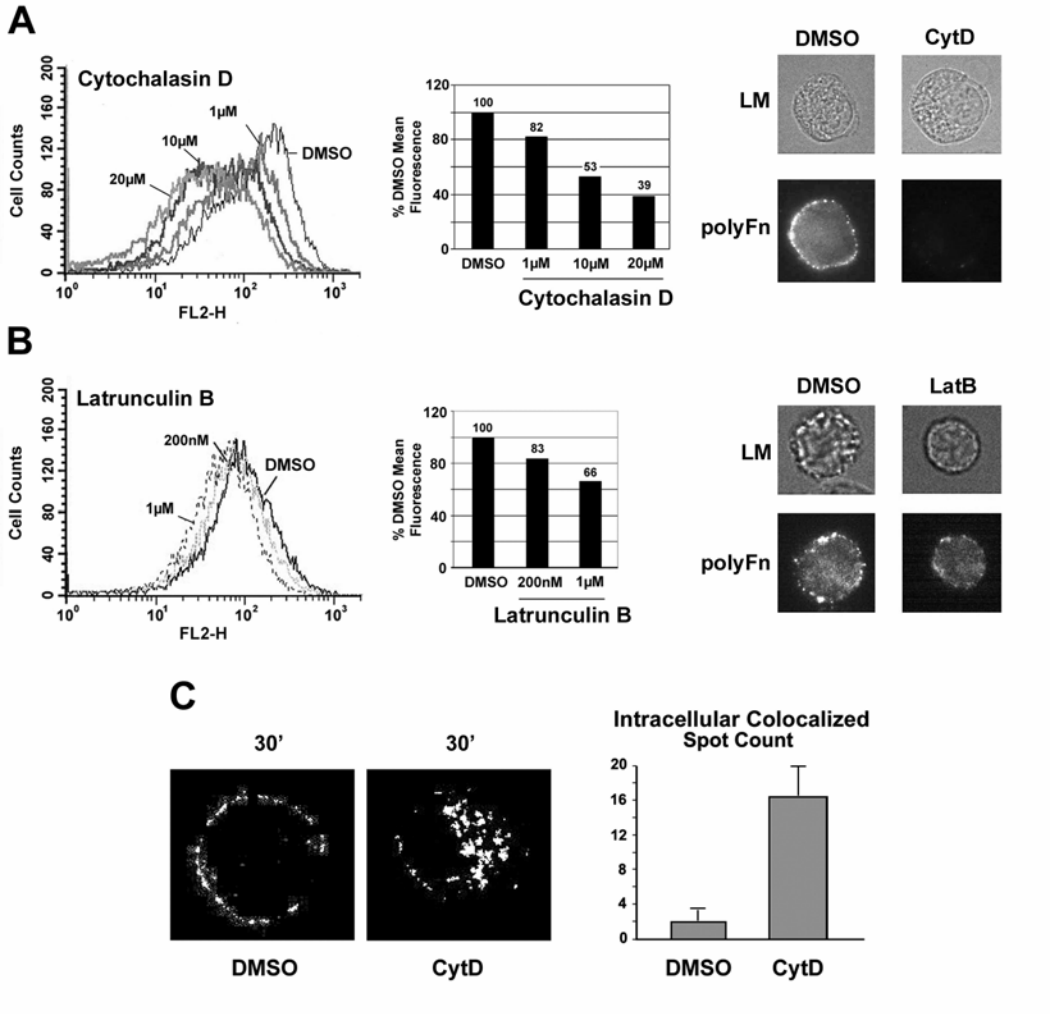
A
Cytochalasin D
Cell Counts
FL2-H
1μM
10μM
20μM
DMSO
% DMSO Mean Fluorescence
100
82
53
39
DMSO
1μM
10μM
20μM
Cytochalasin D
DMSO
CytD
LM
polyFn
B
Latrunculin B
200nM
1μM
DMSO
100
83
66
DMSO
200nM
1μM
Latrunculin B
DMSO
LatB
LM
polyFn
C
30'
30'
DMSO
CytD
Intracellular Colocalized Spot Count
DMSO
CytD

critical for polyFn assembly of breast cancer cells during suspension, we used two inhibitors known to disrupt actin polymerization, Cytochalasin D and Latrunculin B. Both inhibitors were able to block polyFn assembly in MTF7L cells in dose-dependent manners (Fig 3.4A&B), with Cytochalasin D having a more prominent effect. Cytochalasin D impedes actin polymerization by binding to barb ends of actin filaments, blocking addition of monomeric actin to actin filaments, while Latrunculin B blocks actin polymerization by binding to monomeric actin (17,18). The distinct mechanisms of the two inhibitors may explain the differences in the inhibitory activity on polyFn assembly.

To determine whether disturbance of actin cytoskeletal organization would perturb the subcellular localization of the PKCε-actin complex, we used the stronger inhibitor of polyFn assembly, Cytochalasin D. Cytochalasin D treatment resulted in increased cytoplasmic localization of the PKCε-actin binding complex (Fig 3.4C), which is paralleled by diminished polyFn. By altering the subcellular localization of PKCε-actin, Cytochalasin may render PKCε unable to activate downstream signaling components leading to inhibited polyFn assembly. These results suggest that an intact cytoskeletal structure is necessary for and supports the proper localization of the PKCε complex to transduce signals leading to polyFn assembly.

Deletion of proposed Protein kinase Cε actin-binding site is insufficient to block polyFn assembly

A unique actin binding domain of PKCε that is homologous to other actin binding proteins has been identified and localized to amino acids 223-228, located between the C1A and C1B domains (19). A mutant protein lacking this actin binding site is able to perturb proper neurite formation but does not alter its subcellular

Figure 3.5: PKCε actin binding motif is not essential for polyFn assembly: MTF7L breast cancer cells were transfected with wild type PKCε or PKCε deleted of its actin binding domain (cloned into pEGFR-N1), immunostained and analyzed for poly-Fn on FACS. X-axis gates were selected based on the staining of MTF7L cells with non-immune rabbit IgG. Y-axis gates were selected based on 50% Fn staining intensity of the vector transfected GFP-positive cells. Cells in the upper right quadrant of the scatter gram (strong expressers of PKCε and Fn) were expressed as percent of the sum of cells in the right upper and lower quadrants (strong PKCε expressers), providing a quantitative measure of the inhibitory activity of PKCε−△ABD (A). Cell lysates from transfected cells were blotted with anti-GFP antibody to show equal expression levels (B) and also immunoprecipitated with anti-GFP and blotted with actin to show the actin binding activity of each construct (C). (D) Adenovirus-mediated expression of PKCε−△ABD shows identical results. AdWTε, adenoviral PKCε−WT. AdABDε, adenoviral PKCε−△ABD.

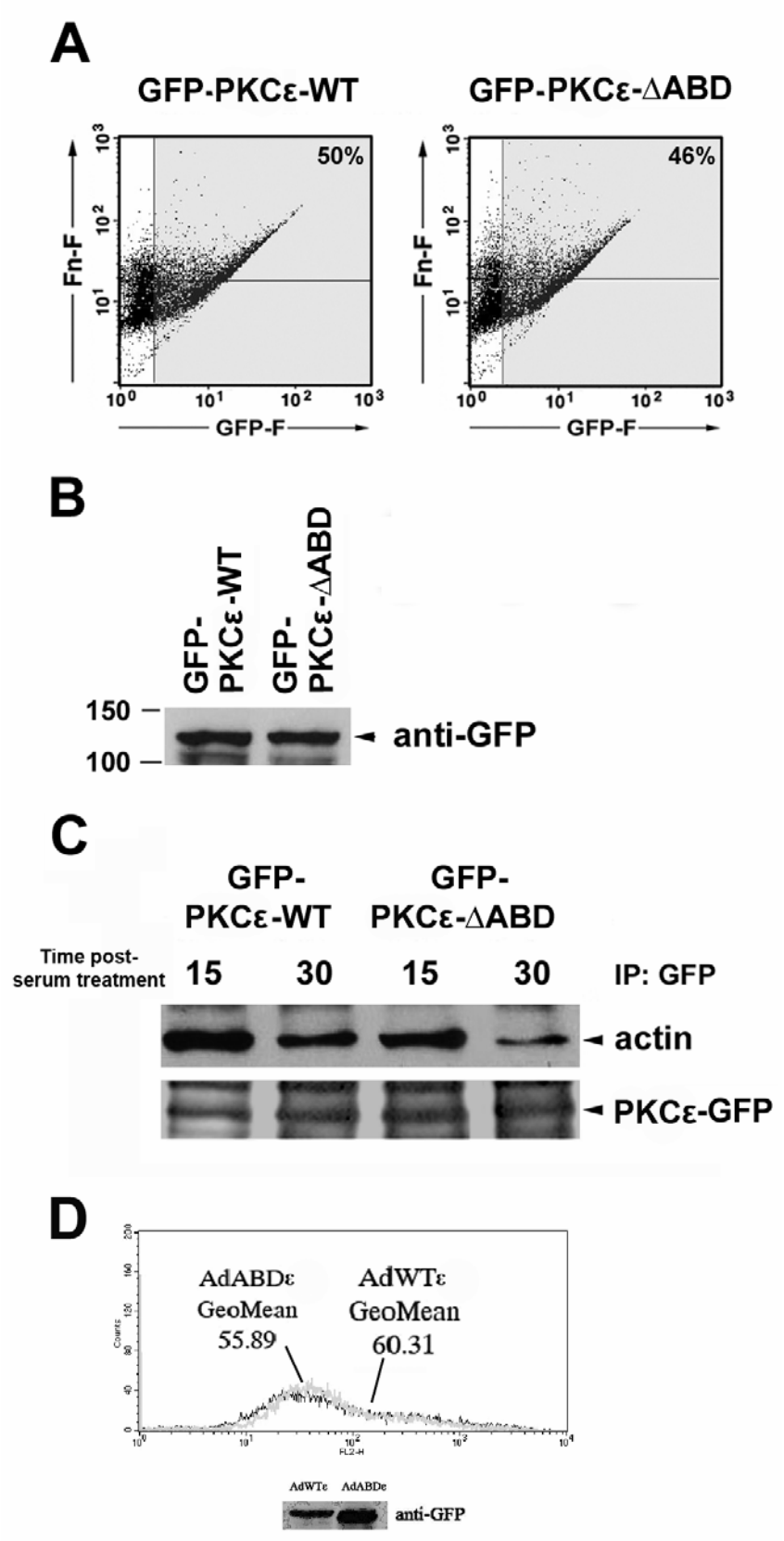
A
GFP-PKCε-WT
GFP-PKCε-ΔABD
50%
46%
Fn-F
GFP-F
B
GFP-PKCε-WT
GFP-PKCε-ΔABD
150
100
anti-GFP
C
GFP-PKCε-WT
GFP-PKCε-ΔABD
Time post-serum treatment
15
30
15
30
IP: GFP
actin
PKCε-GFP
D
AdABDε GeoMean 55.89
AdWTε GeoMean 60.31
Counts
FL2-H
AdWTε
AdABDε
anti-GFP

localization in cells compared to the wild type protein (20). We generated a PKCε construct lacking amino acids 223-228 (PKCε–△ABD) in order to investigate whether deletion of this domain will negatively affect PKCε mediated polyFn assembly. Surprisingly, transfection of PKCε–△ABD into MTF7L cells failed to block surface expression of polyFn (Fig 3.5A). This was not due to differential expression of the transfected proteins, as shown by equal GFP-tagged protein expression (Fig 3.5B). Overexpression of PKCε–△ABD from adenoviral vectors with over 90% transduction rate in MTF7Ls also failed to have any effect on polyFn (Fig 3.5D). These data suggest that the proposed actin binding domain does not have a direct role for PKCε regulated polyFn assembly in MTF7L cells. We then examined whether the mutant PKCε, PKCε–△ABD, is still able to bind β-actin. Immunoprecipitation of the transfected protein PKCε–△ABD revealed that this mutant PKCε still binds β-actin, but seems to have weaker affinity compared to wild type PKCε (Fig 3.5C). It is possible that this residual actin binding still plays a role in supporting polyFn assembly, and that under these circumstances, an alternative pathway or accessory proteins exists in MTF7L cells that is able to compensate for the loss of the actin binding domain in PKCε. The fact that PKCε–△ABD was previously found to localize to the same compartments as wild type PKCε (20) also further highlights the importance of proper PKCε localization to the cortical cytoskeleton.

Pyk2 kinase activity is required for polyFn assembly

Pyk2 has been known to have a role in actin cytoskeleton organization in processes such as cell adhesion and cell migration of several cell types (21). The autophosphorylation and activation of Pyk2 is stress fiber-dependent (21) and its activation is PKCε-dependent in myocytes (7). These facts prompted us to investigate whether or not Pyk2 kinase activity plays a role in polyFn assembly. A Pyk2 kinase

dead (K475A) mutant (Pyk2-KD) was used to transfect MTF7L cells in comparison to Pyk2 wild type (Pyk2-WT). Wild type and kinase dead mutant of the other focal adhesion kinase member, FAK, were also transfected in MTF7 cells for comparison. 24 hours after transfection, the cells were subjected to EoE suspension culture for 1h, then stained with anti-Fn antibody to detect surface assembled polyFn. Results show that the introduction of kinase dead Pyk2 partially impaired the ability of the cells to form surface Fn aggregates (Fig 3.6A&B), demonstrating the active role of Pyk2 during the course of polyFn formation on the cancer cell surface. In contrast, kinase-dead FAK had no effect on polyFn assembly (Fig 3.6A).

To further examine whether or not Pyk2 autophosphorylation correlates with the course of polyFn assembly in our assay, MTF7L cells were serum-starved overnight and incubated in an EoE suspension culture in FBS for the indicated time points. Cell lysates were probed for phosphorylated Pyk2 content (pPyk2). The time course experiment indicated that pPyk2 peaked at 10 minutes of incubation (Fig 3.6C), coinciding with the peak of PKCε phosphorylation as previously shown (4). The close occurrence of phosphorylation of PYK2 and PKCε suggests that one protein could be regulating the phosphorylation of the other. Since a previous study in rat ventricular myocytes has shown that PKCε regulates Pyk2, we were eager to know whether or not diminished PKCε will have an effect on Pyk2 activation. Indeed, the PKCε inhibitor BIMXI concentration markedly decreased phosphorylation of Pyk2 (Fig 3.6D). Similar results were obtained when cells were treated with Cytochalasin D (Fig 3.6D). This suggests that Pyk2 activation is downstream of PKCε and that abnormal subcellular localization of PKCε under disrupted cytoskeletal organization will abrogate PKCε downstream signaling to Pyk2.

Salicylate, the known Pyk2 inhibitor, is able to abrogate the phosphorylation of the PKCε mediated Pyk2 phosphorylation (22). We tested this inhibitor for its effects

Figure 3.6: Pyk2 kinase activity is required for polyFn assembly: (A&B) MTF7L breast cancer cells were transiently transfected with wild type or kinase-dead FAK and Pyk2 and 24h later subjected to EoE suspension culture in DMEM+20%FBS for 1h at 37℃. Cells expressing equal amounts of wild type and kinase-dead FAK and Pyk2 were stained with anti-Fn antibodies and analyzed by dual-color FACS as described. **(A)** and Fn-immunocytochemistry **(B).** Kinase-dead Pyk2 but not FAK impairs polyFn assembly. **(C)** Time-dependent Pyk2 phosphorylation: Pyk2-transfected MTF7L cells were suspended for the indicated time periods in DMEM+20%FBS, then lysed. Lysates were separated by SDS-PAGE, blotted onto nitrocellulose and probed with phosphor-specific Pyk2(Y402) antibody or anti-Pyk2 antibody. (D) BIMXI and Cytochalasin D (CytD) inhibit Pyk2 phosphorylation: MTF7 cells were trypsinized and treated with BIMXI (500nM) or CytD(1μM) for 15 min, then subjected to EoE suspension in 20% FBS/DMEM for 0,15, and 30 min, lysed and lysates resolved by SDS-PAGE (10% gel) and Western probed with anti-Pyk2 and phosphor-specific anti-Pyk2 antibodies. (E) MTF7L cells pretreated with sodium salicylate (10 or 20mM) for 30 min, then subjected to EoE suspension (1h; DMEM+20%FBS) were stained with anti-Fn and analyzed by FACS. The Pyk2 inhibitor salicylate inhibits polyFn assembly in a dose-dependent manner.

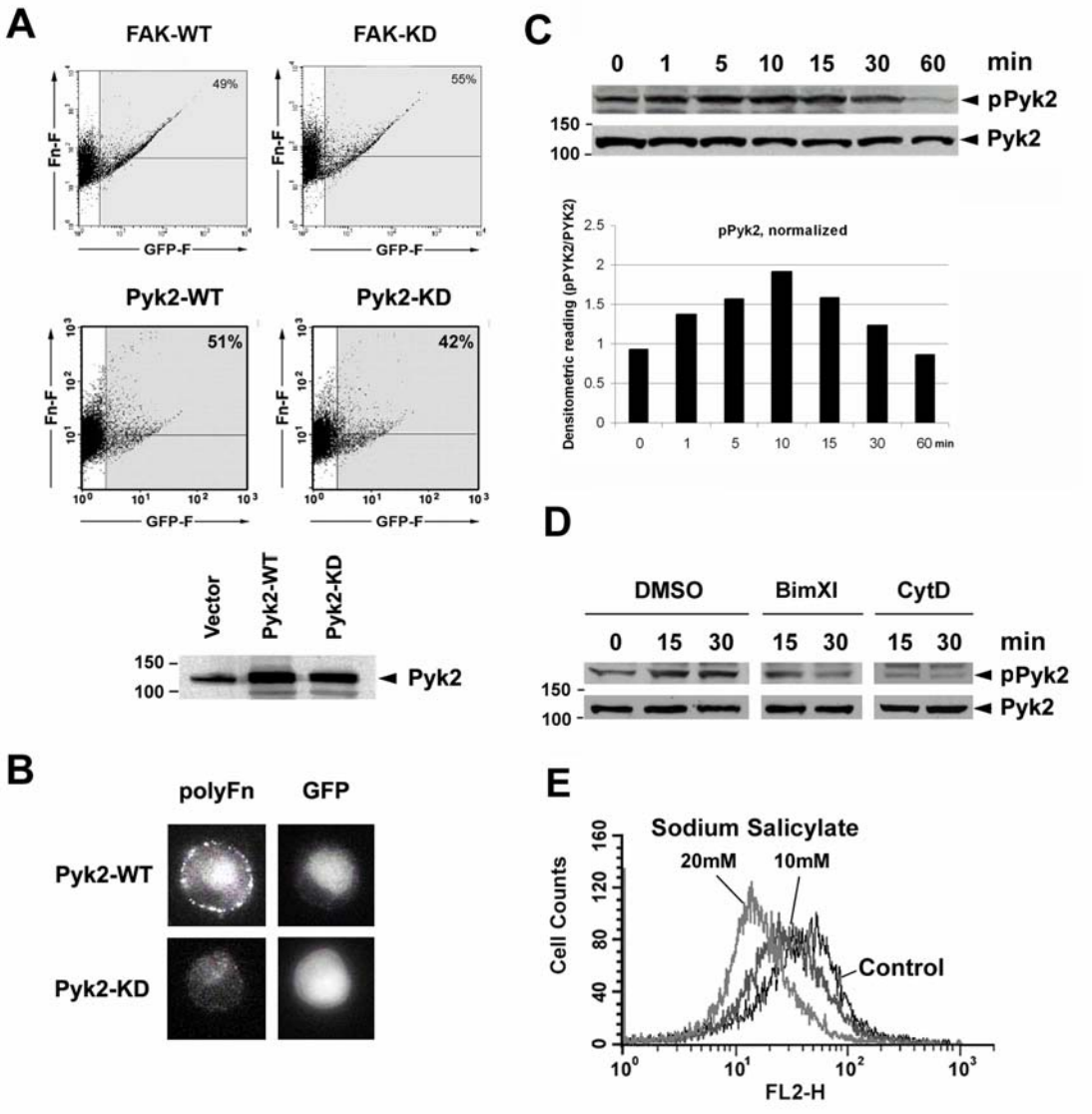
A
FAK-WT
FAK-KD
49%
55%
Fn-F
GFP-F
Pyk2-WT
Pyk2-KD
51%
42%
Vector
Pyk2-WT
Pyk2-KD
150
100
Pyk2
B
polyFn
GFP
Pyk2-WT
Pyk2-KD
C
0 1 5 10 15 30 60 min
pPyk2
Pyk2
pPyk2, normalized
Densitometric reading (pPYK2/PYK2)
2.5
2
1.5
1
0.5
0
0 1 5 10 15 30 60 min
D
DMSO
BimXI
CytD
0 15 30 15 30 15 30 min
pPyk2
Pyk2
E
Sodium Salicylate
20mM
10mM
Control
Cell Counts
FL2-H

on polyFn and found that it abolished polyFn formation at the proposed working concentrations (Fig 3.6E).

DISCUSSION

Early work on PKCε has linked it to oncogenic transformation of cells. The oncogenic activity has been reported in fibroblasts, colonic cell lines, prostate epithelial cell lines and breast cancer cell lines (23-26). In mice, epidermis-specific transgenic overexpression of wild type PKCε resulted in development of metastatic squamous cell carcinomas (27). High-density tissue microarray analysis revealed significant positive correlation between PKCε and tumor histologic grade, while knockdown of PKCε reduced breast cancer cell invasiveness and lung metastasis (26). In our previous study, impairment of PKCε in rat breast cancer cells by a dominant negative construct and specific drug inhibitors leads to decreased polyFn assembly and reduced lung colonization (4). The converging signaling events of PKCε and the actin cytoskeleton is a potential mechanism underlying these oncogenic processes.

Many approaches have been used to identify PKC binding partners in order to understand the role of PKC in different cellular functions (28). Mass spectrometry results have showed that PKCε associates with proteins including β'Cop, cytokeratins, cardiac myofibrils, matrin3, transferin, Rac GAP1 and vimentin. (16,29,30). Many of the binding proteins identified within the PKCε complex are putative PKC substrates such as MARCKS and STICKS, while others are not phosphorylated by PKC and may function as anchoring proteins or regulators of substrate phosphorylation, facilitating integration of PKC signaling into other pathways (5,16,19,29). Our current study presents two cytoskeletal interacting partners of PKCε potentially involved in mediating polyFn assembly. This finding is consistent with a previous study

performed in fibroblasts (28), which found that both actin and myosin IIa co-immunoprecipitated with PKCε but are not substrates of PKCε. We have tested the myosin ATPase inhibitors 2,3-Butadione monoxime (31) and blebbistatin (32) and it seems that myosin ATPase activity is not involved in our cellular function in polyFn assembly (Fig 3.7 A&B). Although PKCε does not directly regulate myosin phosphorylation (28), it is still possible that PKCε is able to modulate myosin activity non-catalytically or that myosin can regulate PKCε activity. The role of myosin IIa in the PKCε complex may also be to bridge PKCε to actin stress fibers or to strengthen the association of PKCε and F-actin.

PKC activity is regulated through differential recruitment by PKC isotype-specific binding proteins localized in different subcellular domains, which facilitates PKC localization to activate proteins in a particular cellular compartment (19,30,33). Subcellular localization is a key event in PKC functional and regulatory specificity. We show that both PKCε activity and cytoskeletal integrity is required for PKCε-actin association in MTF7L cells and that PKCε increasingly associates with actin in a time dependent manner. Inhibition of PKCε activity diminishes this response, suggesting that the catalytic component of PKCε could play a role in either its initial binding to actin or strengthen the binding interaction and that PKCε must be activated before binding to the actin cytoskeleton. Perturbing the cytoskeleton by Cytochalasin D prevents PKCε translocation from the cytoplasm to the plasma membrane, resulting in abrogation of polyFn assembly on tumor cell surfaces. Therefore, we propose that upon PKCε activation, PKCε binds to intact F-actin cytoskeleton, which sustains PKCε activity and PKCε translocation to the plasma membrane and facilitates downstream activation of Pyk2 to promote successful polyFn assembly.

Interaction between PKCε and F-actin has been shown to activate PKCε (19,34) and the PKCε actin binding domain has been mapped to amino acids 223-228.

Figure 3.7: Inhibitors of myosin ATPase activity had no effect on polyFn assembly: MTF7L cells pretreated with blebbistatin (100μM or 200μM) (A) and 2,3-Butadione monoxime (BDM) (20 μM) (B) for 30 min, then subjected to EoE suspension (1h; DMEM+20%FBS) were stained with anti-Fn and analyzed by FACS.

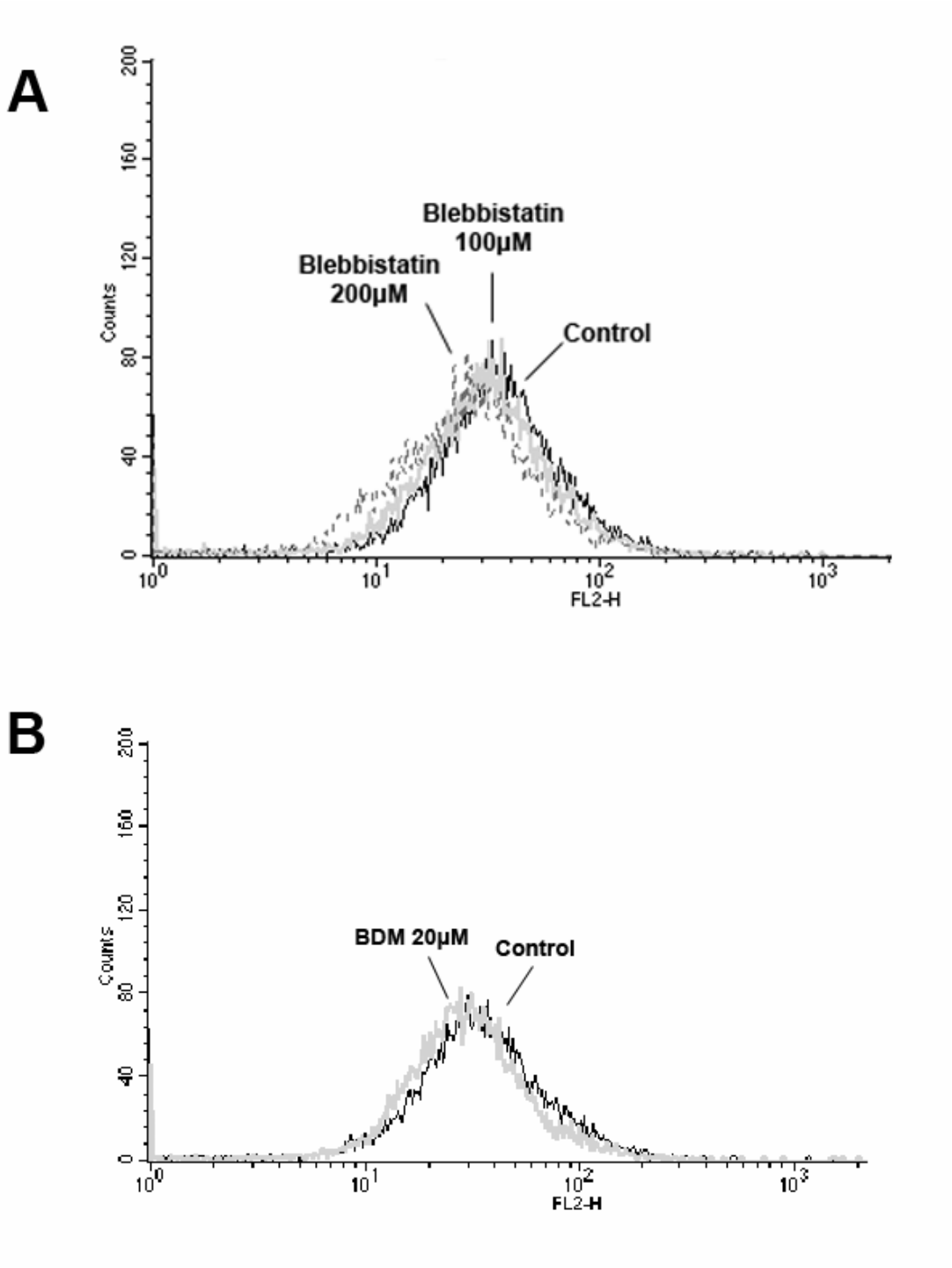
A
Blebbistatin
100μM
Blebbistatin
200μM
Control
Counts
FL2-H
B
BDM 20μM
Control
Counts
FL2-H

In our results, deletion of the proposed actin binding site of PKCε was insufficient to block the formation of polyFn on breast cancer cells and PKCε activation seems to be a prerequisite for actin binding. Immunoprecipitation of wtPKCε-GFP and PKCε−△ ABD -GFP revealed residual levels of actin binding. The residual actin binding may be due to the existence of an alternate actin binding site of PKCε or through alternative pathways via supporting proteins such as other actin-binding proteins within the cells that can bind PKCε to the cytoskeleton. On the other hand, the fact that PKCε−△ABD overexpression failed to abrogate polyFn assembly could be due to the fact that PKCε−△ABD still retains the wild type protein subcellular localization (20) and that subcellular localization is the crucial factor in the relationship of actin cytoskeleton and PKCε in this study. The proximity of both wild type PKCε and PKCε−△ABD, which both possess the catalytic domain, to the cytoskeleton and/or plasma membrane compartment may be the main feature responsible for downstream signaling leading up to polyFn assembly. Hence, the mere absence of the actin-binding site may not be truly sufficient to induce a significant effect on polyFn formation when the mutant protein maintains proper localization that supports PKCε to activate the necessary proteins at its cytoskeletal signaling site.

Pyk2 and FAK are highly homologous in sequence and share a similar structural organization (35). Despite of the high similarity, the two proteins seems to be differentially regulated. Although phosphorylation of FAK and Pyk2 can both be controlled by integrin engagement, Pyk2 response to soluble factors such as angiotensin II is dramatically stronger in certain cells, while FAK is mainly regulated by integrin-mediated cell adhesion (35). Pyk2 and FAK also associate with the cytoskeleton and with integrin signaling complexes by complexing to proteins such as Src kinases, p130 Cas, paxillin and Graf1 (36). FAK C-terminal domain binds the integrin-associated protein talin while Pyk2 binds the actin-associated protein gelsolin

(37), which can further account for their differential functions. In this study, we show that Pyk2 is the main adhesion kinase responsible for downstream signaling from PKCε to polyFn assembly of MTF7L cells, indicated by the ability of kinase dead Pyk2 and the Pyk2 inhibitor salicylate to impair polyFn formation. Inhibition of PKCε by BIMXI, which also blocks polyFn assembly (4), inhibits time-dependent activation of Pyk2 in MTF7L cells. The relationship of PKCε and Pyk2 is consistent with a previous study which shows that constitutively active PKCε increases endothelin-1 induced Pyk2 phosphorylation while kinase inactive PKCε inhibited Pyk2 phosphorylation (7). Pyk2 has been implicated in integrin inside-out signaling by associating with beta3 integrins (38) and this could be a possible pathway by which Pyk2 regulates polyFn assembly. The phosphorylated beta3 integrin cytoplasmic tail provides a binding site for Pyk2 (8). Pyk2 has the FERM domain that contains a phosphotyrosine binding domain (PTB) domain similar to talin, which is also able to bind beta3 tail and trigger activation for ligand binding (39). Cellular signal induces the conformational change of talin allowing it to bind to the beta integrin tail and unclasps the complex between the alpha and beta integrin cytoplasmic tails, which causes a conformational shift in the extracellular head domain and renders it more extended for high affinity ligand binding (39). Pyk2 binding to the integrin cytoplasmic tails could have a similar impact on the polyFn receptor and activate the integrins for fibronectin binding and subsequent polyFn assembly.

Results obtained in this study are summarized in Fig 3.8A. In our working model (Fig 3.8B), we propose that in MTF7L cells subjected to EoE suspension culture PKCε is activated and phosphorylated and associates with F-actin in the cytoplasm, presumably at secretory vesicle located in the vicinity of the Golgi complex (Fig 3.2, arrows). The PKCε-actin complex then translocates in increasing

Figure 3.8: Diagram of cellular processes in polyFn assembly: (A) Summary of effects of various treatments performed in this study, providing the relationship of subcellular localization of PKCε, actin and polyFn. (B) Signaling pathway in polyFn assembly. Soluble ligands in the plasma activates PKCε through receptor binding, PKCε translocates to the membrane and cortical cytoskeleton, activates PYK2 in proximity. Activated PYK2 activates the beta integrin cytoplasmic tail domain and extracellular domain of integrin is rendered extended for ligand binding. Phosphorylated protein marked with "p".

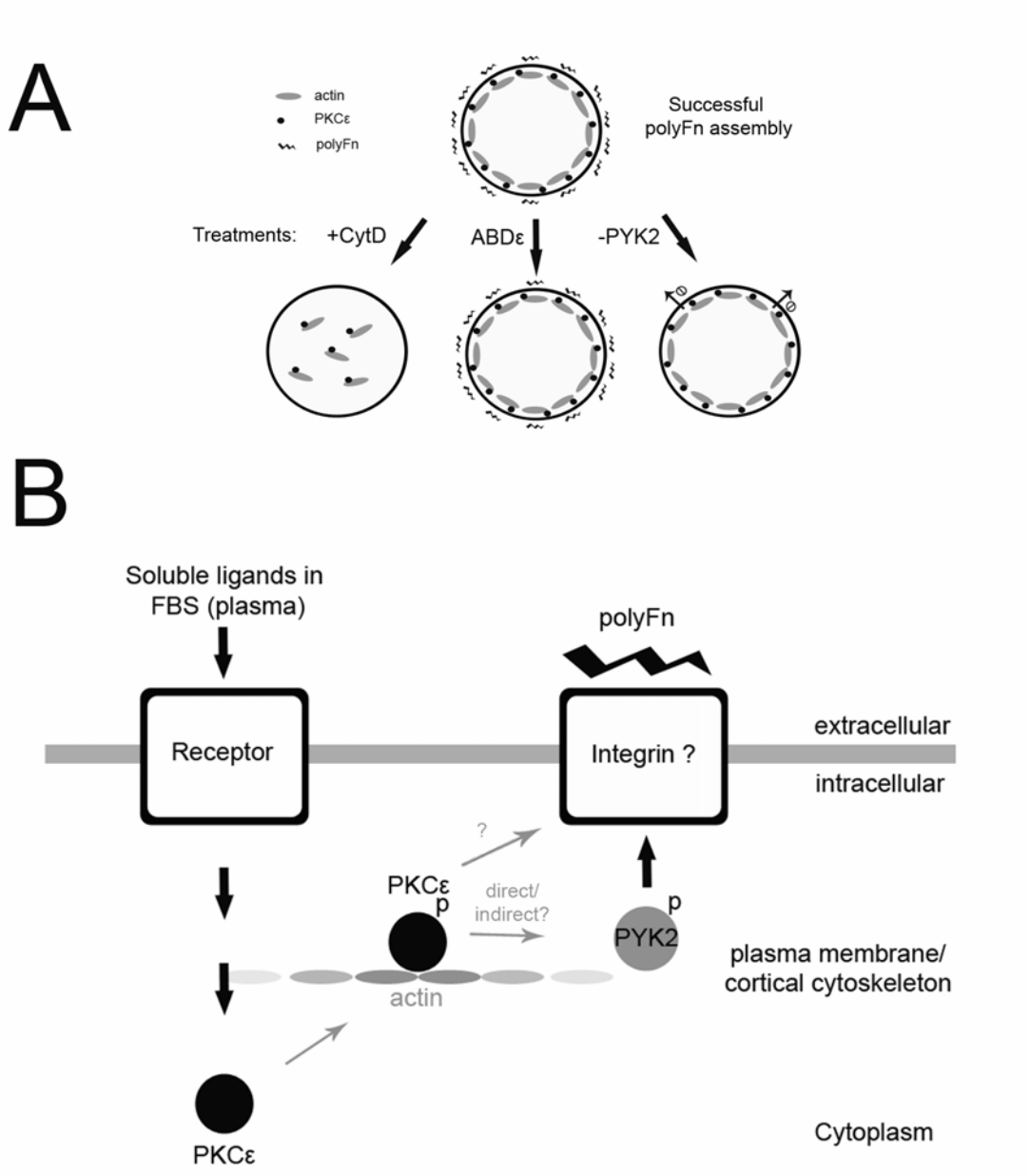
A
actin
PKCε
polyFn
Successful
polyFn assembly
Treatments:
+CytD
ABDε
-PYK2
B
Soluble ligands in
FBS (plasma)
polyFn
Receptor
Integrin ?
extracellular
intracellular
?
PKCε
p
direct/
indirect?
p
PYK2
plasma membrane/
cortical cytoskeleton
actin
PKCε
Cytoplasm

amounts (10-30min) to the subplasmalemmal space, which is prevented by Cytochalasin D as shown by the intracellular accumulation of PKCε/actin complexes (Fig 3.4). Whether the PKCε-mediated activation of Pyk2 happens immediately following complexing of PKCε/F-actin in the cytosolic compartment or at the plasma membrane in unclear. However, strong phosphorylation of Pyk2 as early as 1-5 min after subjecting MTF7L cells to EoE suspension culture (Fig 3.6C), i.e., prior to the appearance of PKCε/F-actin complexes in the subplasmalemmal space (Fig 3.2), suggests that Pyk2 is activated in the cytosol. At Golgi-derived secretory vesicles (Fig 3.2, arrows), PKCε and/or Pyk2 could well serve as activator(s) of β integrins, collaborating with talin to promote integrin activation and clustering (39) and to initiate the assembly of Fn/integrin complexes in secretory vesicles. As secretory vesicles fuse with plasma membrane, Fn is exposed at the cell surface, where it serves as a scaffold for Fn-Fn self association with plasma Fn into insoluble polymeric complexes (1). Such mechanism is supported by siRNA Fn-knockdown experiments in which polyFn is dramatically reduced, albeit cancer cells are exposed to high plasma Fn concentration in EoE suspension culture (4). Similarly, human MCF7 breast cancer cells that do not express Fn yet have a similar β1 integrin expression profile as MTF7L (40) are unable to assemble polyFn on their surfaces in medium containing 20% FBS or plasma Fn (Pauli et al., personal communication). Together, our data provided novel information of the polyFn assembly process, that in previous studies from our laboratory has been shown to be an integral part of cancer cells' ability to colonize the lungs (1,2,4).

REFERENCES

1. Cheng, H. C., Abdel-Ghany, M., Elble, R. C., and Pauli, B. U. (1998) J Biol Chem 273(37), 24207-24215

2. Cheng, H. C., Abdel-Ghany, M., Zhang, S., and Pauli, B. U. (1999) Clin Exp Metastasis 17(7), 609-615

3. Johnson, R. C., Zhu, D., Augustin-Voss, H. G., and Pauli, B. U. (1993) J Cell Biol 121(6), 1423-1432

4. Huang, L., Cheng, H. C., Isom, R., Chen, C. S., Levine, R. A., and Pauli, B. U. (2008) J Biol Chem 283(12), 7616-7627

5. Jaken, S., and Parker, P. J. (2000) Bioessays 22(3), 245-254

6. Disatnik, M. H., Boutet, S. C., Pacio, W., Chan, A. Y., Ross, L. B., Lee, C. H., and Rando, T. A. (2004) J Cell Sci 117(Pt 19), 4469-4479

7. Bayer, A. L., Heidkamp, M. C., Howes, A. L., Heller Brown, J., Byron, K. L., and Samarel, A. M. (2003) J Mol Cell Cardiol 35(9), 1121-1133

8. Butler, B., and Blystone, S. D. (2005) J Biol Chem 280(15), 14556-14562

9. Stawowy, P., Margeta, C., Blaschke, F., Lindschau, C., Spencer-Hansch, C., Leitges, M., Biagini, G., Fleck, E., and Graf, K. (2005) Cardiovasc Res 67(1), 50-59

10. Besson, A., Wilson, T. L., and Yong, V. W. (2002) J Biol Chem 277(24), 22073-22084

11. Palmantier, R., George, M. D., Akiyama, S. K., Wolber, F. M., Olden, K., and Roberts, J. D. (2001) Cancer Res 61(6), 2445-2452

12. Zeidman, R., Lofgren, B., Pahlman, S., and Larsson, C. (1999) J Cell Biol 145(4), 713-726

13. Cheng, H. C., Abdel-Ghany, M., and Pauli, B. U. (2003) J Biol Chem 278(27), 24600-24607

14. Abdel-Ghany, M., Cheng, H. C., Elble, R. C., and Pauli, B. U. (2001) J Biol Chem 276(27), 25438-25446

15. Wu, C., Keivens, V. M., O'Toole, T. E., McDonald, J. A., and Ginsberg, M. H. (1995) Cell 83(5), 715-724

16. Keenan, C., and Kelleher, D. (1998) Cell Signal 10(4), 225-232

17. McAvey, B. A., Wortzman, G. B., Williams, C. J., and Evans, J. P. (2002) Biol Reprod 67(4), 1342-1352

18. Wakatsuki, T., Schwab, B., Thompson, N. C., and Elson, E. L. (2001) J Cell Sci 114(Pt 5), 1025-1036

19. Prekeris, R., Mayhew, M. W., Cooper, J. B., and Terrian, D. M. (1996) J Cell Biol 132(1-2), 77-90

20. Zeidman, R., Troller, U., Raghunath, A., Pahlman, S., and Larsson, C. (2002) Mol Biol Cell 13(1), 12-24

21. Wu, S. S., Jacamo, R. O., Vong, S. K., and Rozengurt, E. (2006) Cell Signal 18(11), 1932-1940

22. Wang, Z., and Brecher, P. (2001) Hypertension 37(1), 148-153

23. Tachado, S. D., Mayhew, M. W., Wescott, G. G., Foreman, T. L., Goodwin, C. D., McJilton, M. A., and Terrian, D. M. (2002) J Cell Biochem 85(4), 785-797

24. Perletti, G. P., Concari, P., Brusaferri, S., Marras, E., Piccinini, F., and Tashjian, A. H., Jr. (1998) Oncogene 16(25), 3345-3348

25. Wu, D., Foreman, T. L., Gregory, C. W., McJilton, M. A., Wescott, G. G., Ford, O. H., Alvey, R. F., Mohler, J. L., and Terrian, D. M. (2002) Cancer Res 62(8), 2423-2429

26. Pan, Q., Bao, L. W., Kleer, C. G., Sabel, M. S., Griffith, K. A., Teknos, T. N., and Merajver, S. D. (2005) Cancer Res 65(18), 8366-8371

27. Jansen, A. P., Verwiebe, E. G., Dreckschmidt, N. E., Wheeler, D. L., Oberley, T. D., and Verma, A. K. (2001) Cancer Res 61(3), 808-812

28. England, K., Ashford, D., Kidd, D., and Rumsby, M. (2002) Cell Signal 14(6), 529-536

29. Csukai, M., Chen, C. H., De Matteis, M. A., and Mochly-Rosen, D. (1997) J Biol Chem 272(46), 29200-29206

30. Xu, T. R., and Rumsby, M. G. (2004) FEBS Lett 570(1-3), 20-24

31. Soeno, Y., Shimada, Y., and Obinata, T. (1999) Cell Tissue Res 295(2), 307-316

32. Shu, S., Liu, X., and Korn, E. D. (2005) Proc Natl Acad Sci U S A 102(5), 1472-1477

33. Csukai, M., and Mochly-Rosen, D. (1999) Pharmacol Res 39(4), 253-259

34. Prekeris, R., Hernandez, R. M., Mayhew, M. W., White, M. K., and Terrian, D. M. (1998) J Biol Chem 273(41), 26790-26798

35. Zheng, C., Xing, Z., Bian, Z. C., Guo, C., Akbay, A., Warner, L., and Guan, J. L. (1998) J Biol Chem 273(4), 2384-2389

36. Ivankovic-Dikic, I., Gronroos, E., Blaukat, A., Barth, B. U., and Dikic, I. (2000) Nat Cell Biol 2(9), 574-581

37. Mitra, S. K., Hanson, D. A., and Schlaepfer, D. D. (2005) Nat Rev Mol Cell Biol 6(1), 56-68

38. Pfaff, M., and Jurdic, P. (2001) J Cell Sci 114(Pt 15), 2775-2786

39. Qin, J., Vinogradova, O., and Plow, E. F. (2004) PLoS Biol 2(6), e169

40. Morini, M., Mottolese, M., Ferrari N., Ghiorzo, F., Buglioni, S., Mortarini, R., Noonan, D.M., Natali, P.G., and Albini, A. (2000) Int. J. Cancer 87(3), 336-342

CHAPTER 4

CONCLUDING DISCUSSIONS

PKC EPSILON-MEDIATED REGULATION OF POLYMERIC FIBRONECTIN ASSEMBLY

Overexpression of fibronectin (Fn) has been demonstrated in invasive/metastatic breast tumors and tumor cells from primary invasive ductal breast carcinomas (1-3) as well as cell lines such as MDA-MB-231 and MTF7, and is especially prominent in cell lines selected for enhanced lung metastatic ability (4,5). Survey of all our highly lung-metastatic breast cancer cell lines revealed high levels of Fn expression (4). Tumor cells that were isolated from the blood of tumor-bearing animals are characterized by a cell surface coat of multi-globular polyFn, which could be reproduced on the cell surface of cancer cells subjected to suspension culture in the presence of serum. This surface coat of polyFn mediates the docking of breast cancer cells MTF7 to the lung endothelial addressin DPP IV and facilitates lung colonization (4,6-8). In this study, the mechanism of polymeric fibronectin formation on the surface of breast cancer cells was investigated. We found that protein synthesis and secretion is crucial for the polyFn assembly process and knockdown of endogenous cellular fibronectin impedes both the formation of surface polyFn and pulmonary metastasis of the cancer cells. PolyFn assembly is regulated by PKCε. Pharmocological inhibition of PKC, transfection of dominant negative regulatory domain mutant of PKCε and knockdown of PKCε protein all decreased surface polyFn in MTF7 cells. PKCε translocates to the membrane in increasing amounts during the course of polyFn assembly, which is accompanied by phosphorylation of PKCε on serine and threonine residues. In contrast, transfection of dominant negative PKCδ and knockdown of PKCδ promoted polyFn assembly, in accordance with the proposed opposing effects of PKCε and PKCδ (9).

In order to further understand how PKCε reglates polyFn assembly, we utilized mass spectrometry to identify possible regulating factors residing within the PKCε complex formed during suspension incubation. Two cytoskeletal proteins were found within the PKCε complex, β-actin and myosin IIa. Myosin ATPase activity is not required for polyFn assembly, as evidenced by lack of effect of pharmacological inhibitors. On the other hand, β-actin associated with PKCε in a time-dependent and PKC activity-dependent manner, and filamentous actin associated with PKCε increasingly at the subplasmalemmal space. The actin depolymerizing drug, Cytochalasin D, disrupted formation of polyFn and perturbed the subplasmalemmal localization of the PKCε-actin complex. The images of PKCε-actin complexes within the cells showed a few cytoplasmic granule-like existence while images from Cytochalasin D treated cells demonstrated a tremendous amount of cytoplasmic complexes. Since PKCε has been implicated in various exocytic processes (10-12), these observations raise the question of whether the PKCε-actin complexing could be involved in exocytosis of fibronectin or polyFn receptors.

One of the focal adhesion kinase family members, Pyk2, was also shown to be involved in polyFn assembly. Transfection of a kinase dead mutant of Pyk2 and pharmacological inhibition with the Pyk2 inhibitor sodium salicylate both decreased surface polyFn assembly, and time-dependent phosphorylation of Pyk2 was blocked by the PKCε inhibitor BIMXI and Cytochalasin D, suggesting that Pyk2 phosphorylation was downstream of cytoskeletal integrity and PKCε activity. Pyk2 possess the same FERM domain by which talin, a cytoplasmic cytoskeletal protein that regulates integrin ligand binding affinity via inside-out signaling (13), binds integrin cytoplasmic tails. Pyk2 has also been shown to bind to β3 integrin cytoplasmic tails (14). Therefore, we propose in our working model that PKCε regulates polyFn assembly by signaling downstream to Pyk2 and allowing Pyk2 to

relay the signal to β3 integrin cytoplasmic tails, in turn altering integrin ligand binding affinity to bind fibronectin, allowing cells to form a fibronectin scaffold that facilitates fibronectin self-association and build up of polymeric fibronectin globules on the surface of cancer cells.

The soluble factor responsible for triggering the polyFn assembly cascade has not been identified. This factor could be a cytokine secreted by the cancer cells and could act in an autocrine manner. The factors tested in this study are listed in Table 1. Negative results may indicate either: the factor was not involved, the factor was insufficient to trigger an active response, the concentration used was not optimal, or the activating conditions were not optimal. The conditioned medium isolated from MTF7 culture was able to induce an increase in polyFn assembly (Fig 4.1A). Two soluble factors were identified in the conditioned medium of MTF7 cells, monocyte chemotactic protein-1 (MCP-1) and tissue inhibitor of metalloproteinase (TIMP-1) (Fig 4.1B), and MCP-1 was tested and shown to be unable to increase polyFn compared to control (Table 1). Future analysis of the conditioned medium of MTF7 cells with cytokine arrays that test for a greater number of cytokines than the 18-cytokine array used may be helpful in identifying the "trigger" factor.

Future investigations on the receptor(s) of polyFn may present evidence to support the detailed mechanism in PKCε regulation of poly Fn assembly. The first candidate to test would be β3 integrin, binding target of Pyk2. To test the hypothesis that β3 integrin is the polyFn receptor subunit, the first step is to confirm the expression of β3 integrin in MTF7 cells. Subsequently, imaging studies can be done to visualize the colocalization of β3 integrin and polyFn globules. A possible interaction may be further characterized by attempting to co-immunoprecipitate β3 integrin and polyFn in biochemical analysis. To further investigate the requirement for inside-out signaling in β3 integrin activation, mutants of β3 integrin cytoplamic tail, which has

Table 1: Stimulators tested for polyFn assembly.

Reagents tested negative as stimulator of polyFn assembly*	
Drug/reagent	**Concentration used**
Lysophosphatidic acid (LPA)	5μM, 10 μM, 20 μM,
Phosphatidylinositol(3,4) bisphosphate (diC8)	10μg/ml
Inositol hexakisphosphate (InsP6)	200μM
m-3M3FBS, phospholipase C activator	25 μM, 50 μM
Epidermal growth factor (EGF)	100ng/ml
Insulin-like growth factor (IGF-1)	100ng/ml, 200ng/ml, 500ng/ml
Stromal cell-derived factor alpha (SDF-1)	300ng/ml, 600ng/ml
Platelet derived growth factor (PDGF)	20gn/ml, 100ng/ml
Transforming growth factor beta (TGFβ)	10pg/ml, 20pg/ml, 50pg/ml, 500pg/ml
Interleukin-8 (IL-8)	25ng/ml, 50ng/ml
Thrombin	5units, 10units
Sphingosine-1-phosphate (S1P)	500nM, 2.6μM
Platelet-derived growth factor (PDGF)	50ng/ml, 100ng/ml, 500ng/ml, 1μg/ml
Monocyte chemoattractant protein-1 (MCP-1)	100 ng/ml

*comparison between MTF7 cells from 1 hour suspension in the presence of no drug, drug + no Fn, drug + Fn (20 μg/ml) in DMEM

Figure 4.1: Cancer cell secreted factors in polyFn assembly. (A) MTF7 cell overnight conditioned medium (CDME) was used to treat cells in EoE suspension culture, in comparison to medium (DME). Cells were stained with anti-Fn and analyzed with FACS. Results show cells treated with conditioned medium had an increased ability to assemble surface polyFn. (B) Rat cytokine array (Raybiotech, Norcross GA) of MTF7 CDME shows secretion of monocyte chemotactic protein-1 (MCP-1) and tissue inhibitor of metalloproteinase (TIMP-1).

A

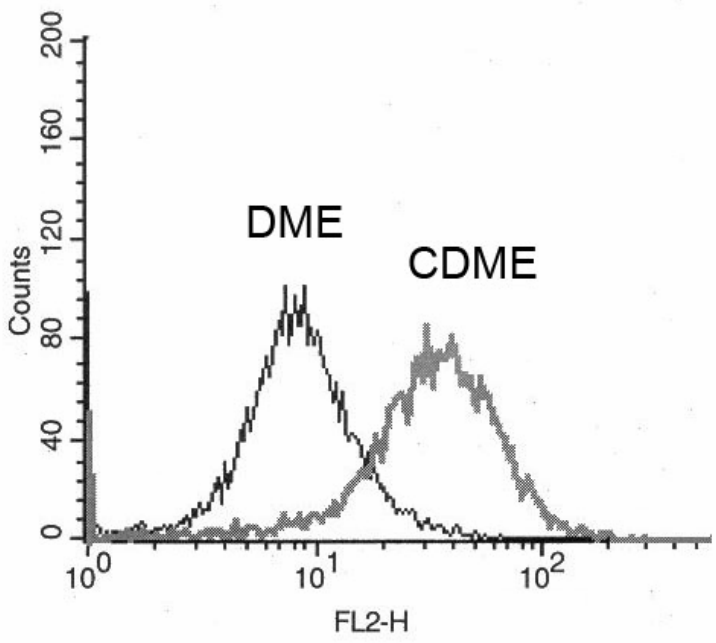

B

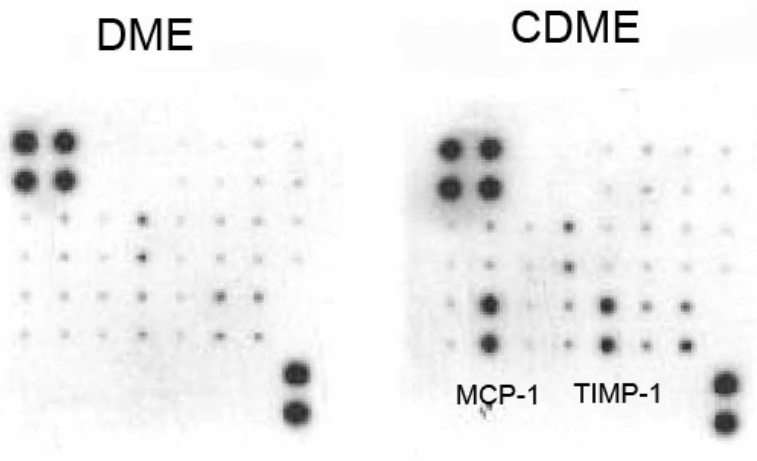

	a	b	c	d	e	f	g	h
1	Pos	Pos	Neg	Neg	CINC-2	CINC-3	CNTF	Fractalkine
2	Pos	Pos	Neg	Neg	CINC-2	CINC-3	CNTF	Fractalkine
3	GM-CSF	IFN-γ	IL-1α	IL-1β	IL-4	IL-6	IL-10	LIX
4	GM-CSF	IFN-γ	IL-1α	IL-1β	IL-4	IL-6	IL-10	LIX
5	Leptin	MCP-1	MIP-3α	β-NGF	TIMP-1	TNF-α	VEGF	BLANK
6	Leptin	MCP-1	MIP-3α	β-NGF	TIMP-1	TNF-α	VEGF	BLANK
7	BLANK	BLANK	BLANK	BLANK	BLANK	BLANK	BLANK	Pos
8	BLANK	BLANK	BLANK	BLANK	BLANK	BLANK	BLANK	Pos

been shown to be crucial in integrin inside-out signaling (15), can be used in transfection experiments. Lastly, effects of knockdown of β3 integrin protein can also be determined. Clarification of the α integrin subunit partner of the possible polyFn β3 integrin receptor could further be investigated by subcellular imaging, biochemistry and mutants. Fibronectin binding sites of β3 integrin could also be blocked using peptides or blocking antibodies.

The involvement of the small GTPases such as Rho, Rac and Cdc42 would also be of interest due to their roles in cytoskeletal organization (16). To test the involvement of the small GTPases Rac and Cdc42 in polyFn assembly, dominant negative or constitutive mutants of Rac and Cdc42 can be transfected into MTF7 cells. Rac or Cdc42 activity can further be characterized by activity assays testing for GTP-form binding to glutathione S transferase–p21-activated kinase (GST-PAK). Functional correlating effects of mutants on polyFn assembly in conjunction with activated Rac or Cdc42 in polyFn assembly phase would indicate a role for a Rho GTPase in surface polyFn formation. Moreover, the possible involvement of a cytokine such as CXCL1(Groα;Cinc1), which is downregulated 8-fold in PKCε-depleted MTF7 cells relative to control cells, must also be considered. In support of this notion, CXCL1 binding to its receptor CXCR2 could have been responsible for the binding of RACK1 with Gβγ subunit of heterotrimeric G proteins and the observed translocation of activated PKCε to the plasma membrane (17).

REFERENCES

1. Amatschek, S., Koenig, U., Auer, H., Steinlein, P., Pacher, M., Gruenfelder, A., Dekan, G., Vogl, S., Kubista, E., Heider, K. H., Stratowa, C., Schreiber, M., and Sommergruber, W. (2004) Cancer Res 64(3), 844-856

2. Hao, X., Sun, B., Hu, L., Lahdesmaki, H., Dunmire, V., Feng, Y., Zhang, S. W., Wang, H., Wu, C., Wang, H., Fuller, G. N., Symmans, W. F., Shmulevich, I., and Zhang, W. (2004) Cancer 100(6), 1110-1122

3. Zucchi, I., Mento, E., Kuznetsov, V. A., Scotti, M., Valsecchi, V., Simionati, B., Vicinanza, E., Valle, G., Pilotti, S., Reinbold, R., Vezzoni, P., Albertini, A., and Dulbecco, R. (2004) Proc Natl Acad Sci U S A 101(52), 18147-18152

4. Cheng, H. C., Abdel-Ghany, M., and Pauli, B. U. (2003) J Biol Chem 278(27), 24600-24607

5. Bandyopadhyay, A., Elkahloun, A., Baysa, S. J., Wang, L., and Sun, L. Z. (2005) Cancer Biol Ther 4(2), 168-174

6. Cheng, H. C., Abdel-Ghany, M., Elble, R. C., and Pauli, B. U. (1998) J Biol Chem 273(37), 24207-24215

7. Abdel-Ghany, M., Cheng, H., Levine, R. A., and Pauli, B. U. (1998) Invasion Metastasis 18(1), 35-43

8. Cheng, H. C., Abdel-Ghany, M., Zhang, S., and Pauli, B. U. (1999) Clin Exp Metastasis 17(7), 609-615

9. Chen, L., Hahn, H., Wu, G., Chen, C. H., Liron, T., Schechtman, D., Cavallaro, G., Banci, L., Guo, Y., Bolli, R., Dorn, G. W., 2nd, and Mochly-Rosen, D. (2001) Proc Natl Acad Sci U S A 98(20), 11114-11119

10. Ivaska, J., Whelan, R. D., Watson, R., and Parker, P. J. (2002) Embo J 21(14), 3608-3619

11. Mendez, C. F., Leibiger, I. B., Leibiger, B., Hoy, M., Gromada, J., Berggren, P. O., and Bertorello, A. M. (2003) J Biol Chem 278(45), 44753-44757

12. Park, Y. S., Hur, E. M., Choi, B. H., Kwak, E., Jun, D. J., Park, S. J., and Kim, K. T. (2006) J Neurosci 26(35), 8999-9005

13. Qin, J., Vinogradova, O., and Plow, E. F. (2004) PLoS Biol 2(6), e169

14. Butler, B., and Blystone, S. D. (2005) J Biol Chem 280(15), 14556-14562

15. Hynes, R. O. (2002) Cell 110(6), 673-687

16. Heasman, S. J., and Ridley, A. J. (2008) Nat Rev Mol Cell Biol 9(9), 690-701

17. Chen, S., Dell, E. J., Lin, F., Sai, J., and Hamm, H. E. (2004) J Biol Chem 279(17), 17861-17868

APPENDIX

CONDITIONAL KNOCKOUT OF FIBRONECTIN IN MAMMARY EPITHELIUM LEADS TO SEVERE LOBULO-ALVEOLAR HYPOPLASIA IN THE MOUSE MAMMARY GLAND*

* Liu K, Cheng L, Flesken-Nikitin A, Huang L, Nikitin AY and Pauli BU. Conditional Knockout of Fibronectin in Mammary Epithelium Leads to Severe Lobulo-Alveolar Hypoplasia in the Mouse Mammary Gland. To be submitted. (Huang L: Biochemistry, mice mating, genotyping, mammary gland extraction)

ABSTRACT

Fibronectin (Fn) plays an important part in the branching morphogenesis of salivary gland, lung, and kidney. Here, we examine the effect of the conditional knockout of Fn in the mammary epithelium [$Fn^{MEp-/-}$] on postnatal mammary gland development, using *Cre-loxP* mediated gene knockout technology. Our data show that $Fn^{MEp-/-}$ mice exhibit (i) a moderate retardation in outgrowth and branching of the ductal tree as well as a reduced number of terminal end buds (TEBs) in adolescent mice (5 weeks old) that became statistically indifferent to control mice [$Fn^{MEp+/-}$; $Fn^{fl+/+}$] in virgin adult mice (16 weeks old), and (ii) severe lobulo-alveolar hypoplasia / aplasia in 15-day pregnant $Fn^{MEp-/-}$ mice, resulting in inability to lactate and nurse. Both heterozygous $Fn^{MEp+/-}$ and $Fn^{fl+/+}$ control mice exhibit normal MG development and Fn expression. Lack of lobulo-alveolar differentiation during pregnancy of $Fn^{MEp-/-}$ mice is associated with significantly decreased rates of MEp proliferation, decreased numbers of MEps that had undergone 'epithelial mesenchymal transition' and invaded the surrounding fat pad, and decreased neovascularization, which was paralleled by a dramatic decrease in Vegf expression. Concomitant downregulation of β1 integrin (Itgb1) and decrease autophosphorylation of FAK suggest that this pathology is mediated, at least in part, by disruption of Fn/Intgb1/FAK signaling pathway. This notion is supported by the fact that conditional knockouts of Itgb1 and FAK generate the same pathology as Fn-deletion.

INTRODUCTION

Fibronectin (Fn) is an adhesive glycoprotein that is present in extracellular matrices (insoluble form) and in body fluids (soluble form; e.g., blood plasma). It exists as a dimer composed of nearly identical ~250 kDa subunits linked covalently near their C-termini by a pair of disulfide bonds. Each monomer consists of 3 types of repeats: 12 type I, 2 types II, and 15 type III (1-3). Although Fn molecules are the product of a single gene, the resulting protein can exist in multiple forms arising from alternative splicing of a single pre-mRNA (~20 variants in humans). Splice sites are EDA (Extra Domain A), EDB (Extra Domain B), and IIICS (type III connecting segment; also called variable [V] region) (4). This multi-domain structure harboring binding sites for cell adhesion receptors (e.g., integrins, syndecans, CD44, CD26), matrix macromolecules (e.g., collagens, hyaluronic acid, proteoglycans, tenascin, thrombospondin, fibrinogen), secreted, biologically important molecules (e.g., factor XIIIa, tissue transglutaminase, fibrinogen, heparin), as well as for Fn-Fn self-association (5-8) makes it a perfect candidate for a 'multi-task' role. As such, it anchors the extracellular matrix to the cell cytoskeleton via adhesion receptors and, in doing so, relays signals from the milieu outside the cell to its inside. This so-called outside-in signaling accounts for the many functions with which Fn has been associated including cell adhesion, differentiation, growth, and migration (6,9,10). Thus, Fn is critical in vertebrate development, tissue morphogenesis and homeostasis, wound healing, angiogenesis, and cancer (1-4,9-13). Fn knockout is embryologically lethal, with abnormalities becoming manifest first at the onset of gastrulation (for details see 14,15).

Many organs, including glands, lung and kidney are formed during embryonic development by epithelial branching through a process of repetitive epithelial cleft and

bud formations. In an elegant organ culture study, Yamada and associates (16) showed that Fn is essential for cleft formation during the initiation of epithelial branching in the submaxillary gland. Fn messenger RNA and fibrils were expressed transiently and focally in forming epithelial cleft regions. Knockdown of Fn by small interfering RNA and by inhibition with anti-Fn or anti-integrin antibodies (anti-α5, -α6, and -β1) blocked cleft formation and branching, while exogenous Fn accelerated cleft formation and branching. Mechanistically, the authors implied that fibrillar Fn mediates cleft formation in branching morphogenesis by downregulating cadherins at cell-cell junctions, thereby converting cell-cell to cell-matrix adhesions. Although a similar scenario has not been established for the mammary gland (MG), the functional role of ECM proteins, including Fn, collagen type I, and laminin, in MG postnatal development has been studied more recently (17). Among the three ECM proteins only the Fn levels changed appreciably, increasing threefold between puberty and sexual maturity and remaining high during pregnancy and lactation. This temporal expression of Fn coincides with the expressions of hepatocyte growth factor (HGF; produced by mammary fibroblasts) (17-19), estrogen and progesterone (both shown to regulate Fn expression) (20). HGF levels rise at midpuberty and are maximal at sexual maturity and remain high during pregnancy, while estrogen is driving ductal development during puberty, and estrogen and progesterone mediate proliferation, ductal branching and alveologenesis at sexual maturity and during pregnancy (21,22). Moreover, blockade of AP-1 transcription factors, which inhibits expression of AP-1-dependent genes (e.g., Fn, cyclin D, c-myc, TIMP-1, vimentin) suppresses branching and budding and reduces gland tree size and fat pad occupancy in developing MGs (23). More details of the genes involved in postnatal MG development have been provided by several, excellent review articles by Hennighausen and associates (24-26). Together these studies suggest that the temporal expression patterns of growth

regulatory molecules (e.g., cyclin D, c-myc, HGF, EGF), matrix macromolecules (e.g., Fn) and steroid hormones modulate mammary epithelial proliferation and morphogenesis by interacting Fn/integrin-, growth factor-, and steroid hormone-signaling pathways, which ultimately may also harbor new clues of the role of these factors, particularly Fn, in mammary cancer progression (27).

In this report, we present data of the role of Fn in the postnatal development of the mammary gland, using mice with MMTV-Cre-loxP conditional knockout of Fn in the mammary epithelium ($Fn^{MEp-/-}$). Our whole-mount, histologic, immunohistochemical, morphometric, biochemical, and functional data show that these mice exhibit (i) moderate retardation in outgrowth and branching of the ductal tree in virgin mice, and (ii) lack of alveolar budding and lobule formation during pregnancy and lactation, resulting in inability to lactate and nurse. Both heterozygous $Fn^{MEp+/-}$ and Fn-floxed ($Fn^{fl+/+}$) control mice exhibited near normal and normal MG development and Fn expression, respectively. Decreased mammary epithelial cell (MEp) proliferative rates in $Fn^{MEp-/-}$ mice and altered signaling via the β1 integrin (Itgb1) Fn receptor and focal adhesion kinase may have accounted, at least in part, for the observed result.

MATERIAL AND METHODS

Conditional Knockout of Fn in Mouse Mammary Epithelium

Heterozygous, male $Fn^{fl+/-}$ carrying *loxP* sites within the 5' untranslated region at the *Msc*1 site and within the first intron at the *Nhe*1 site of the Fn gene were generated in Dr. Fässler laboratory (Max-Planck-Institute, Martinsried, Germany) (28). These mice were backcrossed with wild type FVB mice to produce heterozygous

$Fn^{fl+/-}$ mice. The heterozygous $Fn^{fl+/-}$ mice were crossed with siblings to generated homozygous $Fn^{fl+/+}$ mice. To introduce Cre-recombinase [*an enzyme that cleaves loxP sites, thereby removing the start codon, signal sequence and the exon/intron border of exon 1 of Fn to generate the Fn-null allele 28)*] that is under control of the mammary epithelial cell-specific MMTV LTR promoter into $Fn^{fl+/+}$ mice, $Fn^{fl+/+}$ females were paired with male MMTV-Cre mice with an FVB genetic background (supplied by Dr. Guan, University of Michigan) to ultimately obtain female mice with the genotype MMTV-Cre^{+} $Fn^{fl+/+}$ and the phenotype $Fn^{MEp-/-}$. Offspring with the desired genotypes were identified by PCR analysis of tail DNA, using the same primer sets as described by Fässler and associates (28). Control mice were heterozygous $Fn^{MEp+/-}$ and $Fn^{fl+/+}$ mice. Mice were analyzed at 5- and 16-weeks of age and at day 15 of pregnancy (13 to 14 weeks of age).

To assure selectivity of Cre-recombinase activity in MEp, we stained frozen sections (5 μm thick) of the MGs from offspring of homozygous MMTV-Cre and Rosa26STOP^{loxP}LacZ mice (*expression of β-galactosidase is possible only after Cre-mediated deletion of a stop codon flanked by loxP sites;* Jackson Laboratory) with X-gal solution as described by Bonnerot et al. (29). Sections were counterstained with Nuclear Fast Red. Controls were MGs from Rosa26STOP^{loxP}LacZ mice. To further assess organ-specificity of the MMTV-Cre-mediated Fn knockout in MGs, DNA was extracted from lung (Lu), heart (He), kidney (Ki), mammary gland (MG), salivary gland (SG), uterus (Ut) and liver (Li) of $Fn^{MEp-/-}$ mice. PCR was performed with the primers designed from regions flanking the Fn1 lox-P sites. Fn deletion results in a 320 bp band, while floxed Fn1 revealed a 1,200 bp band.

Mammary Gland Whole Mount Preparation, Staining, and Analyses

The left 4th inguinal mammary fat pad (MFP) was excised essentially as described by Tiran and Elson (30). In brief, excised MFPs were spread onto glass slides and fixed with Tellyesniczky's fixative overnight. MFPs were then soaked in three changes of 100% acetone each for 6h, followed by 2h-treatments with each 100%, 95% and 70% ethanol, and stained with 0.2% carmine red overnight. After rinsing in water, MFPs were dehydrated sequentially in 50%, 70%, 95%, and 100% ethanol each for 2h, cleared with methyl salicylate overnight and examined under a dissecting microscope. MG whole mounts were evaluated as follows: (i) Extent of ductal outgrowth (maximal outgrowth beyond MFP lymph node measured in millimeters; (ii) number of ductal branch points per unit area of MFP; and (iii) number of terminal end buds (TEBs) in MGs from virgin mice (virgin mice 5- and 16-weeks old) as described by Shen et al. (23); and (iv) size and number of alveolar lobules from MGs of pregnant and lactating mice. A minimum of 7 mice per each age-category and genotype were analyzed.

Histologic and Morphometric Techniques

The right 4th inguinal MFP was excised as described above, spread onto glass slides and fixed with phosphate-buffered 4% paraformaldehyde overnight at 4°C. MFPs were then subjected to routine paraffin-embedding, and 4-µm thick, planar sections stained with hematoxylin & eosin (H.&E.). Sections were evaluated as follows: (i) assessment of the tissue architecture and branching pattern; and (ii) estimation of the volume density (V_{MG}) of the glandular structures occupying the MFP as described by Weibel et al. (31) and Pauli et al. (32), using computer-enlarged photographs from entire MFP sections and superimposed test lattices of 1-cm^2

subunits: V_{MG}=Pi (number of line intersection points falling on MG components) / P_T (total number of intersection points falling on MG components + MFP stroma) (32). A minimum of 7 mice per each age-category and genotype were analyzed.

Immunohistochemistry

Paraformaldehyde-fixed sections from the right 4th inguinal MFP mounted on poly-L-lysine coated glass slides were used for immunohistochemical analyzes. Prior to staining with primary antibody (mouse anti-Fn monoclonal antibody directed against the EDA domain of human Fn1: 1:50; overnight; 4°C) (Santa Cruz Biotechnology), 5-µm thick, deparaffinized sections were treated sequentially with 1% pepsin (Sigma) in 10 mM HCl (pH 2.0; 30 min; 37°C) for antigen unmasking, M.O.M. Ig blocking reagent (M.O.M. Immunodetection kit; Vector Laboratories, Burlingame, CA) for blocking endogenous immunoglobulin, and normal horse serum (R.T.U. Vectastain® Universal Elite ABC kit; Vector Laboratories) for blocking unspecific binding of the secondary antibody. Detection of bound primary antibody was by biotinylated horse anti-mouse secondary antibody, ready-to-use, stabilized ABC reagent (R.T.U. Vectastain® Universal Elite ABC kit) and the peroxidase substrate 3-amino-9-ethyl carbozole (AEC; Invitrogen, Carlsbad, CA). Sections were washed vigorously with PBS between each step of this procedure and counterstained with hematoxylin (5 seconds; room temperature). Control section were stained normal mouse IgG instead of primary antibody.

Assessment of MEp Proliferative and Apoptotic Rates

The MEp proliferative rate was estimated by BrdU assay. In brief, mice were injected intraperitoneally with 0.1 ml/10 gm body weight of BrdU solution (Invitrogen) 2 hours prior to sacrifice. BrdU-positive cells were detected by immunohistochemistry using anti-BrdU antibody (1:150 dilution; 1.5 h; 37°C)

(Invitrogen) essentially as described above. The proliferative rate was expressed as the percent BrdU-positive cells of the total number of MEps counted (~1,000 cells/MG counted).

The MEp apoptotic rate was determined by the cleaved caspase 3 immunohistoichemical assay (23). The anti-cleaved caspase 3 antibody was from BD Biosciences (San Jose, CA) and was used at a dilution of 1:150 as described above. The percent cleaved caspase 3-positive cells of the total number of MEps (~1,000 cell counted) was used as an expression of the MEp-apoptotic rate.

Biochemical Analyses

To assess the role of the downstream Fn-signaling partners in the lobulo-alveolar differentiation of the MG, MG were homogenized in lysis buffer (50 mM Tris-HCl, pH 7.4, 150 mM NaCl, 1 mM EDTA, 1 mM EGTA, 1 mM benzamidine chloride, 1 mM PMSF, 2 μg/ml leupeptin, 0.27 TIU/ml aprotinin, 0.1 mM sodium vanadate, and 1% Triton X-100) and incubated for 1h at 4°C (33). Total cell lysates were subjected to SDS-PAGE (~20-50μg protein) and Western blotting (33), using anti-Fn (Sigma), anti-ItgB1 (Sana Cruz Biotechnology), anti-focal adhesion kinase (FAK) (Biomol), anti-FAK(pY397) (Biomol), HRP-conjugated donkey anti-rabbit or goat anti-mouse secondary antibodies and ECL for detection of bound antibody as described (33).

RESULTS

MMTV-Cre Mediated Recombination

Mice used in this study had the following genotypes: (i) $Fn^{fl+/+}$, (ii) MMTV-$Cre^{+}Fn^{fl+/-}$ (phenotype: $Fn^{MEp+/-}$) and (iii) MMTV-$Cre^{+}Fn^{fl+/+}$ (phenotype: $Fn^{MEp-/-}$).

These genotypes were identified by PCR using tail-derived genomic DNA and primer sets that flanked the floxed sites of the Fn gene as described in Material and Methods. The same set of primers was also used to PCR-probe DNA isolated from various organs including lung, heart, kidney, liver, uterus, mammary gland, and salivary gland in order to examine which organs exhibited Cre recombinase activity. In MMTV-$Cre^{+}Fn^{fl+/+}$ mice only mammary gland and salivary gland exhibited strong Cre activity as visualized by deletion of the floxed Fn-segment (320bp band) in these organs (Fig A.1A). In contrast, heterozygous MMTV-$Cre^{+}Fn^{fl+/-}$ mice exhibited both Fn-species (i.e., deleted [320bp] and undeleted [1.2kb] floxed-Fn) and $Fn^{fl+/+}$ mice revealed only undeleted, floxed Fn as expected (data not shown). To further assess the selectivity of Cre recombinase activity and expression in MEp, we stained frozen sections from the mammary gland of MMTV-Cre^{+}- Rosa26STOP^{loxP}LacZ and Rosa26STOP^{loxP}LacZ (control) mice with X-gal. X-gal staining was only observed in the mammary epithelium from MMTV-Cre^{+}- Rosa26STOP^{loxP}LacZ mice, where Cre recombinase activity removed a floxed stop colon to allow expression of LacZ (Fig A.1B). No X-gal staining was observed in non-epithelial tissues. Age-matched, Cre-negative control mice revealed no X-gal staining of the mammary epithelium (Fig A.1C). To examine Fn protein expression we selected mammary gland from 15-day pregnant $Fn^{fl+/+}$ and $Fn^{MEp-/-}$ mice since at stage mammary glands of normal mice express relatively high levels of Fn (17) and since most of the MFP is occupied by glandular tissue thereby keeping the amount contributed by the stromal compartment at a minimum. As expected, $Fn^{fl+/+}$ mice exhibit strong Fn expression, while Fn expression in $Fn^{MEp-/-}$ mice varied from approximately 0 to approximately 40% (Fig A.1D).

Figure A.1: Conditional Knockout of Fn in Mammary Epithelia: (A) DNA was extracted from lung (Lu), heart (He), kidney (Ki), mammary gland (MG), salivary gland (SG), uterus (Ut) and liver (Li) of MMTV-$Cre^{+}Fn^{fl+/+}$ mice. PCR was performed with the primers designed from the regions flanking the Fn loxP sites. Fn deletion results in a 320bp band, while floxed Fn in a 1200bp band. (B) Frozen section from the MG of a 16-week old MMTV-Cre/Rosa26$STOP^{loxP}$LacZ mouse stained with X-Gal solution (Fermentas) and counterstained with Fast Red. Notice the select expression of Cre-recombinase activity in MEp, but not surrounding stromal cells (C) X-Gal staining of a frozen section from the mammary gland of a 16-week old Rosa26$STOP^{loxP}$LacZ control mouse. X-Gal staining is negative. (D) Fn protein expression in $Fn^{fl+/+}$ and $Fn^{MEp-/-}$mice.

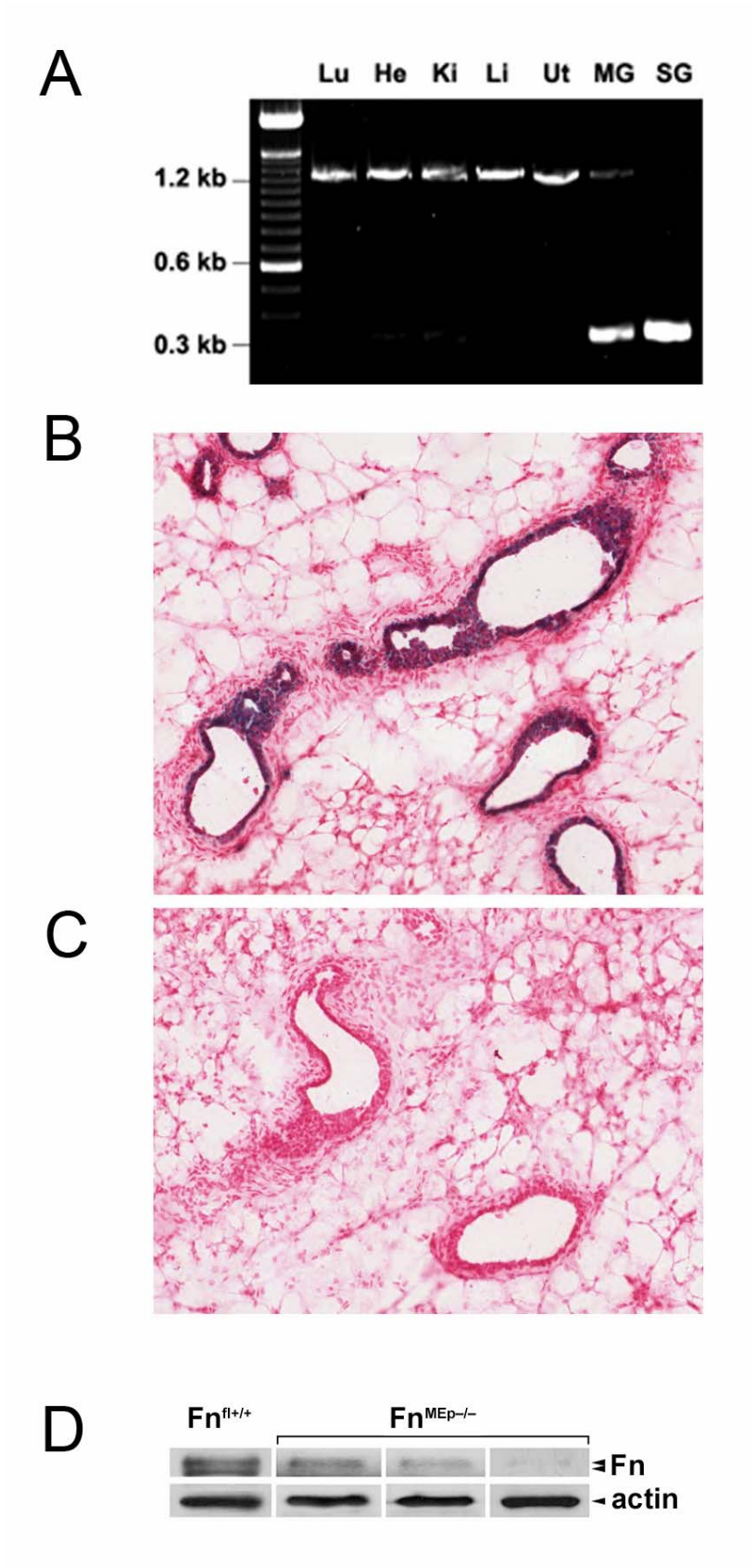
A
Lu
He
Ki
Li
Ut
MG
SG
1.2 kb
0.6 kb
0.3 kb
B
C
D
Fnfl+/+
FnMEp−/−
Fn
actin

Analyses of MFP Whole Mounts

Carmine red-stained MFPs from each age-group and genotypes of mice were analyzed qualitatively and quantitatively. At five weeks of age, mice with MMTV-Cre-mediated deletion of floxed Fn [$Fn^{MEp-/-}$] exhibited a significant retardation in ductal outgrowth of the MG relative to heterozygous $Fn^{MEp+/-}$ and $Fn^{fl+/+}$ mice (Figs A.2 and A.3A&B). Also decreased were the number of ductal branch points and the number of terminal end buds (TEBs) relative to the two control groups [$Fn^{MEp+/-}$; $Fn^{fl+/+}$] (Fig A.3C&D). At 16 weeks of age, ductal outgrowth and number of branch points in $Fn^{MEp-/-}$ mice were still decreased, but statistically indifferent from those of control $Fn^{MEp+/-}$ and $Fn^{fl+/+}$ mice (Fig A.3B&C). The most dramatic changes in MG postnatal development were observed at day 15 of pregnancy. The MG of $Fn^{MEp-/-}$ mice exhibited normal ductal development and branching extending from the nipple to the terminal ductules (Fig A.2), but lobulo-alveolar differentiation, typically observed at this stage of pregnancy in normal mice, was totally missing (Fig A.2). Together, these data show that Fn deletion in MEp caused a minor retardation in ductal outgrowth and number of branch points in adolescent $Fn^{MEp-/-}$ mice relative to the two age-matched control groups [$Fn^{MEp+/-}$; $Fn^{fl+/+}$]. However, at 16 weeks of age MG ductal outgrowth and branching in $Fn^{MEp-/-}$ mice had caught-up to those in age-matched control mice (Fig A.3 B&C), suggesting that Fn-deletion might have slowed the rate of MEp proliferation.

Figure A.2: Mammary Gland Whole Mounts from $Fn^{fl+/+}$ and $Fn^{MEp-/-}$ mice: At 5 weeks, there is a noticeable retardation in the ductal outgrowth, decreased branching, and decreased occupancy of the MFP with glandular elements in $Fn^{MEp-/-}$ relative to $Fn^{fl+/+}$ mice. At 16 weeks (virgin mice; v16w), ductal outgrowth and branching are almost identical and there is only a minor decrease in mammary fat pad (MFP) occupancy in $Fn^{MEp-/-}$ relative to $Fn^{fl+/+}$ mice. In pregnant mice at day 15, there is a total lack in lobulo-alveolar differentiation in $Fn^{MEp-/-}$ mice (see higher magnification) and a normal lobulo-alveolar differentiation in $Fn^{fl+/+}$ mice (see higher magnification). There is a more or less identical density and branching pattern of MG ducts that extend to terminal ductules in $Fn^{fl+/+}$ and $Fn^{MEp-/-}$ mice. Bar: 1mm.

No noticeable differences were observed between heterozygous $Fn^{MEp+/-}$ and $Fn^{fl+/+}$ and wild-type FVB mice (data not shown).

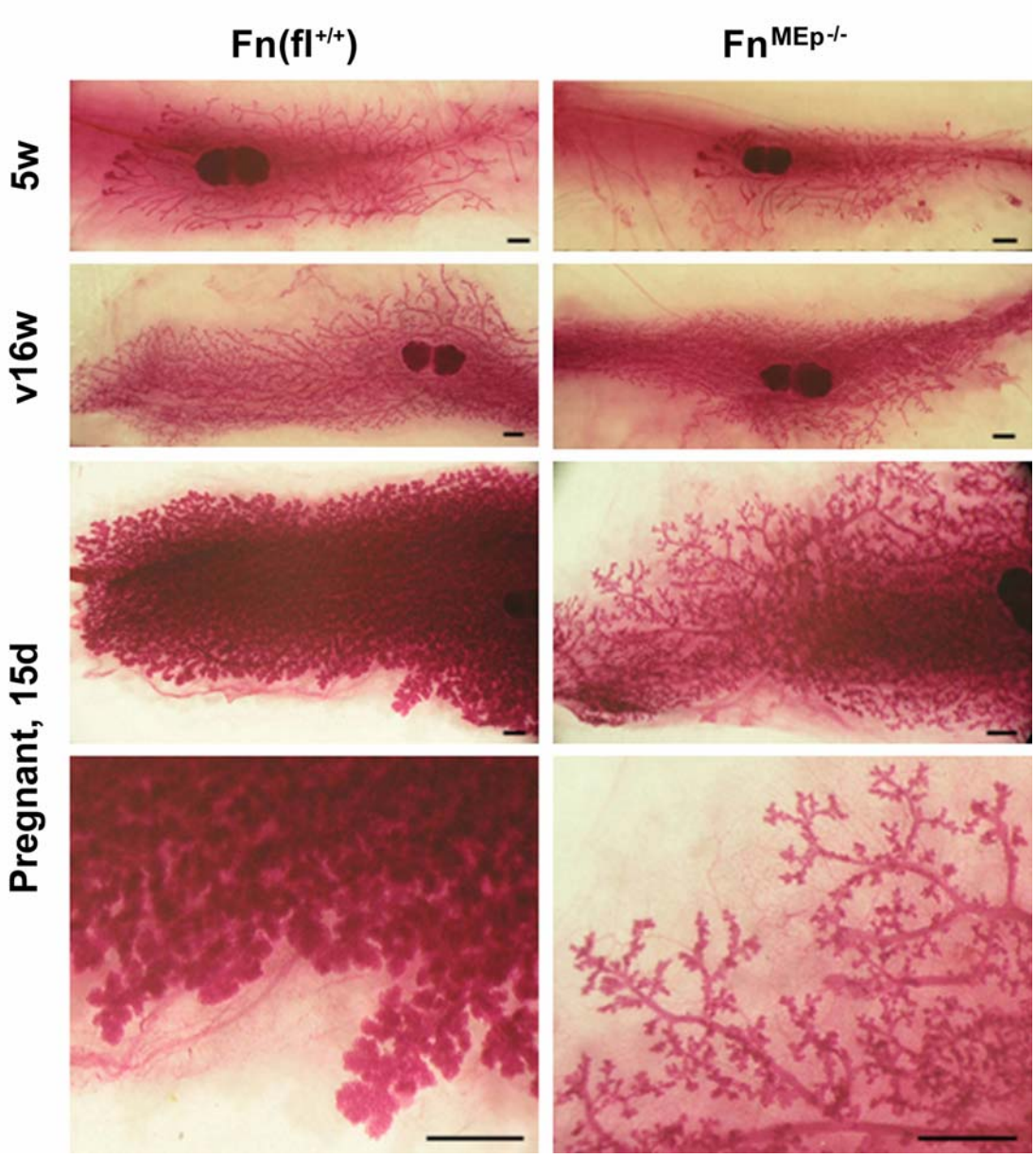
Fn(fl+/+)
FnMEp-/-
5w
v16w
Pregnant, 15d

Figure A.3: Quantitative Aspects of the Effects of Fn-knockout on MG postnatal development: MG whole mounts were used to measure outgrowth of ductal branches beyond the fat pad lymph node (A & B) and to count the number of branch points of outgrowing ducts (C) in 5- and 16-week-old, $Fn^{fl+/+}$, heterozygous $Fn^{MEp+/-}$, and homozygous $Fn^{Mep-/-}$ virgin mice. Also counted was the number of terminal end buds (TEBs) (D) in 5-week old mice from the three groups of mice. Notice retarded ductal outgrowth and decreased numbers of branch points and TEBs in $Fn^{Mep-/-}$ mice, relative to $Fn^{MEp+/-}$ and $Fn^{fl+/+}$ mice at 5 weeks, but no significant differences at 16 weeks.

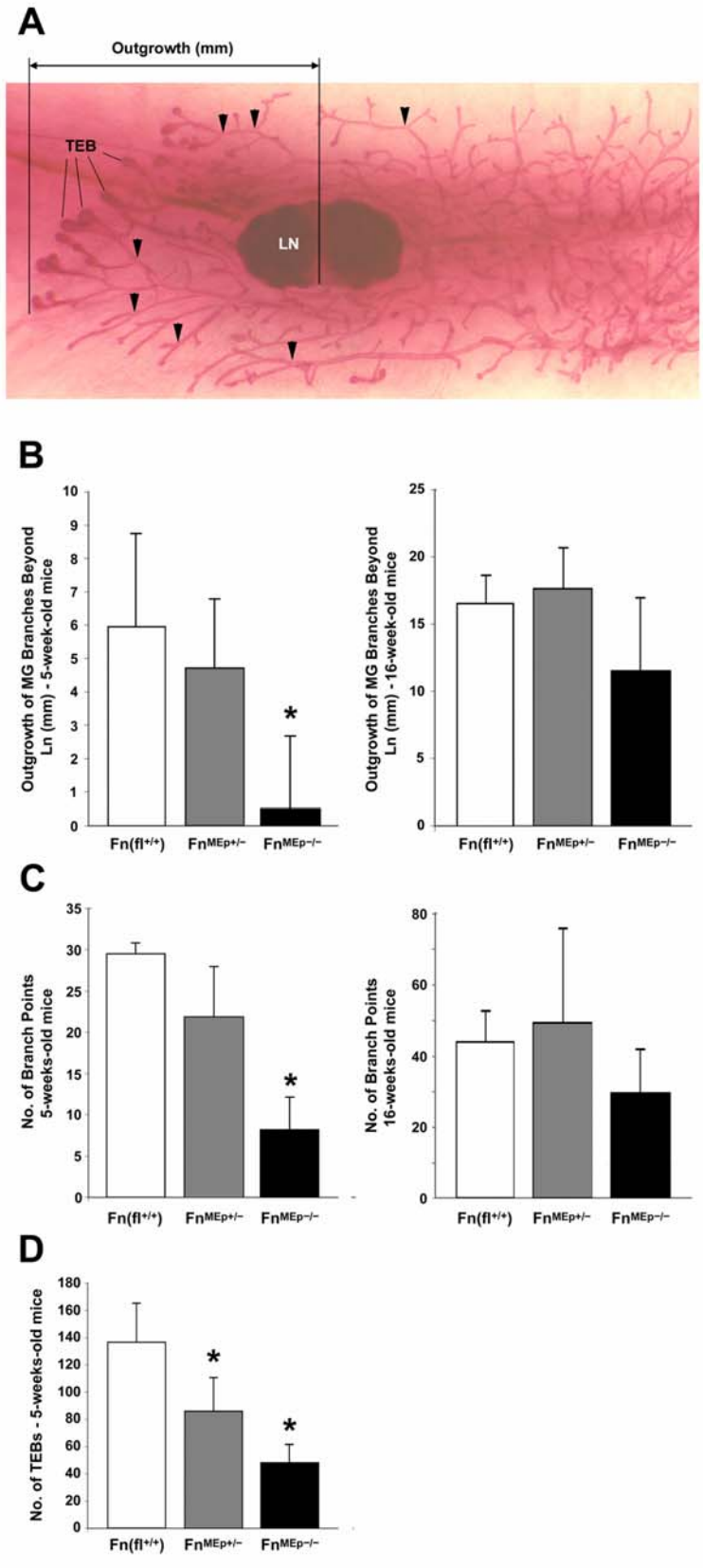
A
Outgrowth (mm)
TEB
LN
B
Outgrowth of MG Branches Beyond Ln (mm) - 5-week-old mice
Outgrowth of MG Branches Beyond Ln (mm) - 16-week-old mice
Fn(fl+/+)
FnMEp+/−
FnMEp−/−
C
No. of Branch Points 5-weeks-old mice
No. of Branch Points 16-weeks-old mice
D
No. of TEBs - 5-weeks-old mice

Histological Analyses

Histological examination of planar sections prepared from mammary glands of mice of the same groups complemented our findings from MG whole mounts. At 5 weeks of age, there was a slightly decreased number of ductal cross-sections in $Fn^{MEp-/-}$ mice relative to $Fn^{fl+/+}$ mice (Fig A.4 & Fig A.5A). However, this did not result in a statistically significant difference in the MG/MFP volume percent. Similar observations were made in 16-week old virgin mice. Glandular cross-sections were more frequent and there was a more pronounced branching in $Fn^{fl+/+}$ relative to $Fn^{MEp-/-}$ mice (Fig A.4 & Fig A.5B). Again, dramatic differences were only observed in 15-day pregnant females. There was normal lobulo-alveolar differentiation in $Fn^{fl+/+}$ mice versus a rudimentary to a total lack of lobulo-alveolar differentiation in $Fn^{MEp-/-}$ mice (Fig A.4 & Fig A.5D&E). This observation was reflective of a significant decrease in MG/MFP volume percent in the latter group of mice (Fig A.5 C-E). No statistical differences were observed between $Fn^{fl+/+}$ and $Fn^{MEp+/-}$ mice. To examine whether the difference in the MG/MFP volume percentages between $Fn^{fl+/+}$ and $Fn^{MEp-/-}$ mice was due to changes in the rates of proliferation and apoptosis of mammary epithelial cells in $Fn^{MEp-/-}$ mice, we performed a BrdU incorporation and cleaved caspase-3 assays. Results show a significant decrease in the rate of proliferation of MEps in $Fn^{MEp-/-}$ mice relative to $Fn^{fl+/+}$ mice (Fig A.6), but no significant differences in the rate of apoptosis (data not shown).

Immunohistochemical Analyses

Anti-Fn staining of mammary gland planar sections from 5 and 16-week old virgin mice of the three animal groups yielded no reportable differences. However, in 15-day pregnant mice, there were intriguing differences between $Fn^{fl+/+}$ and $Fn^{MEp-/-}$ mice. At low magnification, there was little or no Fn-staining in MG sections from

Figure A.4: Horizontal Section of Mammary Glands from $Fn^{fl+/+}$ and $Fn^{MEp-/-}$ Mice Stained with H.&E.: At 5 weeks, there is a decreased number of ductal cross-sections in $Fn^{MEp-/-}$ mice relative to their heterozygous counterparts. At 16 weeks (virgin 16w), MGs from $Fn^{MEp-/-}$ mice show ductal cross-sections (D) and branching ductules (d) and no alveolar development, while MGs from $Fn^{fl+/+}$ mice exhibit a higher density of ductal cross-sections and indications of alveolar differentiation (a). At 15 days of pregnancy, MGs of $Fn^{MEp-/-}$ exhibit good ductal branching, ducts and ductules are collapsed and contain no milk, lobulo-alveolar differentiation is lacking. Newborn pups die within 2 days following birth. In contrast, $Fn^{fl+/+}$ mice show extensive lobulo-alveolar differentiation and ducts (D) and ductules (d) are filled with milk. Pups develop normally. Images are depicted at identical magnifications.

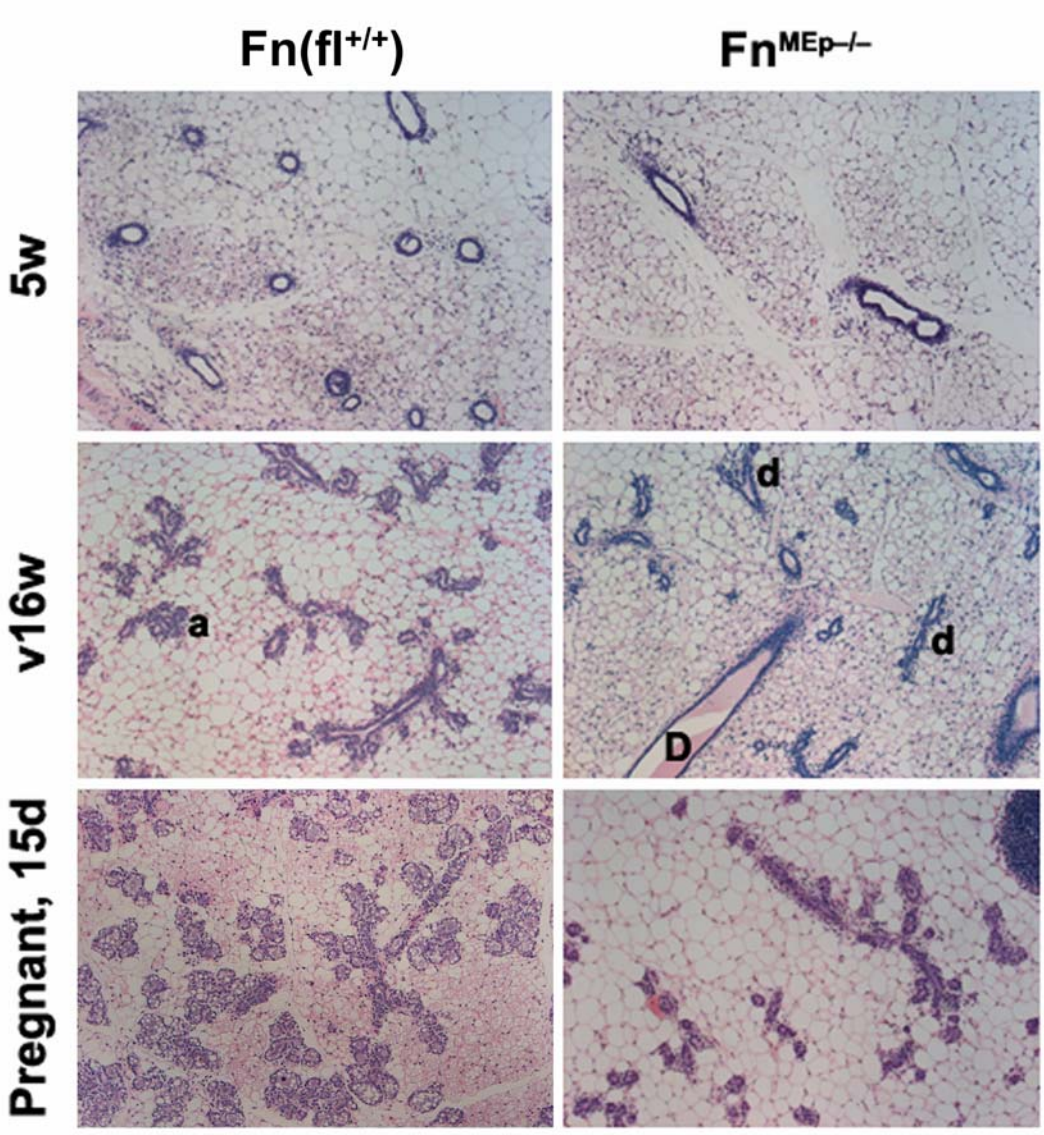
Fn(fl+/+)
FnMEp–/–
5w
v16w
Pregnant, 15d
a
d
d
D

Figure A.5: Mammary Gland Volume Density of the Mammary Fat Pad: Five micron thick paraffin sections were prepared from the mammary gland of 5 adolescent 5-week old mice (A), 5 adult virgin 16-week old mice (B), and 5 15-day pregnant mice (C) with the phenotypes $Fn^{fl+/+}$, $Fn^{MEp+/-}$, and $Fn^{Mep-/-}$. The MG volume density of the mammary fat pad was determined by standard morphometric techniques, using computer-enlarged photographs from entire MFP sections and superimposed test lattices of 1-cm2 subunits: VMG=Pi (number of line intersection points falling on MG components) divided by PT (total number of intersection points falling on MG components + MFP stroma) (150). Statistically significant differences in the volume density of MGs were only observed in 15-day pregnant mice, where the MG volume density in $Fn^{Mep-/-}$ was dramatically decreased relative to the MG volume densities in $Fn^{fl+/+}$ and $Fn^{MEp+/-}$ mice (C). This difference in MG volume densities is readily seen in H.&E.-stained sections from $Fn^{fl+/+}$(D) and $Fn^{MEp+/-}$(E) mice. D & E Insets: Fn protein expression; actin loading control.

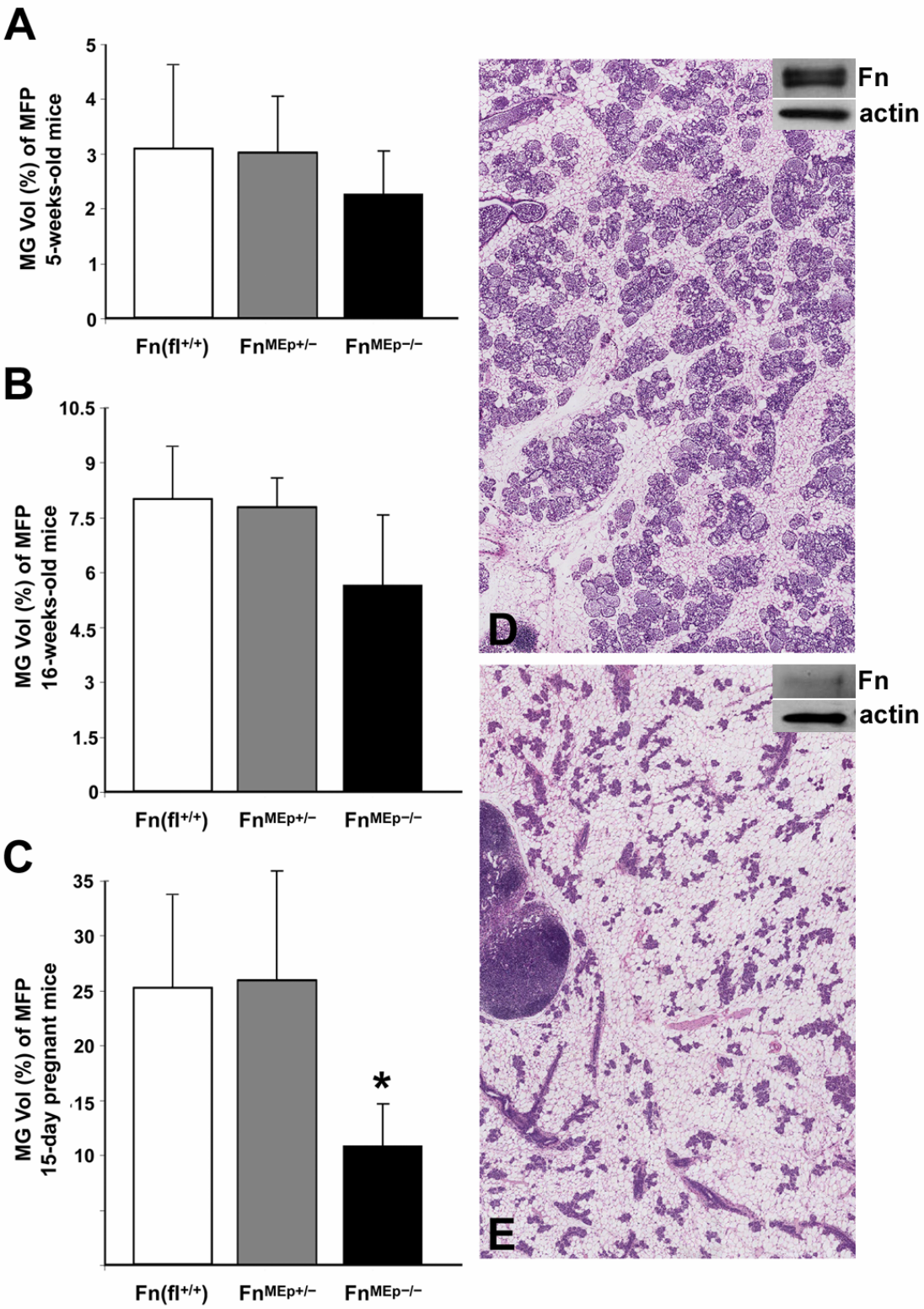
A
MG Vol (%) of MFP
5-weeks-old mice
5
4
3
2
1
0
Fn(fl+/+)
FnMEp+/−
FnMEp−/−
B
MG Vol (%) of MFP
16-weeks-old mice
10.5
9
7.5
6
4.5
3
1.5
0
Fn(fl+/+)
FnMEp+/−
FnMEp−/−
C
MG Vol (%) of MFP
15-day pregnant mice
35
30
25
20
15
10
*
Fn(fl+/+)
FnMEp+/−
FnMEp−/−
Fn
actin
D
Fn
actin
E

Figure A.6: Cell Proliferation Assay: BrdU-staining of mammary gland section from a 10-day pregnant $Fn^{fl+/+}$ control mouse (A) and a 10-day pregnant $Fn^{Mep-/-}$ mouse (B), both injected 2h prior to euthanasia with 100µg BrdU/gm of BW. There is a significant decrease in the number of BrdU-positive MEps in $Fn^{Mep-/-}$ mice relative to control $Fn^{fl+/+}$ mice (counts are from 200 MEps in each of 3 mice per category) (C).

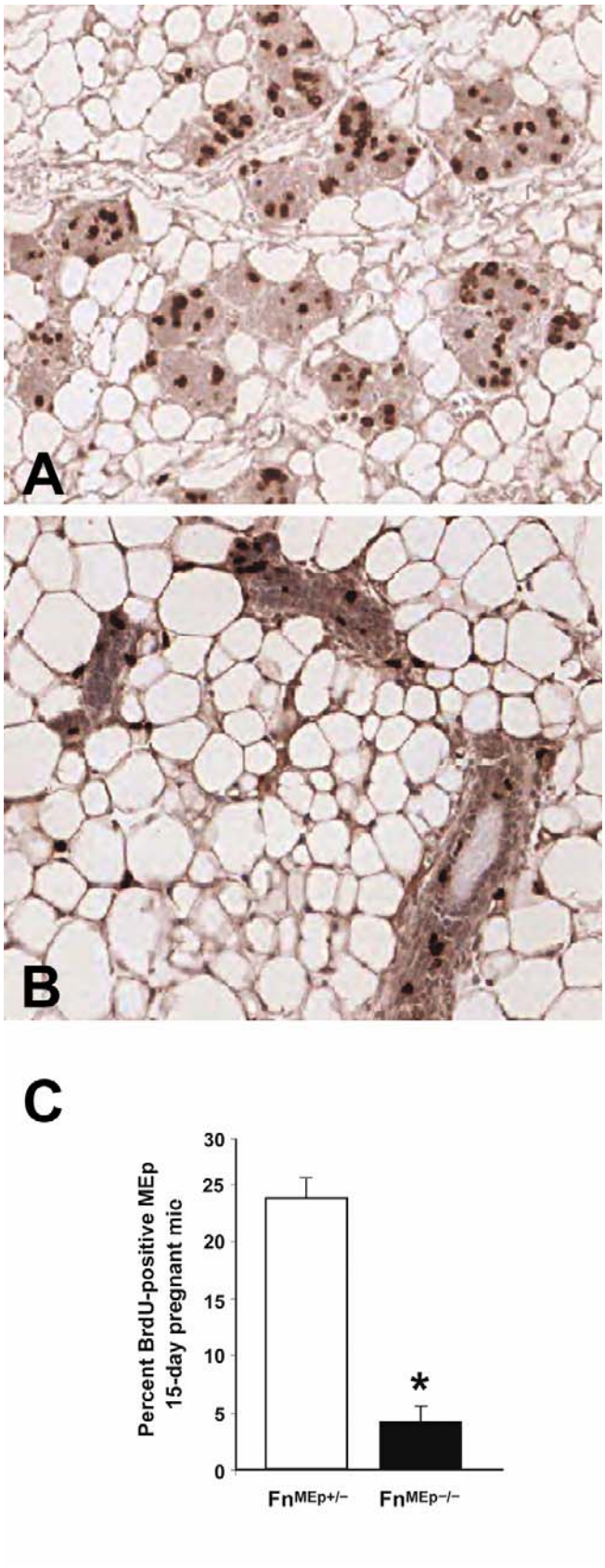
A
B
C
Percent BrdU-positive MEp
15-day pregnant mic
30
25
20
15
10
5
0
*
Fn^MEp+/−
Fn^MEp−/−

$Fn^{MEp-/-}$ mice, showing only rudimentary lobulo-alveolar differentiation (Fig A.7A), while MG sections from $Fn^{fl+/+}$ mice exhibited a haze of Fn staining around small ductules and newly formed alveoli (Fig A.7B). Staining was particularly strong around small blood vessels. At high magnification at the tip of sprouting ductules, epithelial cells lost their cuboidal shape and assumed a spindle- mesenchymal-like shape as they penetrated surrounding connective tissue shape in a manner reminiscent of epithelial-mesenchymal transition of invading cancer cells (Fig A.7C, arrows). At the same time, the cell body of spindle-shaped epithelial cells stained positive for Fn. Such staining was especially prominent at the tip of the invading cell. In other areas of lobulo-alveolar differentiation epithelial cells separating from the tubular confines of alveoli and sprouting into neighboring tissues stain positively for Fn (Fig A.7D&E). These processes are reminiscent of budding alveoli and are accompanied by strong Fn expression. Also noticeable is a strong Fn staining reaction around newly formed blood vessels of the lobulo-alveolar compartment. Such staining was absent around mature blood vessels outside the lobule.

Neovascularization of Mammary Gland Lobules

Lobulo-alveolar differentiation in 15-day pregnant $Fn^{fl+/+}$ mice was associated with a flurry of newly formed blood vessels that was associated with Fn staining at their periphery (Fig A.8; arrows). In contrast, age-matched $Fn^{MEp-/-}$ mice of the same stage of pregnancy exhibited rudimentary alveolar differentiation with few blood vessels and little or no Fn-staining (Fig A.7A). To examine whether the increased neovascularization was associated with increased expression of vascular endothelial cell growth factor (Vegf) expression, we extracted total RNA from $Fn^{fl+/+}$ and $Fn^{MEp-/-}$ mice and determined Vegf expression levels relative to the housekeeping gene Gapdh, using RT-PCR. Data show a more than 8-fold decrease in Vegf expression in

Figure A.7: MG Immunohistochemistry: Five μm-thick sections from MGs of 10-day pregnant $Fn^{Mep-/-}$ (A) and $Fn^{fl+/+}$(B-E) mice were stained with anti-Fn polyclonal Ab. At low magnification (A & B), there is little or no Fn-staining in MG sections from $Fn^{Mep-/-}$ mice showing only rudimentary lobulo-aveolar differentiation (A), while MG sections from $Fn^{fl+/+}$mice exhibit a haze of Fn-positive staining around small ducts and particularly within areas of early lobulo-alveolar differentiation that is especially prominent around small blood vessels (B). At higher magnification of MG sections from $Fn^{fl+/+}$ mice (C-E), there are Fn-positive cells that have undergone epithelial-mesenchymal transition at the tip of a sprouting terminal ductule (arrows, C), Fn-positive epithelial cells "dropping out" from the alveolar lining (arrows D) and forming new alveolar structures (arrows E).

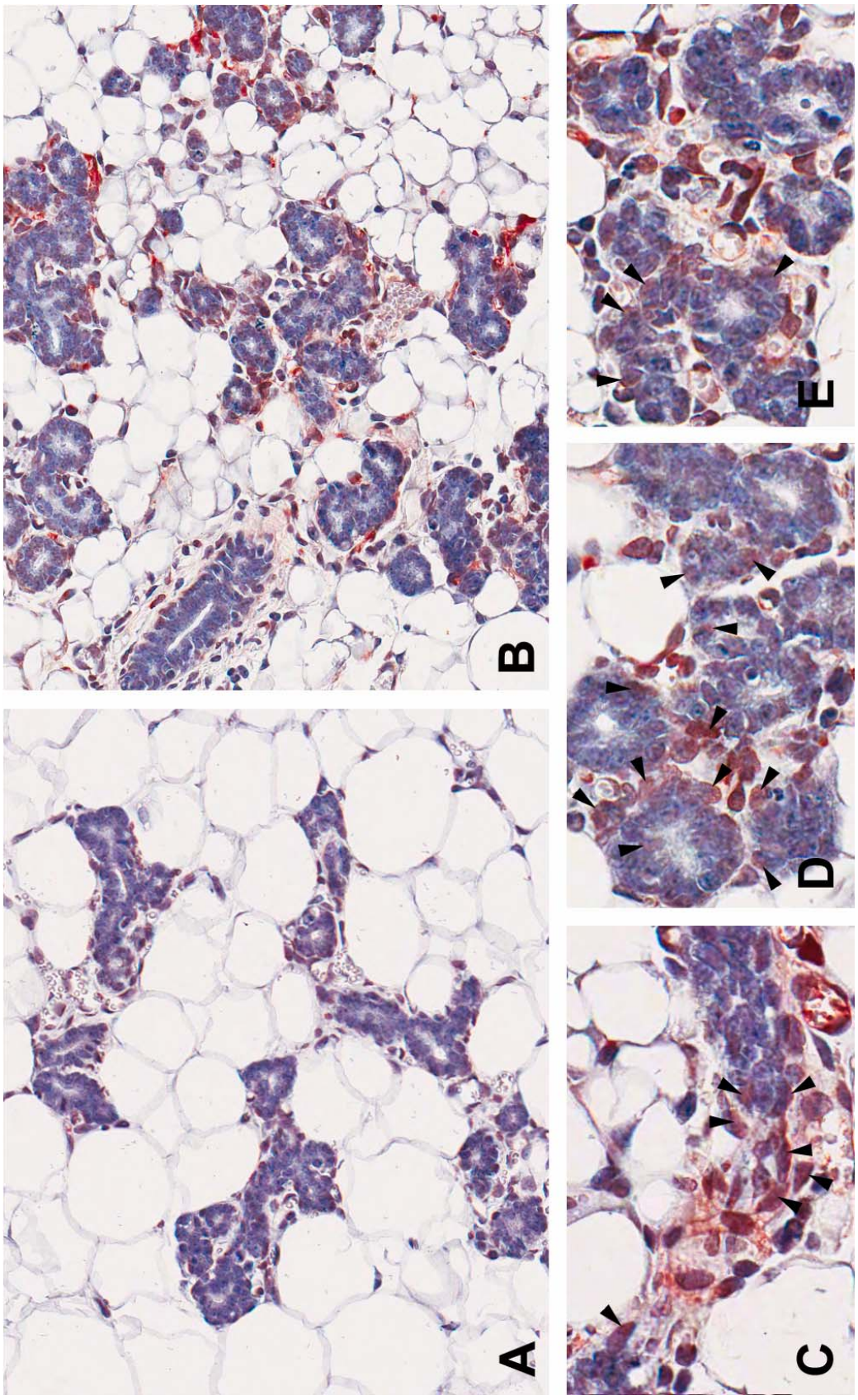
A
B
C
D
E

mammary glands from 15-day pregnant $Fn^{MEp-/-}$ mice over $Fn^{fl+/+}$ mice $Fn^{fl+/+}$ mice (Fig A.8).

Fn, Integrin β1, and Focal Adhesion Kinase - Mediators of Lobulo-Alveolar Morphogenesis?

Conditional knockout of either Fn, integrinβ1 (Itgb1) (35,36), or focal adhesion kinase (FAK) (37) in mammary epithelium appeared to have a similar effect on mammary gland postnatal morphogenesis. They all caused failure of lobulo-alveolar differentiation during pregnancy. To test whether Itgb1 and FAK might act downstream of Fn, we examined expression of these proteins and in the case of FAK, the activation status, in the mammary glands of $Fn^{fl+/+}$ and $Fn^{MEp-/-}$ mice. Indeed, knockout of Fn triggered a decrease in Itgb1 expression and autophosphorylation of FAK, but no decrease in FAK protein expression (Fig A.9).

DISCUSSION

Fibronectin has been introduced as a multi-domain glycoprotein that regulates a variety of cellular functions including differentiation, proliferation, apoptosis, migration (1-3). As such it is involved in embryologic and postnatal development (14-16), tissue homeostasis, wound healing, angiogenesis, and cancer (1-10). Here, we have analyzed the effects of conditional knockout of Fn in mammary epithelial cells on postnatal development of the mammary gland. Studies of adolescent (5 weeks) and adult virgin (16 weeks) mice of the three phenotypes $Fn^{fl+/+}$, $Fn^{MEp+/-}$, and $Fn^{MEp-/-}$ yielded quantitative differences in the expansion and differentiation of the ductal tree within the mammary fat pad between groups, but no significant differences in the branching pattern. Noteworthy are statistically decreased distances of branch

Figure A.8: Neovascularization of the Lobulo-Alveolar Compartment in $Fn^{fl+/+}$ Mice: Histologic section of the lobulo-alveolar compartment of a 15-day pregnant $Fn^{fl+/+}$ mouse exhibits a high vascular density (arrows), that is absent in 15-day pregnant $Fn^{Mep-/-}$ mice (see Fig. A.7A). This result is mimicked by a strong message for Vegf in MGs from $Fn^{fl+/+}$ mice and a very weak Vegf message in MGs from $Fn^{Mep-/-}$ mice.

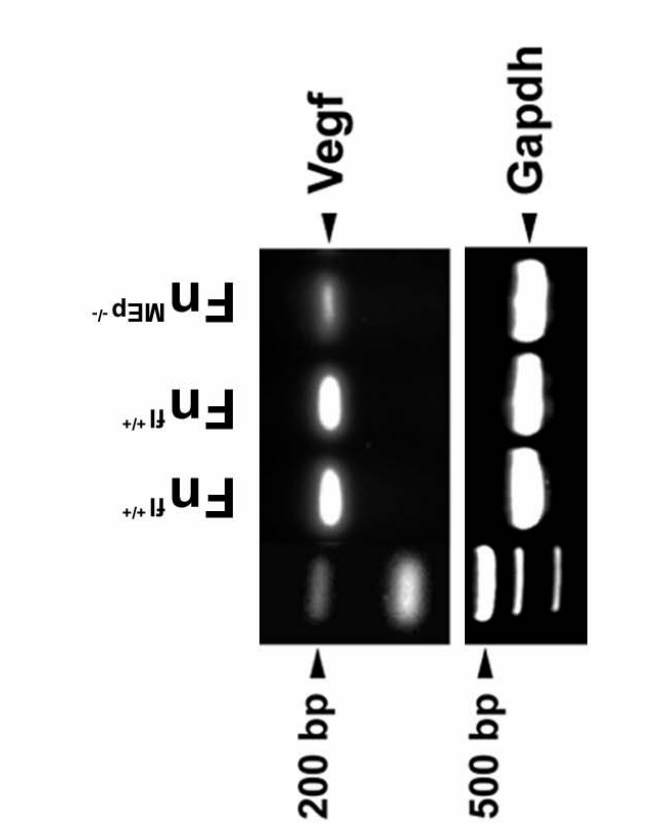
Vegf
Gapdh
Fn MEp -/-
Fn fl +/+
Fn fl +/+
200 bp
500 bp

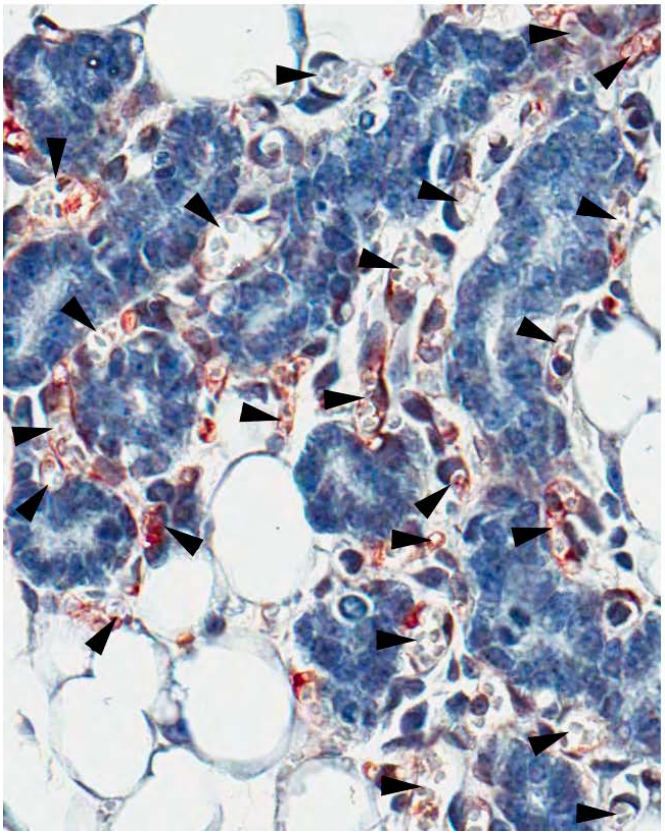

Figure A.9: Fn-Signaling via Itgb1 and FAK during MG Development in 15-day Pregnant $Fn^{fl+/+}$, but not $Fn^{MEp-/-}$ Mice: MGs (4th; inguinal) were extracted in lysis buffer and subjected to Western blotting with anti-Fn, anti-Itgb1, anti-FAK, and anti-FAK(pY397). $Fn^{fl+/+}$ MGs exhibit strong Fn, Itgb1, and FAK(pY397) expression, while $Fn^{Mep-/-}$ MGs fail to activate FAK and have somewhat reduced Itgb1 expression.

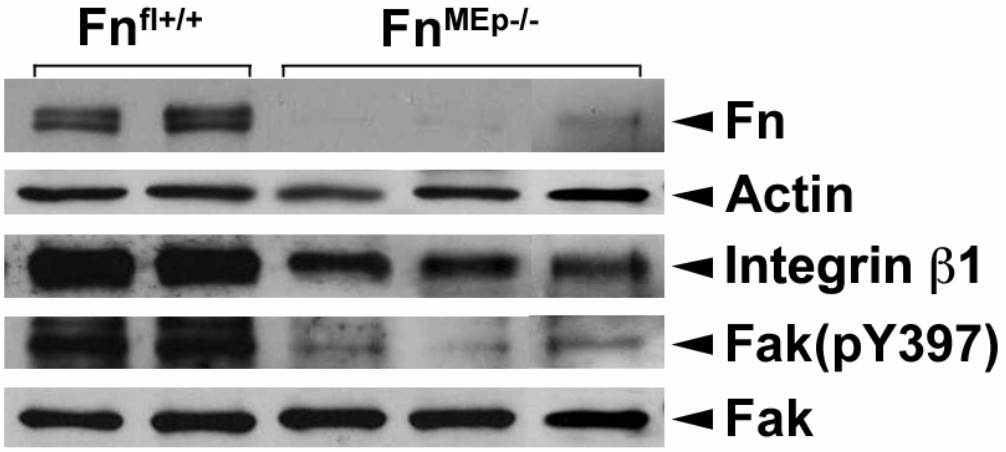
Fn^fl+/+
Fn^MEp-/-
Fn
Actin
Integrin β1
Fak(pY397)
Fak

outgrowth, numbers of branch points, and number of TEBs in 5- week old $Fn^{MEp-/-}$ mice. These differences were still present in 16-week old $Fn^{MEp-/-}$ mice, but were less pronounced and statistically not significant due to variability between samples asvisualized by large standard deviations in our statistical analyses, likely due to the mosaic Cre expression (34). Dramatic, statistically sound differences were observed only in pregnant mice, where the mammary glands of $Fn^{MEp-/-}$ mice exhibited severe deficiencies in the typical lobulo-alveolar differentiation observed in the two control groups, i.e., $Fn^{fl+/+}$ and $Fn^{MEp+/-}$ mice (see Fig A.5). The degree of lobulo-alveolar impairment in $Fn^{MEp-/-}$ mice ranged from severe hypoplasia to aplasia and was closely associated with the amount of Fn protein recovered from these glands. Failure of lobulo-alveolar differentiation resulted in lack of milk production and early death of newborn pups (<2days).

Our data mimic to a large extent those reported for mice with the conditional knockout of the β1 integrin (Itgb1) (35,36) and focal adhesion kinase (FAK) (37) in the mammary epithelium. Fn-knockout in mammary epithelium, like Itgb1- (35,36) and FAK-knockout (37), did not affect the pattern of ductal outgrowth and branching, albeit both were slowed down somewhat in $Fn^{MEp-/-}$ and $FAK^{MEp-/-}$ mice. In pregnant mice, deletion of Fn, Itgb1, and FAK left only a skeleton of ducts and ductules (Fig A.2) with lack of lobulo-alveolar differentiation and ensuing inability of females to produce milk and nurse their pups (35-37). These data suggest that Fn may operate proximal of Itgb1 and FAK (38). In support of this notion Fn deletion was followed by significant decreases in Itgb1 expression and autophosphorylation of FAK, while FAK protein expression remained constant. Disruption of Fn-Itgb1-FAK interactions and associated malformation of focal adhesions (35) may have accounted for the observed decreased rate of proliferation that was most prominent in 16-week old virgin and 15-day pregnant $Fn^{MEp-/-}$ mice. Such impaired proliferation has also been noticed in

Itgb1- and FAK-knockouts in the mammary epithelium as well as in mammary glands of mice that expressed a dominant-negative chimeric form of Itgb1 (39). Moreover, consistent with our in vivo observation, mammary epithelial cells isolated from $Itgb1^{MEp-/-}$ mice expressed decreased levels of tyrosine phosphorylation at residue 397 of FAK relative to mammary epithelial cells from Itgb1-floxed mice (35).

In the mammary gland of $Fn^{MEp-/-}$ mice branching initiation, branch outgrowth, elongation and ramification seem to occur independent of Fn, albeit epithelial-mesenchymal transition (EMT), which involves expression of Fn, has been implicated to be responsible for the expansion (invasion) of the ductal tree within the mammary fat pad (40). However, our morphologic studies are more indicative of "cohort-type" of invasion of ducts into the mammary fat pad, rather than a "mesenchymal-type" of invasion (41) that involves individual spindle-shape cells of files of cells to penetrate MFP tissue. In contrast, at sites of alveologenesis epithelial cells arising from terminal ductules and primary alveolar buds seem to separate themselves from the epithelial lining and enter the mammary fat pad. These cells are spindly (mesenchymal) in shape and are strongly Fn positive and appear highly motile (42). The driving forces behind these processes are not well established, but could well be mediated by Fn itself, which has been shown to exert an EMT promoting effect (43). Differentiation of the newly created lobuloalveolar compartment could then be achieved by Jak2/Stat5a-signaling, reversing EMT and promoting differentiation of epithelial cells as shown by accompanying increased expression of E-cadherin, zonula occludens-1 and cytokeratins 8 and 18 (44).

Lobulo-alveolar differentiation in the mammary gland of $Fn^{fl+/+}$ mice is associated with an elaborate neovascularization process, as shown by the formation of vascular honeycombs around the alveolar structures (45) and high levels of Vegf expression. Such neovascularization is missing in $Fn^{MEp-/-}$ mice and, correspondingly,

Vegf expression is low. This result may be in response to extensive, new, lobulo-alveolar growth in $Fn^{fl+/+}$ mice and lack thereof in and $Fn^{MEp-/-}$ mice. However, several studies suggest a more direct involvement of Fn in Neovascularization. For example, (i) rat coronary neovascularization during prenatal and early postnatal development was preceded by the deposition of Fn suggesting that Fn may provide a primary scaffolding for the migration of primordial endothelial cells/angioblasts (46); (ii) Retinal vasculogenesis follows the spread of astrocytes into the nerve fiber layer of the retina and the deposition of Fn in the zone of vasculogenesis (47); (iii) Proliferative diabetic retinopathy, a condition which entails proliferation of microvascular endothelial cells and retinal neovascularization is associated with upregulation of Fn extra domain B (EDB) (48); (iv) Exposure of endothelial cells to EDB+-Fn or EDB- polypeptide significantly increased Vegf expression and promotes endothelial proliferation and tube formation in vivo (49).

In summary, we have present novel evidence of the role of Fn in postnatal mammary gland morphogenesis. Conditional knockout of Fn in mammary epithelium leads to severe lobulo-alveolar hypoplasia/aplasia. Concomitant downregulation of Itgb1 and decrease autophosphorylation of FAK suggest that this pathology is mediated, at least in part, by disruption of Fn/Itgb1/FAK signaling pathway. This notion is supported by the fact that conditional knockouts of Itgb1 and FAK generate the same pathology as Fn-deletion (35-37). Moreover, a more that 6-fold downregulation of Vegf and significantly impaired neovascularization in $Fn^{MEp-/-}$ mice further compromised lobulo-alveolar differentiation.

REFERENCES

1. Mosher DF (1989) Fibronectin. San Diego, CA: Academic Press, Inc.

2. Hynes RO (1990) Fibronectin. New York, NY: Springer-Verlag

3. Pankov P and Yamada KM (2002) J. Cell Sci., **115**, 3861-3963

4. ffrench-Constant C (1995) Exp. Cell Res., **221**, 261-271

5. Johansson S, Svineng G, Wennerberg K, Armulik A, and Lohikangas L (1997) Front. Biosci., **2**, 126-146

6. Danen EHJ and Yamada KM (2001) J. Cell. Physiol., **189**, 1-13

7. Couchman JR, Austria MR and Woods A (1990) J. Invest. Dermatol., **94**, 7S-14S

8. Wierzbicka-Patynowski I and Schwarzbauer JE (2003) J. Cell Sci., **116**, 3269-3276

9. Kumar CC (1998) Signaling by integrin receptors. Oncogene, **17**, 1365-1373.

10. Geiger B, Bershadsky A, Pankov R and Yamada KM (2001) Nat. Rev. Mol. Cell. Biol., **2**, 793-805

11. Yamada KM and Clark RAF (1996) Provisional matrix. In: *The Molecular and Cellular Biology of Wound Repair* (ed. Clark RAF), pp. 51-93. New York: Plenum Press.

12. Cheng HC, Abdel-Ghany M and Pauli BU (2003) J. Biol. Chem., **278,** 24600-24607

13. Miyamoto S, Katz BZ, Lafrenie RM and Yamada KM (1998) Ann. NY Acad. Sci., **857**, 119-129

14. George EL, George-Labouesse EN, Patel-King RS, Rayburn H and Hynes RO (1993) Development, **119**, 1079-1091

15. Watt FM and Hodivala KJ (1994) Curr. Biol., **4**, 270-272

16. Sakai, T., Larsen, M., and Yamada, K. M. (2003). Nature 423, 876-81

17. Haslam, S. Z., and Woodward, T. L. (2003). Breast Cancer Res 5, 208-15

18. Wang Y, Selden AC, Morgan N, Stamp GW and Hodgson HJ (1994) Am. J. Pathol., **144**, 675-682

19. Yang Y, Spitzer E, Meyer D, Sachs M, Niemann C, Hartmann G, Weidner KM, Bichmeier C and Birchmeier W (1995). J. Cell Biol., **131**, 215-226

20. Woodward TL, Mienaltowski A, Modi R, Bennet JM and Haslam SZ (2000) Endocrinol., **142**, 3214-3222

21. Woodward TL, Xie JW and Haslam SZ (1998) J. Mammary Gland Biol. Neopl., **3**, 117-131

22. Fendrick JL, Raafat AM and Haslam SZ (1998) J. Mammary Gland Biol. Neopl., **3**, 7-22

23. Shen, Q., Zhang, Y., Uray, I. P., Hill, J. L., Kim, H. T., Lu, C., Young, M. R., Gunther, E. J., Hilsenbeck, S. G., Chodosh, L. A., Colburn, N. H., and Brown, P. H. (2006). Dev Biol 295, 589-603

24. Hennighausen L and Robinson GW (2001) Dev. Cell, **1**, 467-475

25. Shillingford JM and Hennighausen L (2001) Trends Endocrinol. Metab., **12**, 402-408

26. Hennighausen L and Robinson GW (2005) Nat. Rev. Mol. Cell Biol., **6**, 715-725

27. Labat-Robert J (2002) Cancer Biol., **12**, 187-195

28. Sakai T, Johnsoin KJ, Murozono M, Sakaio K, Magnuson MA, Wieloch T, Cronberg T, Isshiki A, Erickson HP and Fässler R (2001) Nat. Med., **7**, 324-330

29. Bonnerot C, Nicolas JF (1993) Methods Enzymol. 225:451-469

30. Tiran Z and Elson A (2003) Meth. Enzymol., **366**, 124-132

31. Weibel ER and Bolender RP (1973) Stereological Techniques for electron microscopic morphometry. In: *Principles and Techniques of Electron Microscopy*, (ed. Hayat MA), Vol. **3**, 237-296.

32. Pauli BU, Cohen SM and Weinstein RS (1983) J. Urol., **129**, 646-652

33. Abdel-Ghany M, Cheng HC, Elble RC, Pauli BU. (2002) J Biol Chem. 277, 34391-3400

34. White DE, Kurpios NA, Zuo D, Hassell JA, Blaess S, Mueller U, Muller WJ. (2004) Cancer Cell, 6, 159-170

35. Naylor, M. J., Li, N., Cheung, J., Lowe, E. T., Lambert, E., Marlow, R., Wang, P., Schatzmann, F., Wintermantel, T., Schuetz, G., Clarke, A. R., Mueller, U., Hynes, N. E., and Streuli, C. H. (2005) J Cell Biol 171, 717-728

36. Li, N., Zhang, Y., Naylor, M. J., Schatzmann, F., Maurer, F., Wintermantel, T., Schuetz, G., Mueller, U., Streuli, C. H., and Hynes, N. E. (2005) Embo J 24, 1942-53

37. Nagy, T., Wei, H., Shen, T. L., Peng, X., Liang, C. C., Gan, B., and Guan, J. L. (2007) J Biol Chem 282, 31766-76

38. Mitra SK, Schlaepfer DD. (2006) Curr Opin Cell Biol., 18, 516-523

39. Faraldo MM, Deugnier MA, Lukashev M, Thiery JP, Glukhova MA (1998) EMBO J. 17, 2139-2147

40. Fata JE, Werb Z, Bissell MJ. (2004) Breast Cancer Res. 6, 1-11

41. Friedl P and Wolf K. (2003) Nat. Rev. Cancer 3:362-374, 2003

42. Larsen M, Wei C, Yamada KM. (2006) J Cell Sci. 119, 3376-3384

43. Taliana L, Evans MD, Ang S, McAvoy JW. (2006) Mol Vis. 12, 1233-1242

44. Sultan AS, Brim H, Sherif ZA. (2008) Cancer Sci. 99, 272-279

45. Djonov V, Baum O, Burri PH. (2003) Cell Tissue Res. 314, 107-117

46. Rongish, B. J., Hinchman, G., Doty, M. K., Baldwin, H. S., and Tomanek, R. J. (1996) J Mol Cell Cardiol 28, 2203-15

47. Jiang, B., Liou, G. I., Behzadian, M. A., and Caldwell, R. B. (1994) J Cell Sci 107 (Pt 9), 2499-508

48. Khan ZA, Cukiernik M, Gonder JR, Chakrabarti S. (2004) Invest Ophthalmol Vis Sci. 45, 287-295

49. Khan, Z. A., Chan, B. M., Uniyal, S., Barbin, Y. P., Farhangkhoee, H., Chen, S., and Chakrabarti, S. (2005)Angiogenesis 8, 183-96